

**UNIVERSIDADE FEDERAL DE SANTA CATARINA  
DEPARTAMENTO DE ENGENHARIA MECÂNICA**

Julian Esteban Barrera Torres

**USO DOS CICLOS RANKINE ORGÂNICOS PARA O  
APROVEITAMENTO DO CALOR RESIDUAL EM  
INSTALAÇÕES DE PRODUÇÃO DE PETRÓLEO E GÁS**

Florianópolis

2014



Julian Esteban Barrera Torres

**USO DOS CICLOS RANKINE ORGÂNICOS PARA O  
APROVEITAMENTO DO CALOR RESIDUAL EM  
INSTALAÇÕES DE PRODUÇÃO DE PETRÓLEO E GÁS**

Dissertação submetida ao Programa  
de Pós-Graduação em Engenharia Mecânica  
para a obtenção do Grau de Mestre  
em Engenharia Mecânica.  
Orientador: Edson Bazzo, Dr.Eng.

Florianópolis

2014

Catálogo na fonte elaborada pela biblioteca da  
Universidade Federal de Santa Catarina

Barrera Torres, Julian Esteban

Uso dos ciclos Rankine orgânicos para o aproveitamento do calor residual em instalações de produção de petróleo e gás / Julian Esteban Barrera Torres ; orientador, Edson Bazzo - Florianópolis, SC, 2014.

158 p.

Dissertação (mestrado) - Universidade Federal de Santa Catarina, Centro Tecnológico. Programa de Pós-Graduação em Engenharia Mecânica.

Inclui referências

1. Engenharia Mecânica. 2. Engenharia mecânica. 3. Eficiência energética. 4. Plataformas de petróleo e gás. 5. Ciclos Rankine orgânicos. I. Bazzo, Edson. II. Universidade Federal de Santa Catarina. Programa de Pós-Graduação em Engenharia Mecânica. III. Título.

Julian Esteban Barrera Torres

**USO DOS CICLOS RANKINE ORGÂNICOS PARA O  
APROVEITAMENTO DO CALOR RESIDUAL EM  
INSTALAÇÕES DE PRODUÇÃO DE PETRÓLEO E GÁS**

Esta Dissertação foi julgada aprovada para a obtenção do Título de “Mestre em Engenharia Mecânica”, e aprovada em sua forma final pelo Programa de Pós-Graduação em Engenharia Mecânica.

Florianópolis, 01 de Abril 2014.

---

Armando Albertazzi Gonçalves Jr, Dr.Eng.  
Coordenador do Curso

---

Edson Bazzo, Dr.Eng.  
Orientador

**Banca Examinadora:**

---

Edson Bazzo, Dr.Eng.  
Presidente

---

Silvio de Oliveira Junior, Dr.Eng

---

Ricardo Antonio Machado, Dr.Eng.

---

Alexandre Kupka da Silva, Ph.D.



For anyone who reads this dissertation  
with a purpose.





## ACKNOWLEDGMENTS

I would like to express my very great appreciation to Professor Edson Bazzo for his valuable and constructive suggestions during the planning and development of this research work. His willingness to give his time so generously has been very much appreciated.

I would also like to express my deep gratitude to Professor Silvio Oliveira, Professor Ricardo Machado and Professor Alexandre Kupka, my research examining board, for their enthusiastic encouragement and useful critiques of this research work.

Special thanks should be given to Eduardo Kami, for his professional guidance and constructive recommendations on this project.

Finally, I wish to thank my parents for their support and encouragement throughout my study.



*Our intelligence and our technology have given us the power to affect the climate. How will we use this power? Are we willing to tolerate ignorance and complacency in matters that affect the entire human family? Do we value short-term advantages above the welfare of the Earth? Or will we think on longer time scales, with concern for our children and our grandchildren, to understand and protect the complex life-support systems of our planet? The Earth is a tiny and fragile world. It needs to be cherished.*

Carl Sagan, *Cosmos* (1980)



## RESUMO

A presente dissertação contempla o melhoramento do desempenho de uma plataforma de processamento de óleo e gás por meio da incorporação hipotética de um ciclo Rankine orgânico (ORC). Esse ciclo termodinâmico recuperaria parte do calor residual associado aos gases de exaustão das turbinas na planta, para geração de potência adicional, permitindo um decréscimo na carga das mesmas e, portanto no consumo de combustível. O modelamento do processo foi desenvolvido com o propósito de caracterizar a operação normal da plataforma e assim estabelecer as condições de referência para comparar o desempenho energético da mesma. A partir da informação obtida do modelo, uma análise exérgica permitiu identificar as operações com maior irreversibilidade e também com potencial para recuperação da exergia perdida. Além disso demonstrou diferenças significativas na ordem de grandeza entre os fluxos de exergia associados às correntes de óleo e gás produzidos e as demais correntes relacionadas com o seu processamento. Considerando isto, foram considerados três indicadores de eficiência, dois relacionados com os fluxos de exergia e um relacionado com o gasto energético. De outro lado, o sistema ORC foi definido tendo em conta os resultados de estudos recentes focados na seleção do fluido de trabalho e na configuração do ciclo, visando as melhores condições de operação do ciclo enquadrado dentro das restrições impostas pelo processo. Considerando a grande variabilidade dos parâmetros de produção deste tipo de instalação, a comparação dos resultados do modelo incluindo o ORC integrado com o processo foi feita ao longo de um perfil de produção que contempla a variação de cinco parâmetros de maneira independente: (i) vazão de óleo, (ii) vazão de água de produção, (iii) pressão de poço, (iv) vazão de gás injetado e (v) vazão de água injetada. Os resultados mostraram que a implementação do ciclo traz um melhoramento dos indicadores de eficiência energética propostos, independentemente da variação nos parâmetros de produção, com um melhoramento dos indicadores relativamente uniforme ao longo do perfil analisado. Os parâmetros de produção com maior impacto sobre a potência gerada pelo ORC correspondem às vazões de gás e de água injetadas no reservatório, sendo essas as operações que demandam maior potência e portanto uma maior produção de gases de exaustão nas turbinas. Em geral, a metodologia adotada pretende avaliar o impacto de uma tecnologia para o melhoramento da eficiência energética

(nesse caso o ORC) em um processo industrial existente, considerando a caracterização detalhada do processo em questão e a variação dos parâmetros mais relevantes de produção, de tal forma que os resultados ofereçam um panorama mais amplo na hora de aplicar este tipo de sistema.

**Palavras-chave:** Eficiência Energética, Processamento de Óleo e Gás, Análise Exergética, Ciclo Rankine Orgânico, FPSO.

## ABSTRACT

The present dissertation contemplates the energy performance enhancement of an oil and gas processing platform by means of the hypothetical incorporation of an Organic Rankine Cycle (ORC). This thermodynamic cycle would recover part of the waste heat associated with exhaust gases coming from gas turbines in order to produce additional power, allowing a decrease in their load and consequently in their fuel consumption. The process modeling was developed with the aim of characterizing the plant normal operation and thereby establish the reference conditions for comparing its energy efficiency. With the information obtained from the model, a detailed exergy analysis enabled the identification of the operations with greatest irreversibility and with potential for the exergy losses recovering. In addition, it showed a great difference between the exergy fluxes associated with produced oil and gas streams when compared with the other streams associated with their processing. Considering that, the use of three energy efficiency indicators was analyzed, two of these indicators are related to the exergy fluxes and the other with the energetic expense. On the other side, the ORC system was defined taking into account the results of recent studies focused on the selection of the ORC working fluid and the ORC configuration, aiming the best operating conditions framed into process constraints. Considering the great variability of the production parameters in this kind of installations, the comparison of the model results with the ORC integrated was made along a production profile that comprises the variation of five parameters independently: (i) oil flow, (ii) production water flow, (iii) well pressure, (iv) injected gas flow and (v) injected water flow. The results demonstrated that the implementation of the ORC improves the proposed indicators, independently of the variation of the chosen production parameters. The energy improvement was found relatively uniform along the production profile. The production parameters with a greater impact over the ORC output correspond to the gas and water flows injected back into the reservoir. These operations demand the highest amount of power and thus the greatest production of exhaust gases at gas turbines. This procedure pretends to evaluate the effect of an energy enhancement technology (in this case the ORC) in an existing process, characterizing its behavior under variable production conditions. In this way, the results can give a wider panorama when applying this kind of systems for energy

performance improvement.

**Keywords:** Energy Efficiency, Oil and Gas Processing, Exergy Analysis, Organic Rankine Cycle, FPSO.



## LIST OF FIGURES

|           |   |    |
|-----------|---|----|
| Figure 1  | World oil and gas demand (IEA, 2012).....   | 7  |
| Figure 2  | Production profiles of some Brazilian fields (SIMMONS, 2009).....   | 8  |
| Figure 3  | Typical operation scheme of an oil and gas production plant (WILKINSON, 2006).....  | 11 |
| Figure 4  | Schemes of most common types of offshore platforms (MAHONEY, 2013).....   | 13 |
| Figure 5  | Basic operation scheme of an FPSO (WILKINSON, 2006).....  | 14 |
| Figure 6  | Basic layout of an FPSO topside.....  | 18 |
| Figure 7  | Example of an FPSO topside.....   | 19 |
| Figure 8  | Basic PFD of a typical FPSO process plant.....  | 20 |
| Figure 9  | Basic scheme of an ORC system.....  | 22 |
| Figure 10 | Basic scheme of an regenerative ORC system.....   | 23 |
| Figure 11 | Types of fluids (HEBERLE; PREIBINGER; BRÜGGEMANN, 2012).....  | 25 |
| Figure 12 | Effect of the enthalpy of vaporization of the working fluid (BAO; ZHAO, 2013).....  | 26 |
| Figure 13 | Difference between cycle efficiency and power output (DECLAYE, 2009).....   | 27 |
| Figure 14 | Relation between the critical temperature and the parameter $\xi$ for various candidates (CHEN; GOSWAMI; STEFANAKOS, 2010)..... | 28 |
| Figure 15 | Determination of the normal boiling point (NBP) of each pseudocomponent (ASPENTECH, 2011).....                                  | 37 |
| Figure 16 | Specific heat of crude fractions as a function of temperature and its standard specific gravity (MAXWELL, 1968).....            | 39 |
| Figure 17 | Heat of combustion of crude fractions as function of its standard specific gravity (MAXWELL, 1968).....                         | 40 |
| Figure 18 | Basic PFD (Process Flow Diagram) of the separation plant.....   | 42 |
| Figure 19 | Basic PFD (Process Flow Diagram) of the boost system.....   | 44 |
| Figure 20 | Basic PFD (Process Flow Diagram) of the gas injection/export system.....  | 45 |
| Figure 21 | Basic PFD (Process Flow Diagram) of the power gene-   |    |

|  |    |
|--|----|
| ration system.....   | 46 |
| Figure 22 Operating parameters of gas turbines (SIEMENS AG, 2009).   | 47 |
| Figure 23 Basic PFD (Process Flow Diagram) of the water injection system. ....   | 47 |
| Figure 24 Analyzed production profiles.....  | 52 |
| Figure 25 Model general algorithm. ....  | 60 |
| Figure 26 Power supply distribution for: (a)-Hysys model and (b)-EES model. ....   | 65 |
| Figure 27 Rejected heat distribution for: (a)-Hysys model and (b)-EES model. ....  | 66 |
| Figure 28 Simplified Grassmann diagram of the plant, exergy flows in MW.....   | 69 |
| Figure 29 Exergy destruction rate distribution for: (a)-Hysys model and (b)-EES model. ....  | 71 |
| Figure 30 Exergy losses distribution for: (a)-Hysys model and (b)-EES model. ....  | 71 |
| Figure 31 Exergy efficiencies ( $\eta_p$ ) for Hysys and EES models. ....  | 74 |
| Figure 32 Exergy efficiencies ( $\Phi_p$ ) for Hysys and EES models. ....  | 74 |
| Figure 33 Variation of (i) cyclopentane mass flow, (ii) ORC performance, (iii) Rejected heat and (iv) ORC output with the evaporation temperature of cyclopentane..... | 76 |
| Figure 34 Variation of the HTF outlet temperature and HTF mass flow with the evaporation temperature of cyclopentane.....  | 77 |
| Figure 35 T-s diagram of the ORC at different evaporation temperatures.....  | 78 |
| Figure 36 Variation of ORC input and cyclopentane specific work with the evaporation temperature.....  | 79 |
| Figure 37 Total rejected heat vs. ORC $T_{ev}$ for selected scenarios.   | 82 |
| Figure 38 Total rejected heat (i), power demand (i) and thermal efficiency of power generation (ii) profiles. ....   | 83 |
| Figure 39 ORC input and output, MW.....  | 84 |
| Figure 40 $\eta_P$ and $\lambda$ : (i) for cases 0 through 15 and (ii) for cases 3 through 15. ....  | 85 |
| Figure 41 $\eta_{II}$ variation along the production profile. ....   | 87 |
| Figure 42 Influence factor $f$ for each production parameter. (i) current configuration, (ii) ORC integrated. ....   | 88 |
| Figure 43 Influence factor $f$ for each production parameter applied   |    |

|  |     |
|--|-----|
| in the ORC performance.....  | 89  |
| Figure 44 Process flow diagram of a power subsystem turbine ( <b>A</b> ).....                    | 107 |
| Figure 45 Process flow diagram of the separation plant ( <b>B</b> ).....                         | 108 |
| Figure 46 Process flow diagram of gas boosting subsystem ( <b>C</b> )..                          | 109 |
| Figure 47 Process flow diagram of gas injection/export subsystem<br>( <b>D</b> ).....            | 109 |
| Figure 48 Process flow diagram of ORC subsystem ( <b>F</b> ).....                                | 110 |
| Figure 49 Process flow diagram of seawater injection subsystem<br>( <b>H</b> ).....              | 110 |
| Figure 50 Scheme of operation of EES model.....  | 130 |
| Figure 51 Scheme of operation of gas boost system in EES model.                                  | 131 |
| Figure 52 Scheme of operation of gas injection/export system in<br>EES model.....                | 131 |
| Figure 53 TBP curve and normal boiling point (NBP) of each pseu-<br>docomponent.....             | 155 |
| Figure 54 Some physical properties and lower heating value (LHV)<br>of each pseudocomponent..... | 157 |
| Figure 55 Elemental composition of each pseudocomponent.....                                     | 158 |
| Figure 56 Specific heat of crude (oily phase).....   | 158 |



## LIST OF TABLES

|          |   |     |
|----------|---|-----|
| Table 1  | RD&D needs for addressing WHR Barriers (BCS, 2008) .                              | 9   |
| Table 2  | Simulation input data for separation plant. ....                                  | 48  |
| Table 3  | Simulation input data for boost subsystem. ....                                   | 48  |
| Table 4  | Simulation input data for gas injection/export subsystem.                         | 49  |
| Table 5  | Simulation input data for power generation subsystem. .                           | 49  |
| Table 6  | Simulation input data for seawater injection subsystem..                          | 49  |
| Table 7  | Model assumptions . ....  | 49  |
| Table 8  | Oil characterization parameters. ....   | 50  |
| Table 9  | Gas composition. ....   | 50  |
| Table 10 | Subsystems exergy product definition. ....  | 57  |
| Table 11 | Main physical properties of the cyclopentane. ....                                | 58  |
| Table 12 | ORC parameters and assumptions . ....   | 59  |
| Table 13 | Comparison of mass and energy balances of models. ....                            | 64  |
| Table 14 | Power consumption per subsystem, kW. ....   | 65  |
| Table 15 | Power supply distribution, % . ....   | 65  |
| Table 16 | Rejected heat per subsystem, kW. ....   | 66  |
| Table 17 | Exergy losses per subsystem, kW. ....   | 68  |
| Table 18 | Exergy destruction rate per subsystem, kW. ....                                   | 68  |
| Table 19 | Exergy destruction rate distribution. ....  | 70  |
| Table 20 | Exergy destruction rate distribution (only separation and gas processes). ....    | 70  |
| Table 21 | Exergy losses distribution. ....  | 72  |
| Table 22 | Exergy performance indicators by system - Hysys model.                            | 73  |
| Table 23 | Exergy performance indicators - EES model . ....                                  | 73  |
| Table 24 | Effect of the ORC integration over some production parameters of the plant . .... | 80  |
| Table 25 | Production parameters profiles. ....  | 81  |
| Table 26 | ORC $T_{ev}$ chosen for each case. ....   | 81  |
| Table 27 | PFD nomenclature. ....  | 105 |
| Table 29 | Mass balances per system in EES model, kg/h. ....                                 | 137 |
| Table 30 | Mass balances per system in Hysys model, kg/h. ....                               | 138 |
| Table 31 | Power demand distribution according to EES and Hysys                              |     |

|  |     |
|--|-----|
| models, kW. ....   | 139 |
| Table 32 Heat rejection distribution according to EES and Hysys models, kW. .... | 140 |
| Table 33 Exergy balances per equipment. ....                                     | 143 |
| Table 34 Exergy losses per system, kW. ....                                      | 145 |
| Table 35 Exergy destruction rate per equipment, kW. ....                         | 146 |
| Table 36 Exergy balances per system in EES model, kW. ....                       | 149 |
| Table 37 Exergy balances per system in Hysys model, kW. ....                     | 150 |
| Table 38 General exergy balance, kW. ....  | 151 |
| Table 39 Crude composition (oily phase). ....                                    | 156 |

## ACRONYMS

|         |   |
|---------|---|
| API     | American Petroleum Institute.                     |
| BOE     | Barrels of Oil Equivalent.                        |
| BSW     | Bottom Sediments and Water.                       |
| C       | Carbon element.                                   |
| CHP     | Combined Heat and Power.                          |
| COSTALD | Corresponding States Liquid Density.              |
| DOE     | Department of Energy of United States.            |
| EES     | Engineering Equation Solver.                      |
| EOS     | Equation of State.                                |
| FPSO    | Floating Production, Storage and Offloading unit. |
| FTP     | Flowing Tubing Pressure.                          |
| GOR     | Gas to Oil Ratio.                                 |
| GWP     | Global Warming Potential.                         |
| H       | Hydrogen element.                                 |
| HHV     | Higher Heating Value or Gross heat of combustion. |
| HTF     | Heat Transfer Fluid.                              |
| IEA     | International Energy Agency.                      |
| LHV     | Lower Heating Value or Net heat of combustion.    |
| N       | Nitrogen element.                                 |
| NBP     | Normal Boiling Point.                             |
| O       | Oxygen element.                                   |
| ODP     | Ozone Depletion Potential.                        |
| ORC     | Organic Rankine Cycle.                            |

|      |  |
|------|--|
| ORVC | Organic Rankine–Vapor Compression.       |
| PFD  | Process Flow Diagram.                    |
| PPD  | Pinch Point Difference.                  |
| PR   | Peng-Robinson.                           |
| PVT  | Pressure-Volume-Temperature.             |
| RD&D | Research, Development and Demonstration. |
| S    | Sulfur element.                          |
| SG   | Specific Gravity.                        |
| TBP  | True Boiling Point.                      |
| TEG  | Triethylene glycol.                      |
| WHR  | Waste Heat Recovery.                     |



## NOMENCLATURE

### Roman Letters

|           |  |
|-----------|--|
| $B$       | Exergy flow, kW.                           |
| $b$       | Mass specific exergy, kJ/kg.               |
| $\bar{b}$ | Molar specific exergy, kJ/kmol.            |
| $f$       | Parameter influence factor.                |
| $H$       | Enthalpy flow, kW.                         |
| $h$       | Mass specific enthalpy, kJ/kg.             |
| HHV       | Higher heating value, kJ/kg.               |
| $K$       | Watson UOPK factor.                        |
| LHV       | Lower heating value, kJ/kg.                |
| $m$       | Mass flow, kg/s.                           |
| $n$       | Molar flow, kmol/s.                        |
| $P$       | Pressure, kPa.                             |
| $Q$       | Heat flow, kW.                             |
| $S$       | Entropy flow, kW/K.                        |
| $s$       | Mass specific entropy, kJ/kg-K.            |
| $SG$      | Specific gravity (15°C/15°C).              |
| $T$       | Temperature, °C.                           |
| $v$       | Liquid volumetric flow, m <sup>3</sup> /s. |
| $x$       | Mass fraction.                             |
| $y$       | Subsystem contribution fraction.           |
| $z$       | Molar fraction.                            |

## Greek Letters

|             |  |
|-------------|--|
| $\beta$     | Exergy correction factor for oil fractions.  |
| $\Delta$    | Finite difference.   |
| $\Phi$      | Exergy performance indicator.  |
| $\gamma$    | Activity coefficient.  |
| $\eta_P$    | Degree of thermodynamic perfection.  |
| $\eta_{II}$ | Exergy performance indicator.  |
| $\lambda$   | Energy performance indicator, MJ/sm <sup>3</sup> oil.  |
| $\Lambda$   | Production parameter.  |
| $\xi$       | $\partial s/\partial T$ - inverse of the slope of the vapor saturation curve in T-s diagram, J/kg-K <sup>2</sup> . |
| $\omega$    | Acentric factor.   |

## Subscripts

|              |  |
|--------------|--|
| 0            | Dead state conditions, $T_0 = 25\text{ }^\circ\text{C}$ , $P_0 = 101.325\text{ kPa}$ . |
| avg.         | Average.   |
| b            | Boiling point.   |
| C            | Carbon element.  |
| c            | Critical point.  |
| ch           | Chemical.  |
| D            | Destruction.   |
| F            | Fuel, Consumed.  |
| GAS          | Gas injection/injection subsystem.   |
| gen          | Generated.   |
| H            | Hydrogen element.  |
| $i, j, k, m$ | Item $i / j / k / m$ .   |
| in           | Inlet.   |

|      |                               |
|------|-------------------------------|
| L    | Losses.                       |
| mix  | Mixture.                      |
| N    | Nitrogen element.             |
| n    | Normalized.                   |
| O    | Oxygen element.               |
| oil  | Oil / Oil fraction.           |
| out  | Outlet.                       |
| P    | Products.                     |
| phys | Physical.                     |
| PS   | Product streams.              |
| r    | Reduced property.             |
| S    | Sulfur element.               |
| SEA  | Seawater injection subsystem. |

### **Superscripts**

|          |  |
|----------|--|
| <i>o</i> | Property evaluated at dead state conditions. |
| m        | Mixture.                                     |
| v        | Vapor phase.                                 |

### **Others**

|                    |   |
|--------------------|---|
| $\Delta_{mix}b$    | Specific mixing exergy, kJ/kg.            |
| $\Delta_f G^\circ$ | Standard free energy of formation, kJ/kg. |
| $\Delta_r G^\circ$ | Gibbs free energy of reaction, kJ/kg.     |



## CONTENTS

|   |    |
|---|----|
| <b>1 INTRODUCTION</b> .....                                     | 1  |
| 1.1 OBJECTIVES .....  | 4  |
| <b>2 BIBLIOGRAPHIC REVIEW</b> .....                             | 7  |
| 2.1 BACKGROUND .....  | 7  |
| 2.2 OIL AND GAS PRODUCTION PLANTS .....                         | 11 |
| <b>2.2.1 Operation and types</b> .....                          | 11 |
| <b>2.2.2 Process description</b> .....                          | 12 |
| <b>2.2.3 Oil Characterization</b> .....                         | 18 |
| 2.3 ORGANIC RANKINE CYCLE (ORC) .....                           | 21 |
| <b>2.3.1 Fundamentals</b> .....                                 | 22 |
| <b>2.3.2 Working fluid selection</b> .....                      | 24 |
| 2.3.2.1 Types of working fluids .....                           | 24 |
| 2.3.2.2 Enthalpy of vaporization .....                          | 25 |
| 2.3.2.3 Density .....   | 27 |
| 2.3.2.4 Critical temperature .....                              | 27 |
| 2.3.2.5 Chemical stability and corrosiveness of the fluid ..... | 28 |
| 2.3.2.6 Environmental aspects .....                             | 29 |
| 2.3.2.7 Safety .....  | 29 |
| 2.4 EXERGY ANALYSIS OF OIL AND GAS PLATFORMS ...                | 29 |
| 2.5 INTEGRATION OF ORC IN OIL AND GAS PLATFORMS                 | 30 |
| <b>3 METHODOLOGY</b> .....                                      | 33 |
| 3.1 OIL CHARACTERIZATION .....                                  | 35 |
| <b>3.1.1 Physical Properties</b> .....                          | 35 |
| 3.1.1.1 Hysys cases .....                                       | 36 |
| 3.1.1.2 EES cases .....   | 38 |
| <b>3.1.2 Chemical exergy</b> .....                              | 38 |
| 3.2 PLANT MODELING .....  | 42 |
| <b>3.2.1 Plant description</b> .....                            | 42 |
| 3.2.1.1 Separation plant .....                                  | 42 |
| 3.2.1.2 Boost system .....                                      | 43 |
| 3.2.1.3 Gas injection/export system .....                       | 44 |
| 3.2.1.4 Power generation system .....                           | 45 |
| 3.2.1.5 Seawater injection system .....                         | 46 |
| <b>3.2.2 Input data</b> .....                                   | 48 |
| 3.2.2.1 Fluids data .....                                       | 50 |
| <b>3.2.3 EES case</b> .....                                     | 51 |
| <b>3.2.4 Production parameters profiles</b> .....               | 51 |

|   |     |
|---|-----|
| <b>3.3 EXERGY ANALYSIS</b> .....  | 51  |
| <b>3.3.1 Exergy calculation</b> .....                                       | 51  |
| <b>3.3.2 Plant exergy balances</b> .....                                    | 53  |
| <b>3.3.3 Exergy and energy efficiency indicators</b> .....                  | 54  |
| 3.3.3.1 Overall indicators .....  | 54  |
| 3.3.3.2 Subsystems indicators .....   | 56  |
| <b>3.4 ORC MODELING</b> .....   | 56  |
| <b>3.4.1 fluid selection</b> .....  | 56  |
| <b>3.4.2 Configuration</b> .....  | 58  |
| <b>3.4.3 Integration with plant model and parameters of operation</b> ..... | 58  |
| <b>4 RESULTS</b> .....  | 63  |
| 4.1 OIL CHARACTERIZATION .....  | 63  |
| 4.2 MODEL DEVELOPMENT .....   | 63  |
| 4.3 EXERGY ANALYSIS .....   | 67  |
| 4.3.1 Exergy balance .....  | 67  |
| 4.3.2 Exergy performance .....  | 72  |
| 4.4 ORC COUPLED TO THE PLANT .....  | 75  |
| 4.5 PRODUCTION PARAMETER PROFILES .....                                     | 80  |
| 4.5.1 ORC working $T_{ev}$ establishment .....                              | 80  |
| 4.5.2 Influence of production parameters over the plant performance .....   | 82  |
| 4.5.3 Influence of the production parameters over ORC performance .....     | 89  |
| <b>5 DISCUSSION</b> .....   | 91  |
| <b>6 CONCLUSION</b> .....   | 95  |
| <b>REFERENCES</b> .....   | 97  |
| <b>APPENDIX A - Hysys model nomenclature</b> .....                          | 105 |
| <b>APPENDIX B - Hysys code</b> .....  | 113 |
| <b>APPENDIX C - EES case development</b> .....                              | 129 |
| <b>APPENDIX D - Exergy balances per equipment</b> .....                     | 143 |
| <b>APPENDIX E - Oil characterization results</b> .....                      | 155 |

## 1 INTRODUCTION

Recently, the enhancement of the energy efficiency in the oil industry has attracted much attention, mainly due to the different challenges coming from three current circumstances: (i) the growing oil and gas demand, (ii) the necessity of reducing CO<sub>2</sub> and other greenhouse gas emissions and (iii) the increasing production costs. According to a recent forecast done by the International Energy Agency (IEA), considering the existing policy commitments and assuming the implementation of those recently announced, by 2035 the world oil demand will increase around 15% and a remarkable rise of 50% is projected for gas demand (IEA, 2012). On the other hand, a gradual enforcement of the existing legislation and the establishment of new commitments related to the pollution control are expected in order to avoid a dangerous climate change, limiting consequently the CO<sub>2</sub> emissions generated by the industry (IEA, 2008; LUDENA; MIGUEL; SCHUSCHNY, 2012). These factors are aggravated by the rapid depletion of the known reserves of oil and gas (SIMMONS, 2009; IEA, 2012) and the increasing costs associated with the development of the new oil and gas fields (SHIMAMURA, 2002; BULLER, 2009).

The offshore production has been an important part of the development of the oil and gas industry during the past two decades, about 33% of world oil production by 2007 was obtained from offshore platforms (KOCAMAN, 2008) and its contribution is projected to be relatively stable until 2035. Considering that over 45% of currently known oil resources are located under the sea and about a quarter of these resources corresponds to deepwater (water with a depth of 400 meters or above), a production growth of 81% is estimated for this type of fields (IEA, 2012). It should be noted that this notable figure is predicted even considering the technical difficulties and high costs inherent to the exploitation of oil and gas at remote locations.

Diverse types of offshore installations have been spread around the world, of which the floating platforms are the most suitable for deepwater production (BARTON, 2009; KINNEY, 2012). Among them, the Floating Production, Storage and Offloading (FPSO) units present technical advantages especially in the development of short-lived and marginal fields in remote locations where fixed platforms were impractical and uneconomical (SHIMAMURA, 2002; GORDON, 2012). Nowadays, Petrobras has the second largest number of FPSO units (about 10 owned and 30 operated), representing about 15% of all the existing

worldwide (MAHONEY; KITHAS, 2013; CRAGER, 2010).

The main purpose of the production plant on an FPSO is to separate the well fluid into oil, gas and water meeting the specifications for their export or further treatment. The most common operations carried out for the separation of these streams includes (ARNOLD; STEWART, 2008): (i) well fluid gathering and well pressure reduction, (ii) gravity separation, (iii) oil treatment and storage, (iv) gas compression and dehydration and (v) water treatment and pumping. Depending on the specific characteristics of the well fluid and field development, the FPSO may contain operations like (BOTHAMLEY, 2004): (i) gas lift/injection, (ii) gas liquefaction and storage, (iii) gas export via pipelines, (iv) gas flaring or (v) seawater treatment and injection.

These installations include the production of the energy required by their own processes, using a part of the oil (or gas) produced in the plant as fuel for the generation of power, cold and heat. Improving the use of this energy through the plant will reduce the fuel consumption, which has important benefits like the abatement of pollutant emissions and the reduction of operating costs. In that direction, the IEA (2008) has shown the combined heat and power (CHP) as a good alternative to increase the energy efficiency in various industrial sectors in the short term. By other side, the Department of Energy of United States (DOE) (BCS, 2008) has presented the main opportunities, challenges and barriers to the research, development and demonstration (RD&D) for the development of technology related with waste heat recovery (WHR) in some industries.

Numerous investigations have been focused on the utilization of the waste heat to activate thermodynamic cycles supplying power, cold or upgraded heat (LITTLE; GARIMELLA, 2011; DENG; WANG; HAN, 2011). Among these systems, the organic Rankine cycle (ORC) is a recognized technology for power generation that already has been used to improve the efficiency in many industrial operations (TCHANCHE et al., 2011). Particularly, the integration of ORC in offshore processing platforms has been the focus of a handful of recent studies (LARSEN et al., 2013; PIEROBON et al., 2013; PIEROBON; NGUYEN, 2012a). However, these studies have not considered the inherent variation in the platform process conditions along its lifespan. Consequently, more work is needed in order to determine the actual advantages of the ORC integration under variable production circumstances within the platform.

The application of exergy concept and the exergy balance is a well-known and accepted technique employed to delimit and quantify



the energy efficiency in chemical and physical operations, which determines the maximum useful work obtainable from a system interacting with its surroundings, as well its potential destroyed by irreversibility (SZARGUT; MORRIS; STEWARD, 1988). Despite its usefulness, this method has not yet been fully adopted in many industrial sectors – including the petrochemical segment, principally due to the absence of a strategy of implementation, the low priority given and the lack of information to work with such kind of analysis (GRIP et al., 2011).

Considering the usefulness of the exergy balance and the current situation of the offshore industry, this study formulates an exergy analysis of a Brazilian FPSO to characterize its energy performance, and then analyzes the effect of the incorporation of an ORC over its efficiency. The development of this work contemplates the following subjects: (i) production plant and ORC modeling, (ii) calculation of the exergy associated with petroleum and its fractions, (iii) use of adequate energy performance indicators, (iv) coupling of the ORC to the plant and (v) effect of the main production parameters over the energy efficiency of the plant. The document is organized in sections as described in the paragraphs below.

The first section corresponds to the bibliographic review, where the main concepts and theoretical basis are summarized. This section covers aspects as the oil and gas production, the ORC operation and its utilization in the waste heat recovery.

The methodology section describes the steps proposed in order to obtain the results expected in this work. The process model was developed considering the design conditions of the plant, in order to establish the magnitude of its operations as well as their mass and energy balances. Next, a rigorous exergy analysis was carried out in order to identify the operations and processes with the greatest irreversibility and the highest exergy losses. Based on these results, various performance indicators were proposed for the comparison of the energy efficiency of the plant when coupling the ORC. The configuration and the working fluid of this system were established based on previous studies focused on its optimization (BRANCHINI; PASCALE; PERETTO, 2013; PIEROBON et al., 2013). Finally, the behavior of the proposed indicators was analyzed along a production profile formed by 16 scenarios varying five production parameters independently. The parameters considered are: (i) produced oil flow, (ii) production water flow, (iii) well pressure, (iv) injected gas flow and (v) injected water flow.

The third section summarizes and discusses the obtained results in order to recognize the impact of the ORC over the energy perfor-

mance of the plant accounting the variation of its main production parameters.

Finally, in the conclusion section, the main findings of this work are presented. The main contribution of the present study consists in the proposal of a procedure aiming the effect of an energy enhancement technology (in this case the ORC) in an existing process, characterizing its behavior under variable production conditions. In this way, the results can give a wider panorama when applying this kind of systems where it could lead a great impact increasing the energy efficiency (*e.g.* offshore oil and gas processing).

## 1.1 OBJECTIVES

In accordance with the outlined scope, the main purpose of this study is to identify clearly the effect of an ORC over the energetic efficiency of an offshore platform along a variable production profile, such that the influence of each production parameter can be analyzed separately. The following aims are contemplated in order to achieve this purpose:

1. Develop the process model in order to determine the mass and energy balances of each operation within the process. The model must be adequate to analyze the behavior of the process conditions under variable inputs, within the design constraints of the plant.
2. Carry out an exergy analysis of the plant in order to quantify the exergy fluxes within the plant as well as the irreversibility in each operation and the potential exergy losses to be recovered by the ORC. This analysis includes the proper calculation of the exergy fluxes associated with hydrocarbon streams (*i.e.* petroleum and its fractions).
3. Choose appropriate exergy performance indicators, in order to make evident the effect of the chosen production parameters over the plant efficiency. These indicators must be related with the plant purpose and operation.
4. Develop the integrated model (the production plant with integrated ORC) and quantify the effect over the energy efficiency of the platform. This effect will be established by comparison of the indicators proposed in the item above.

5. Determine the behavior of the exergy efficiency indicators under variable operating conditions, such that the convenience of the ORC implementation under different production scenarios can be established.



## 2 BIBLIOGRAPHIC REVIEW

### 2.1 BACKGROUND

According to the data published by IEA (2012), the world oil and gas demand by 2035 will grow about 2.75 million of cubic meters per day and 1765 billion of cubic meters per year respectively, without considering future changes in current environmental policies (see Fig. 1). This fact seems to be positive for oil and gas market, but this would be true if the current sources of oil and natural gas were enough to meet these goals. The present situation indicates that the proved oil and gas reserves are being rapidly depleted and are not enough to supply projected demand. In order to illustrate that, Fig. 2 presents the production profiles of some fields located in Brazil (SIMMONS, 2009). It would be necessary to find new oil and gas resources, but from the information presented by Barton (2009) and Shimamura (2002), it can be inferred that it is becoming more difficult to find new reservoirs with an acceptable technical and economic feasibility. This signifies that costs associated with oil and gas production will tend to increase, which would imply a serious impact over the oil and gas market, and consequently over the world economy.

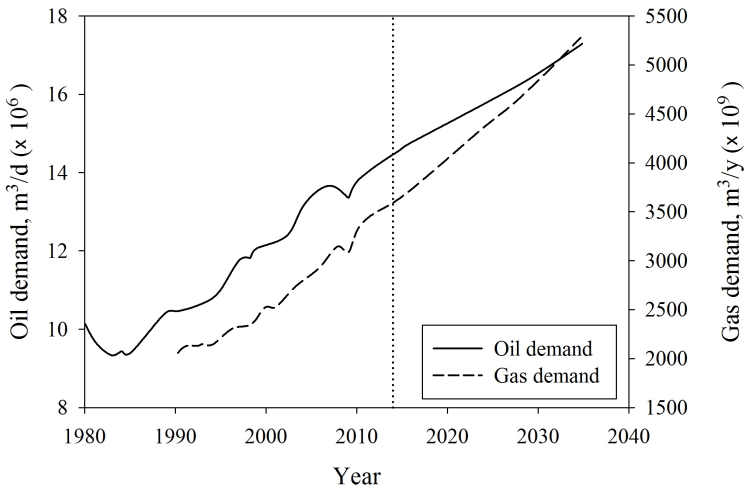


Figure 1 – World oil and gas demand (IEA, 2012).

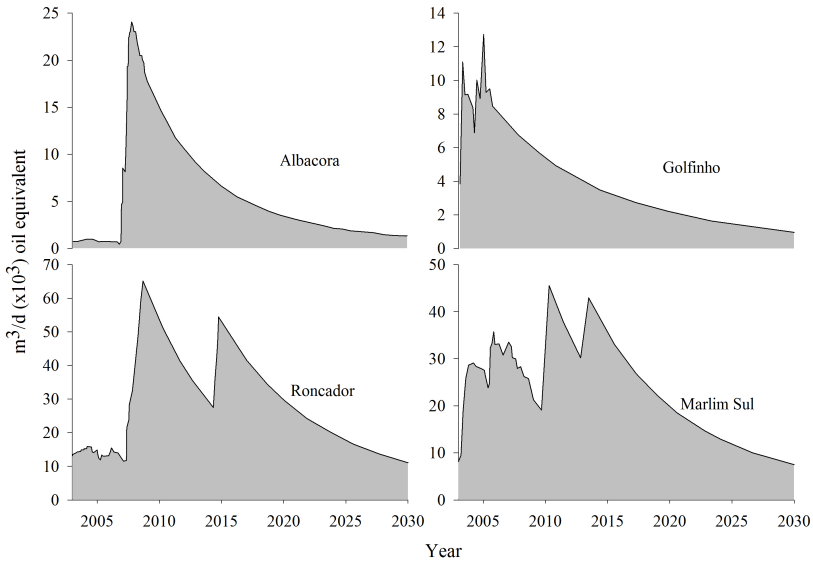


Figure 2 – Production profiles of some Brazilian fields (SIMMONS, 2009).

By the other hand, over the past three decades, the climate change has become the most influencing aspect relating to the humankind sustainability and has compelled governments and policy makers to create commitments about the reduction of CO<sub>2</sub> and other pollutant emissions (LUDENA; MIGUEL; SCHUSCHNY, 2012). These premises affect in a great extent the operation of the oil and gas plants, promoting the investment in cleaner and more efficient systems of production. Considering the goals established about economic and environmental aspects, the use of technologies in order to improve the energy efficiency of new as well as existing plants will be become a requisite more than a choice for this industry.

In that way, DOE through BCS (2008), indicates the WHR as a good alternative to affront this challenging scenario, considering that as much as 20% to 50% of the energy consumed by the industrial sector is ultimately lost via waste heat. According to this reference, the current profile of utilization of WHR is delineated mainly by the following characteristics: (i) WHR frequently implemented, but constrained by factors such as costs and temperature limits, (ii) most unrecovered heat is at low temperatures and (iii) there are sectors where WHR is not common due to factors such as chemical composition of heat carriers or

economic aspects required for recovery. Given that, Tab. 1 summarizes WHR opportunities and addressed barriers in order to guide RD&D works.

Table 1 – RD&D needs for addressing WHR Barriers (BCS, 2008)

| RD&D Opportunity   | Barriers Addressed   |                                |                   |                    |                  |                     |                        |                                     |                              |                 |
|--|----------------------|--------------------------------|-------------------|--------------------|------------------|---------------------|------------------------|-------------------------------------|------------------------------|-----------------|
|  | Long Payback Periods | Material Constraints and Costs | Maintenance Costs | Economies of Scale | Lack of End uses | Heat Transfer Rates | Environmental Concerns | Process Control and Product Quality | Process specific Constraints | Inaccessibility |
| Develop low cost, novel materials for resistance to corrosive contaminants and to high temperatures                                  |                      | X                              | X                 |                    |                  |                     |                        |                                     |                              |                 |
| Economically scaledown heat recovery equipment   | X                    | X                              |                   | X                  |                  |                     |                        |                                     |                              |                 |
| Develop economic heat recovery systems that can be easily cleaned after exposure to chemically active gases                          |                      |                                | X                 | X                  | X                |                     |                        |                                     |                              |                 |
| Develop novel manufacturing processes that avoid introducing contaminants into offgases in energy intensive manufacturing processes  |                      | X                              | X                 |                    |                  |                     | X                      | X                                   | X                            |                 |
| Develop low cost dry gas cleaning systems  |                      | X                              | X                 |                    |                  | X                   | X                      | X                                   |                              |                 |
| Develop and demonstrate low temperature heat recovery technologies, including heat pumps and low temperature electricity generation. |                      |                                |                   |                    | X                |                     |                        |                                     |                              |                 |
| Develop alternative end uses for waste heat  |                      |                                |                   |                    | X                |                     |                        |                                     |                              |                 |

Table 1 – RD&amp;D needs for addressing - WHR Barriers (BCS, 2008)

| RD&D Opportunity   | Barriers Addressed   |                                |                   |                    |                  |                     |                        |                                     |                              |                 |
|--|----------------------|--------------------------------|-------------------|--------------------|------------------|---------------------|------------------------|-------------------------------------|------------------------------|-----------------|
|  | Long Payback Periods | Material Constraints and Costs | Maintenance Costs | Economies of Scale | Lack of End uses | Heat Transfer Rates | Environmental Concerns | Process Control and Product Quality | Process specific Constraints | Inaccessibility |
| Develop novel heat exchanger designs with increased heat transfer coefficients                                 | X                    | X                              |                   |                    |                  |                     | X                      |                                     |                              |                 |
| Develop process specific heat recovery technologies  |                      |                                |                   | X                  |                  | X                   | X                      | X                                   | X                            | X               |
| Reduce the technical challenges and costs of process specific feed preheating systems                          | X                    |                                |                   | X                  |                  | X                   |                        | X                                   | X                            |                 |
| Evaluate and develop opportunities for recovery from unconventional waste heat sources (e.g., sidewall losses) |                      |                                |                   |                    |                  |                     |                        |                                     | X                            | X               |
| Promote new heat recovery technologies such as solid state generation.   |                      |                                |                   |                    | X                |                     |                        |                                     |                              | X               |
| Promote low cost manufacturing techniques for the technologies described above                                 | X                    | X                              | X                 | X                  | X                | X                   | X                      | X                                   | X                            | X               |

Within this context, the contribution of the present work is focused on the demonstration of a heat recovery technology for electricity generation, addressing its specific use in offshore platforms. Among the different options that are being outlined in academic publications, the development of the ORC technology for WHR in oil and gas production plants represents an interesting short-term solution for their energy efficiency improvement. Thus, next sections introduce some key concepts concerning the operation of oil and gas production plants, its energy efficiency, the ORC systems and their process modeling.



## 2.2 OIL AND GAS PRODUCTION PLANTS

### 2.2.1 Operation and types

It is well known that the crude oil and natural gas are the main feedstock of innumerable industries and they are extracted from sedimentary basins, where they have been formed and trapped for over tens of millions of years (WILKINSON, 2006). The only way to extract them is by drilling, that implies a withdrawal of diverse materials as water, sands and salts together with the well fluid. These impurities need to be removed from crude (or gas) before being processed at refineries or used as fuels. This configures the main purpose of the production plant, that consist in separating the well fluid into oil, gas and water meeting the specifications for their export or further treatment or disposal.

The physical and chemical characteristics of crude and gas can vary widely from field to field, influencing the process scheme and conditions of the production plant. A typical scheme of operation is shown in Fig. 3, nevertheless some stages can be added or omitted depending on the crude and gas characterization (see section 2.2.3).

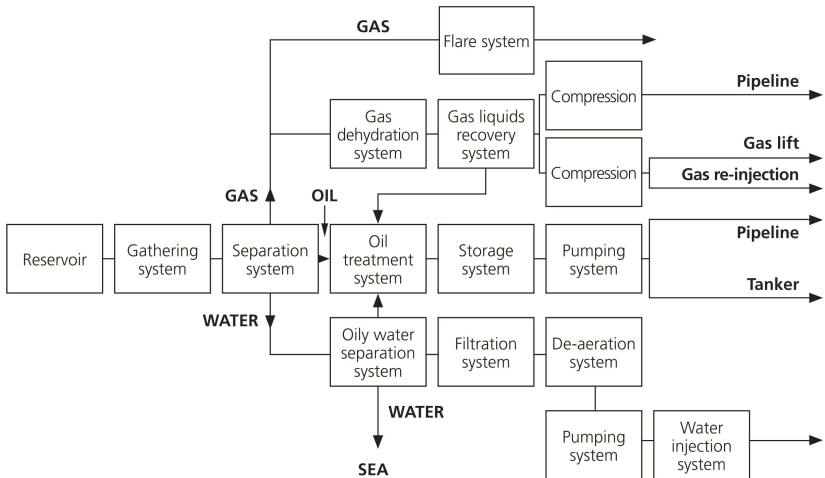


Figure 3 – Typical operation scheme of an oil and gas production plant (WILKINSON, 2006).

It is difficult to classify production plants, because they differ due

to production rates, fluid properties, sale and disposal requirements, location, and operation mode (ARNOLD; STEWART, 2008). Considering only location, production facilities can be separated into two main groups: onshore and offshore installations. According to IEA (2012), the growth potential of the offshore installations (or platforms) is significantly greater, given the estimation of remaining recoverable conventional oil under the sea of about 1200 billion barrels (about 45% of total estimated). Particularly, deepwater production (offshore platforms operating in water depths in excess of 400 m) reports an expansion from 4.8 million of barrels per day in 2011 to about 8.7 million of barrels per day by 2035.

Different types of platforms have been developed, some of these being more adequate to the production at deepwater. Considering the type of anchoring employed, Fig. 4 presents the schemes of various types of platforms. Among these types, the FPSO units present several advantages as (SHIMAMURA, 2002):

- Adaptability for water depth.
- Early deployment.
- These units are self-contained.
- These units are movable and relocatable.
- Can be combined with other offshore facilities.
- Their use can expand oil trading.
- Has segregated storage.

As the industry tackles deeper and deeper water, FPSOs connected to subsea wellheads are replacing fixed platforms as the main development technique. Figure 5 shows a more detailed scheme of an FPSO unit (WILKINSON, 2006).

Currently, Brazil accounts 28 FPSO units of 147 existing worldwide (reported until August 2013) and its national oil company Petrobras has a notable participation in FPSO market, accounting 10 owned and operated units (MAHONEY; KITHAS, 2013).

### 2.2.2 Process description

The subsystems (blocks) presented in Fig. 3 can be briefly described as follows (ARNOLD; STEWART, 2008):

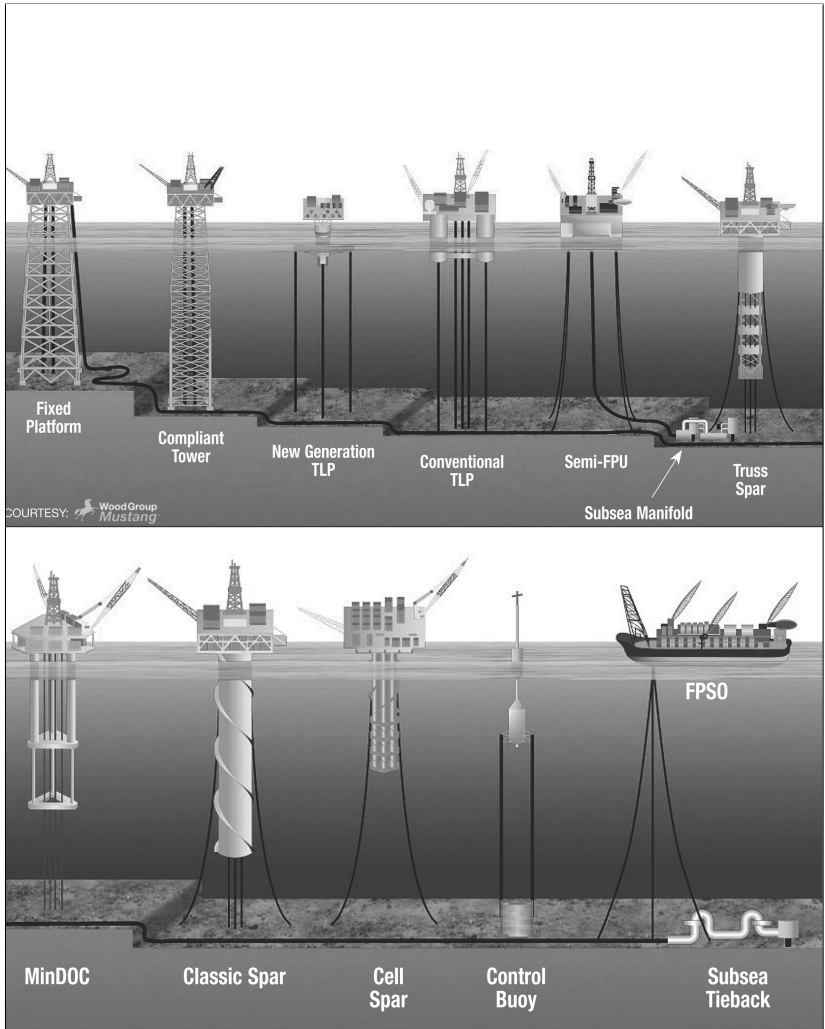


Figure 4 – Schemes of most common types of offshore platforms (MAHONEY, 2013).

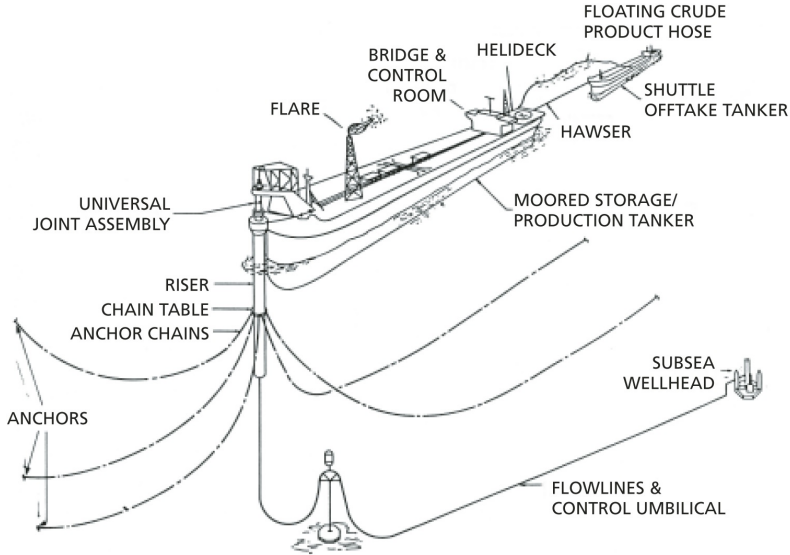


Figure 5 – Basic operation scheme of an FPSO (WILKINSON, 2006).

### 1. Gathering system

The production systems begins at the wellhead, which should include at least a valve called choke. Most of the pressure drop between the well flowing tubing pressure (FTP) and the initial separator operating pressure occurs across this valve. The choke opening determines the flow through the wellhead and permits a rough control over the depletion rate of well.

When two or more wells are commingled in a production plant, it is necessary to install a piping arrangement called manifold, in order to allow flow from any one well to be isolated and diverted towards the test production systems.

### 2. Separation system

The function of separators and other equipment in this system is to make a gross separation of gas, and water from oil. This separation takes place due to the difference of densities between the aqueous, oily and gas phases. Heating of the inlet stream promotes this separation, up to some degree depending on the composition and water content of oil. Generally, this operation

is accomplished in multiple pressure stages with the purpose of stabilizing the major quantity of light hydrocarbon molecules in the oil phase. In a given separator, a higher pressure favors liquid yield, but incorporates too light components into oil that will be lost in atmospheric storage. On the other hand, a lower pressure favors medium component losses through the gas outlet.

### 3. Oil Treatment system

The purpose of this system is to reduce the water content of oil down to the sales requisite (generally 1% BSW or less). Generally, it implies heating of oil stream and sometimes the application of electrostatic fields. The grade of heating and electrostatic treatment depends on the trend to form stable emulsions between the oil and water. This stage is commonly done at a pressure slightly higher than the atmosphere in order to promote its vapor stabilization.

### 4. Storage system

In the FPSO this system corresponds to the tanker (incorporated in the unit), where the oil is accumulated until it is dispatched to external tankers or to other installations via pipeline.

### 5. Gas dehydration system

This system removes the humidity from gas, in order to meet the sales or injection specification. The dehydration is accomplished generally by contact with a dehydrating agent as triethylene glycol (TEG) or methanol. Depending on the available gas pressure and its water content, an intermediate compression stage (boosting) can be needed before this operation.

### 6. Compression

This system must provide the required pressure to the gas stream in order to accomplish any of the following operations:

- *Gas export (pipeline)*: When possible, the major part of the separated gas is sold and exported onshore via pipelines. The capacity of compressors and therefore their power consumption depends on the gas flow and the pressure drop through the lines. It is common to find subsea gas lines up to 200 km long (WILKINSON, 2006).
- *Gas re-injection*: It consists in a way of achieving a supplementary oil recovery maintaining the reservoir pressure by

returning the natural gas back through strategically placed wells in the field. This technique bolsters the main drive as long as possible.

- *Gas lift*: It involves increasing the amount of gas produced with the oil by injecting gas directly into the flowing column in a well rather than into the reservoir. Gas lift is accomplished by using special valves set up at various depths and then controlling the amount of gas entering the flow stream. The increase in gas/oil ratio reduces the pressure needed to drive the oil to the surface (WILKINSON, 2006).

#### 7. Flare system

This system has two basic functions: (i) vents and/or burn safety the excess of gas of the plant when there is a surplus, and (ii) receives and directs the gas and vapors expelled from safety devices when an overpressure occurs. Normally, continuous gas venting or burning is avoided mainly due to environmental restrictions.

#### 8. Oily water separation system

This system takes the oil and solid traces away from the production water stream in order to meet the specifications to be disposed overboard. Normally, this is accomplished using settling, aeration and other related equipment.

#### 9. Filtration system

This system separates smaller particles than the former stage and is accomplished by means of membranes, activated coal and other filtering media. The purpose of the filtration system is to meet the water specifications requirements in order to be injected back to the reservoir. In addition, it is common to take and filter directly seawater and discard all the production water.

#### 10. Deaeration system

This system removes the dissolved gas from filtrated water in order to avoid the growth of aerobic bacteria that can favor a collapse of the reservoir.

#### 11. Pumping and water injection system

The treated water is injected back into the reservoir to maintain the reservoir pressure and thus take a secondary oil recovery. The power consumed by this system depends on the injection depth

and the required water flow. Generally, several pumping stages are necessary to achieve the required pressure rise.

There are other subsystems that are not included in Fig. 3, but also are necessary in the plant operation:

- Safety system

Includes alarms, automatic shutdowns, back-up units, flare stacks (as mentioned above) and firefighting equipment, plus strict administrative procedures and frequently practiced emergency containment and evacuation plans.

- Utility systems

Include power generation and facilities for normal services, all of which can be, and frequently are, powered by gas or oil being processed in the plant.

Commonly, the power generation system of an FPSO unit consists in a set of turbines (gas or diesel fueled) working at part-load for availability and reliability reasons.

The above-mentioned operations can vary according with the main purpose of the platform. According to the work of Bothamley (2004), which summarizes the primary options available for offshore processing, the majority of the offshore platforms falls into the following two categories:

- Stabilized, crude meeting sales specifications and dehydrated gas produced offshore.
- Unstabilized, wet crude and dehydrated gas produced offshore.

Additionally, there is a relatively small number of oil platforms offshore that employ additional gas processing, (e.g. Hydrocarbon dew point control, natural gas liquids recovery or liquefaction of natural gas) in order to produce both oil and gas products meeting sales specifications.

Figure 6 presents a typical layout of the process plant on board of an FPSO, showing the distribution of the main subsystems of the plant. On the other hand, a photograph of an FPSO topside is presented in Fig. 7 in order to illustrate the equipment arrangement within the plant.

In order to analyze the streams and processes that are performed within a plant, a simplified PFD (Process Flow Diagram) is presented

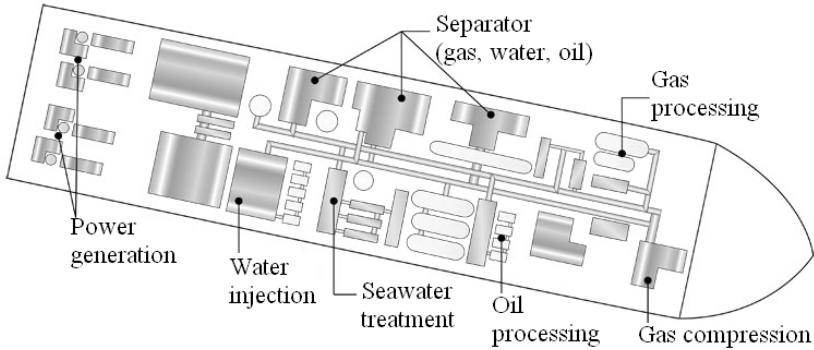


Figure 6 – Basic layout of an FPSO topside.

in Fig. 8. This scheme corresponds to an FPSO operating in the Santos basin (WASCO, 2012), which is analyzed in the present work. Appendix A presents the complete scheme of operation, which includes secondary material and energy streams, as well as the operations within each subsystem (shown as blocks in Fig. 8). The symbols and nomenclature used are also presented there. A detailed process description is presented in Sec. 3.2.1.

### 2.2.3 Oil Characterization

This subsection introduces the most common methods for characterizing crude oils and petroleum fractions, and for estimating their thermophysical properties. In order to simulate properly the oil-related processes, it is necessary to have a good understanding of the composition information and thermophysical properties of crude oils and petroleum fractions. However, the complexity of molecular composition of crude oils and petroleum fractions makes it hardly possible to identify individual molecules. Instead, there are standardized methods to characterize crude oils and petroleum fractions, which are commonly compiled in a technical summary known as crude assay.

A typical crude assay includes two types of information for an oil sample: (i) bulk properties and (ii) fractional properties. Bulk properties include specific gravity, sulfur content, nitrogen content, metal (Ni, V, Fe etc.) content, Watson (UOP) K factor, C/H ratio, pour point, flash point, freeze point, smoke point, aniline point, cloud point,





Figure 7 – Example of an FPSO topside.

viscosity, carbon residue, light hydrocarbon yields (C1-C4), acid number, refractive index, lower and higher heating values and boiling point curve. The most representative bulk properties are briefly described in following paragraphs. Chang, Pashikanti e Liu (2012) presents a detailed description of all above-mentioned properties.

*Specific gravity (SG)* : generally is measured using the API (American Petroleum Institute) gravity to specify the specific gravity of the crude oil as  $^{\circ}\text{API} = (141.5/\text{SG}) - 131.5$ . SG is the specific gravity defined as the ratio of the density of the crude oil to the density of water both measured at 15.6 °C (60 °F). The API gravity reports a value lower than 10°API for very heavy crudes, from 10 to 30°API for heavy crudes, from 30 to 40°API for medium crudes, and a value above 40°API for light crudes.

*Gross heat of combustion or higher heating value (HHV)*: is the amount of heat released by the complete combustion of a unit quantity of fuel. The gross heat of combustion is obtained by cooling down all products of the combustion to the temperature before the combustion, and by condensing all the water vapor formed during combustion.

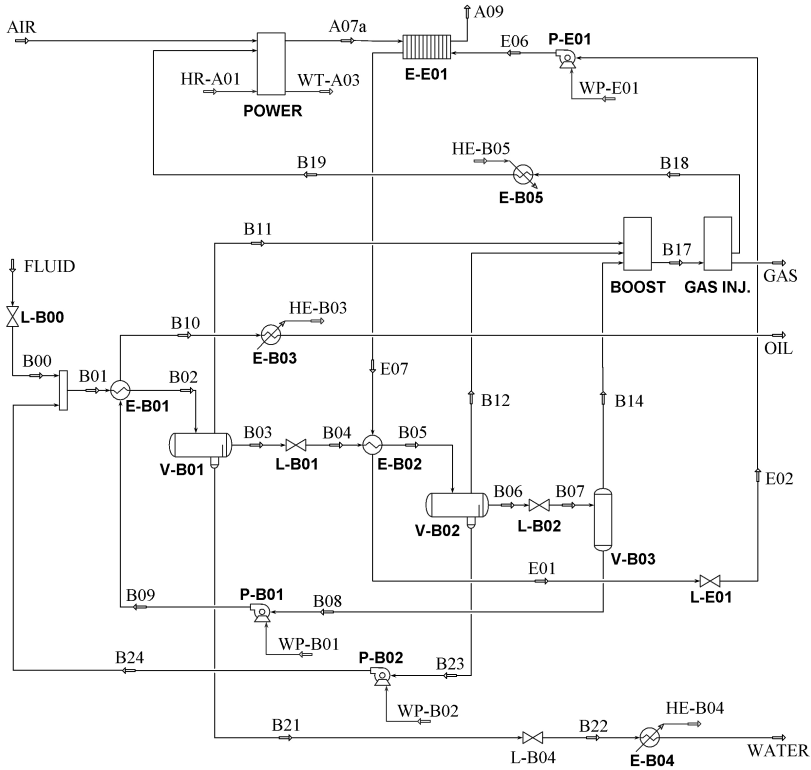


Figure 8 – Basic PFD of a typical FPSO process plant.

*Net heat of combustion or lower heating value (LHV)*: is obtained by subtracting the enthalpy of vaporization of the water vapor formed by the combustion from the higher heating value.

*True boiling point (TBP) distillation curve*: results from using the U. S. Bureau of Mines Hempel method and the ASTM D-285 test procedure. However, there is a trend toward applying the ASTM D2892 procedure, instead of the TBP. A key result from a distillation test is the boiling point curve, that is, the boiling point of the oil fraction versus the fraction of oil vaporized.

*Watson (UOP) K factor*: Is an approximate index of paraffinicity, with higher values corresponding to a high degree of saturation. It is related to the mean average boiling point by the following expression (WATSON; NELSON, 1933):

$$K = \frac{1.216 \sqrt[3]{T_{b,avg.}}}{SG} \quad (2.1)$$

where

$K$ : Watson UOPK factor.

$T_{b,avg.}$ : Mean Average Boiling Point, K.

$SG$ : Bulk specific gravity (15°C/15°C).

This factor must be between 8 (highly aromatic or naphthenic) and 15 (highly paraffinic)(ASPENTECH, 2011).

By the other hand, fractional properties of the oil sample reflect the property and composition for specific boiling-point range to properly refine it into different end products such as gasoline, diesel and raw materials for chemical process. Fractional properties usually contain paraffins, naphthenes and aromatics (PNA) contents, sulfur content, nitrogen content for each boiling-point range, octane number of gasoline, freezing point, cetane index and smoke point for kerosene and diesel fuels. These properties and methods to obtain them are detailed by Chang, Pashikanti e Liu (2012).

Two indicators affect directly the material balance of the plant: the bottom sediments and water (BSW) and the gas to oil ratio (GOR). BSW corresponds to the volumetric ratio of water extracted together with the well fluid (expressed as a percentage) and GOR is the ratio of volumetric flow of produced gas to the volumetric flow of crude oil for crude oil and gas mixture at standard conditions (measured at T=15°C and P=101.325 kPa). The importance of these parameters is associated with their variability over the period of development of a field.

## 2.3 ORGANIC RANKINE CYCLE (ORC)

According to Chen, Goswami e Stefanakos (2010), Bao e Zhao (2013) and Little e Garimella (2011), previous studies have analyzed various advanced thermodynamic cycles such as the ORC, supercritical Rankine cycle, Kaline cycle, Goswami cycle, Maloney-Robertson cycle and trilateral flash cycle for the conversion of heat into available power.

Particularly, the ORC appears with some key advantages when compared with Kalina cycle and trilateral flash cycle (BAO; ZHAO, 2013):

- ORC has simpler structure.
- ORC presents less expansion complexity.

- ORC has a high reliability.
- ORC has a simpler maintenance.

In addition, with the aim to improve the energy efficiency, the ORC can be easily combined with other thermodynamic cycles such as thermo-electric generator, fuel cell, internal combustion engine, microturbines, seawater desalinization system, Brayton cycle, and gas turbine-modular helium reactor. Furthermore, it also can be used as prime movers of combined cooling and power systems as the ORVC (Organic Rankine–Vapor Compression) cycle.

### 2.3.1 Fundamentals

The ORC, which has the same configuration as conventional steam Rankine cycle but uses organic substances with low boiling points as working fluids, can use various types of heat source. Tchanche et al. (2011) present a review of some ORC applications such as industrial waste heat, solar energy, geothermal energy, biomass energy, ocean energy, etc. Figure 9 shows the basic scheme of operation of the ORC.

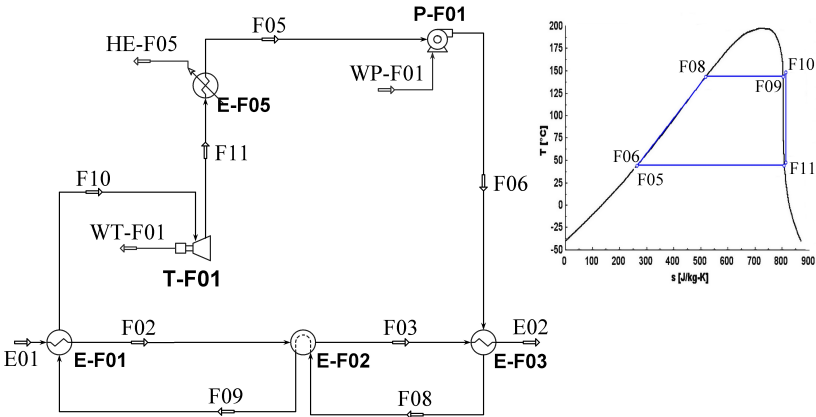


Figure 9 – Basic scheme of an ORC system

The ORC working fluid (state F05) is fed to the pump (P-F01) that increases its pressure (state F06) and leads the fluid to the economizer (E-F03) where it reach its saturation temperature (F08). Next, the fluid across the evaporator (E-F02), wherein the fluid phase change

occurs (state F09). Normally, the saturated vapor is then superheated across E-F01 and expanded in T-F01 (state F11), which produces the shaft work of the cycle (WT-F01). It should be noted that the heat consumed by the economizer, the evaporator and the superheater is supplied by the waste heat source (directly or indirectly). Finally, the vapor stream from expander outlet is condensed in E-F05, and returned back to the pump. Depending on the characteristics of the expansion of fluid (explained in sec. 2.3.2), it may be appropriated the use of a regenerator, which transfers heat from the expander outlet to the economizer inlet. Figure 10 shows the configuration and the cycle of a regenerative ORC.

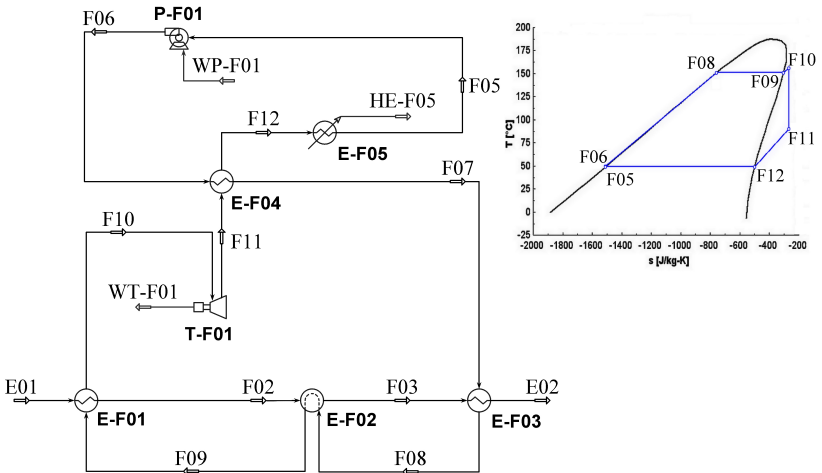


Figure 10 – Basic scheme of an regenerative ORC system

Compared with the conventional Rankine cycle, the ORC demonstrates several advantages such as (TCHANCHE et al., 2011):

- Commonly, it is necessary a lesser amount of heat during the evaporation process.
- The evaporation process takes place at lower pressure and temperature.
- Particularly for dry fluids, the expansion process ends in the vapor region and hence the superheating is not required and the risk of blade erosion is avoided.

- The smaller temperature difference between evaporation and condensation also means that the pressure drop ratio will be smaller, thus simple single stage turbines can be used.

### 2.3.2 Working fluid selection

One of the most important aspects in the development of ORCs is the working fluid selection. The quantity of generated power, the energy efficiency and economic viability of the ORC are strongly affected by the working fluid choose. A working fluid must not only have the necessary thermo-physical properties that match the application but also possess adequate chemical stability in the desired temperature range. There are numerous investigations carried out about the screening, comparison and selection of the best candidates. Particularly Bao e Zhao (2013), and Chen, Goswami e Stefanakos (2010) have reviewed extensively the research done in this area and their work is the main information source of following subsections.

#### 2.3.2.1 Types of working fluids

The working fluids can be categorized according to the vapor saturation curve. This characteristic affects the fluid applicability, cycle efficiency and arrangement of ORC equipment. There are three types of vapor saturation curves in the temperature-entropy (T-s) diagram: (i) dry fluids with a positive slope, (ii) wet fluids with a negative slope and (iii) isentropic fluids with nearly infinitely slopes. Figure 11 shows the T-s diagrams for these three types of fluids.

The manner how this characteristic influences the performance and the number of equipment within the ORC is related with the condensation in the expander outlet. A wet fluid condensates during the expansion process because the negative slope of its vapor saturation curve. This effect must be avoided since the presence of liquid inside expander may damage its blades and reduces its isentropic efficiency. Normally a superheating is required before the fluid enters to the expander, implying an increasing cost of the system and a reduction its efficiency.

On the other side, the main advantage of the dry and isentropic fluids consist in that they expand without phase change, thus superheating is not required. In spite of this, a slight superheating is rec-

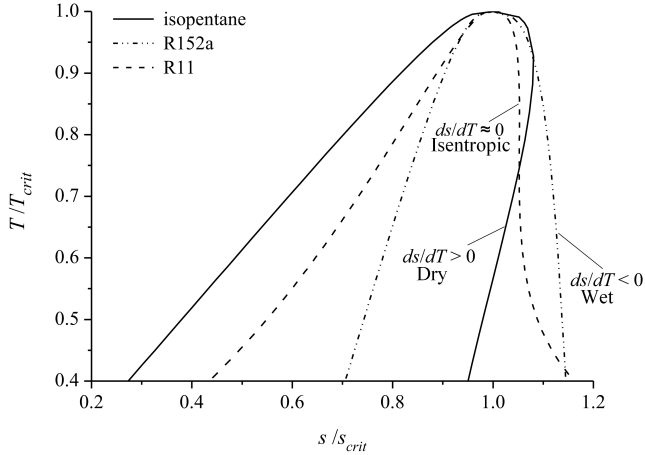


Figure 11 – Types of fluids (HEBERLE; PREIBINGER; BRÜGGEMANN, 2012).

ommended to guarantee only vapor at expander outlet. Moreover, in the case of dry fluid, generally a regenerator is used in order to reduce the condenser load and increase the efficiency of the cycle, which implies an increasing complexity and cost. This preliminarily indicates isentropic fluids as the most interesting candidates to be implemented in an ORC. However, a more detailed analysis (HUNG et al., 2010) has indicated that wet fluids with very steep saturated vapor curves have better overall performance in energy conversion efficiencies than dry fluids and isentropic fluids. In spite of that, they are not always suitable for ORC systems when other thermophysical properties are taken into consideration.

A practical indicator used to visualize how "dry" or "wet" a working fluid is, consists in the inverse of the vapor saturation curve slope ( $\partial T/\partial s$ ). Defining  $\xi = \partial s/\partial T$ , the type of fluid can be classified by its value, *i.e.*  $\xi < 0$  corresponds to a wet fluid,  $\xi = 0$  corresponds to an isentropic fluid and  $\xi > 0$  to a dry fluid.

### 2.3.2.2 Enthalpy of vaporization

High enthalpy of vaporization enables most of the available heat to be added to the ORC and produces a larger quantity of work per

unit of circulating fluid with the evaporation temperature and other parameters defined (CHEN; GOSWAMI; STEFANAKOS, 2010). However, when the heat source is the waste heat, organic fluids with lower specific vaporization heat are preferred. As explained by Bao e Zhao (2013), a lower specific heat of vaporization allows the temperature profile across the economizer-evaporator-separator to be closer to the waste heat profile, which means less irreversibility through the process, thus better performance of the ORC. This is shown in Fig. 12, where the pinch point difference (PPD) is indicated.

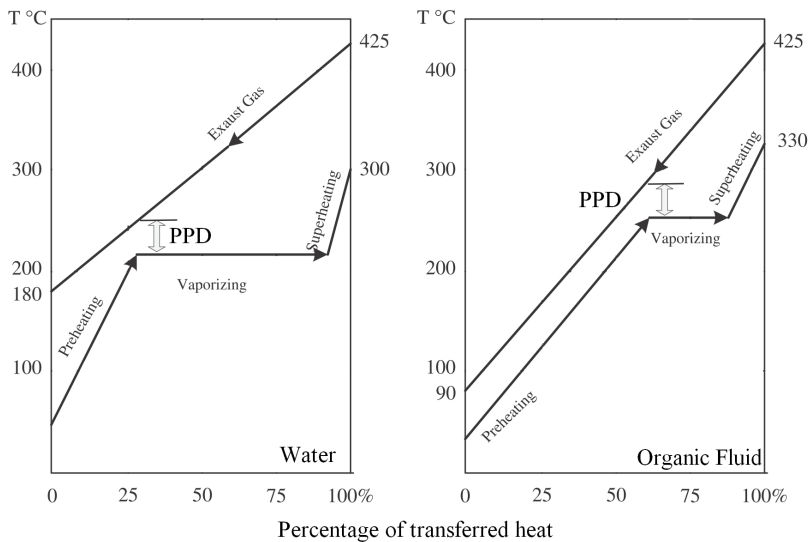


Figure 12 – Effect of the enthalpy of vaporization of the working fluid (BAO; ZHAO, 2013).

Declay (2009) mentions that the purpose of an ORC for waste heat recovery is not always meet the best energy efficiency, but produce the greater amount of power and presents the case illustrated in Fig. 13. This system recovers heat coming from a hot water source at 105 °C using a ketone as working fluid. The operation conditions in the second case (right side) demonstrated the worst efficiency (more irreversibility) but generated more than three times the power reported by the first case (left side).



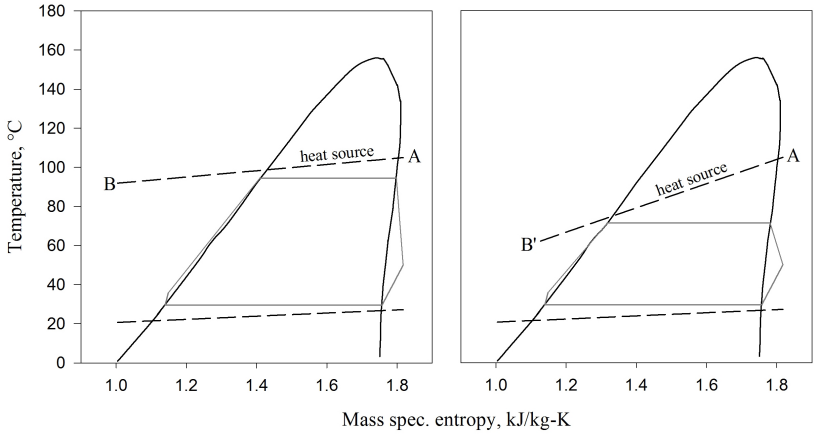


Figure 13 – Difference between cycle efficiency and power output (DECLAYE, 2009).

### 2.3.2.3 Density

This parameter has a great impact over the sizing, and thus over the initial investment of the ORC equipment. Considering that a low density leads to a higher volume flow rate, the pressure drop in the heat exchangers is increased (thus the power consumed by the pump) and the size of the expander must be increased.

### 2.3.2.4 Critical temperature

Previous study (BRUNO et al., 2008) has demonstrated that employing a fluid with higher critical temperature results in higher efficiency but lower condensing pressure, when the optimum high and low pressure were determined in order to meet the maximum first law efficiency of the saturated cycle. However, a high critical temperature also involves working at specific vapor densities much lower than the critical density. This reduced density shows a great impact on the design of the cycles, since the components need to be oversized (QUOILIN et al., 2012).

In a general way, the critical point of a working fluid suggest the proper operating temperature range for the working fluid in liquid and

vapor forms. Figure 14 presents a relation between the critical temperature and the parameter  $\xi$  for various working fluids studied previously, according to the review done by Chen, Goswami e Stefanakos (2010).

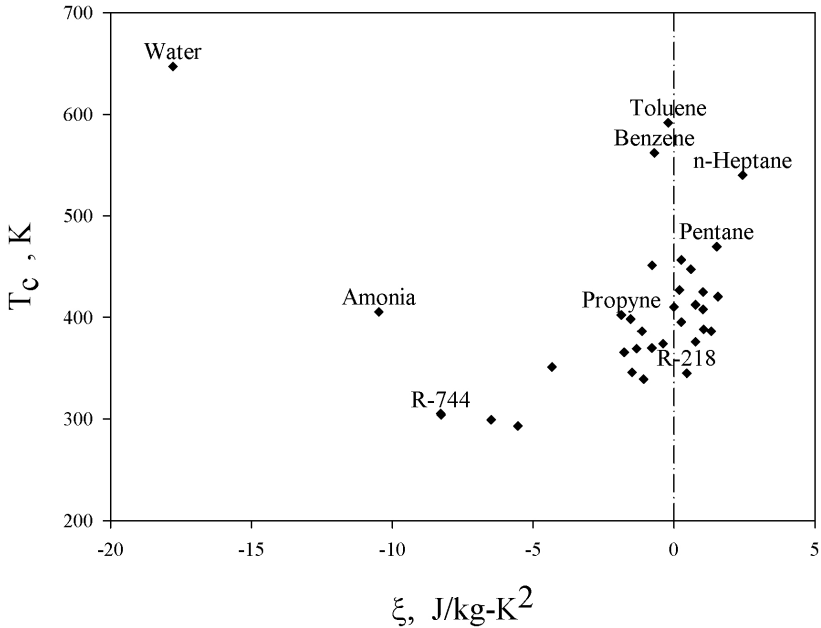


Figure 14 – Relation between the critical temperature and the parameter  $\xi$  for various candidates (CHEN; GOSWAMI; STEFANAKOS, 2010).

### 2.3.2.5 Chemical stability and corrosiveness of the fluid

Organic fluids usually suffer chemical deterioration at high temperatures. Thus, commonly the maximum operating temperature is limited by the chemical stability of the working fluid. In addition, as mentioned by BCS (2008), the corrosion and scaling inside of the equipment associated with waste heat recovery is an important barrier to the implementation of these systems. Hence, the working fluid should be as chemically stable and non-corrosive as possible.

In many cases, the stability characteristics of the working fluid have promoted the use of intermediate fluid in order to transfer heat

from higher temperature sources at a lower temperature level.

### 2.3.2.6 Environmental aspects

The main environmental parameters are: (i) the ozone depletion potential (ODP) and (ii) global warming potential (GWP), which represent substances potential to contribute to ozone degradation and global warming. Due to environmental concerns, some working fluids have been phased out, such as R-11, R-114 and R-115, while some others are being phased out in 2020 or 2030 (CHEN; GOSWAMI; STEFANAKOS, 2010). This criterion can be used in order to screen preliminarily the working fluids candidates and discard those that must be avoided by international protocols.

### 2.3.2.7 Safety

This parameter is related to the level of danger when dealing with the working fluid. Generally, characteristics as non-corrosive, non-flammable and non-toxic are expected, but are not practically found for a specific candidate. Particularly for longer alkanes, autoignition is a problem at temperatures above 200°C.

Another important thermodynamic property is the freezing point of the fluid, which must be below the lowest operating temperature in the cycle. The fluid must also work in an acceptable pressure range. Very high pressure or high vacuum has a tendency to impact the reliability of the cycle or increase the cost (CHEN; GOSWAMI; STEFANAKOS, 2010).

## 2.4 EXERGY ANALYSIS OF OIL AND GAS PLATFORMS

Relatively few works have been focused on analyzing the exergy performance of the oil and gas production installations. Oliveira e Hombeeck (1997) studied a Brazilian platform, whose process includes the crude heating using a WHR system in combination with a furnace in order to improve the separation of phases. Also the gas compression system and the oil pumping system were included. Their analysis indicated the compression and the separation as the most exergy-consuming processes within the plant. In the same way, the worst exergy efficiency was reported for the separation operation (22%) due to the high tem-

perature difference between the crude and exhaust gases. This work was conducted using Hysim (predecessor of Hysys) and an overall exergy efficiency of 9.7% was obtained.

By other side, Silva (2008) developed an exergy analysis of two Brazilian production installations, one located onshore and another located offshore. The methodology proposed in this dissertation adopts the entire plants as the combination of three independent systems: (i) the separation module, (ii) the gas compression module and (iii) the power generation module. The reported efficiencies for the base case were 24.9% using the thermodynamic degree of perfection ( $\eta_P$ —see Sec. 3.3.3) and 7.9%, reported as the actual exergy efficiency. The software used in this dissertation was EES.

Voldsund et al. (2010) simulated a specific North Sea offshore platform by using Hysys. The platform analyzed included separation, recompression (boost), gas injection and oil pumping systems. Results indicated the gas boost and injection as the systems with largest exergy destruction. In this case, an overall exergy efficiency of 32% was reported and the main exergy losses were associated with the gas recycling in compressors.

More recently, Nguyen et al. (2013) simulated a platform including auxiliary systems as the gas dehydration unit, production manifold and production water treatment. Results were obtained combining three different programs: (i) Aspen plus for the processing plant, (ii) DNA for modeling the gas turbines and (iii) Hysys for modeling the dehydration unit. The authors separated the analysis of the processing plant from that carried out for power generation system, and pointed out the gas injection as the process with highest exergy destruction when the combustor chambers of the power generation system are not considered. Analogously, the largest exergy losses were found in the exhaust gases outlet.

## 2.5 INTEGRATION OF ORC IN OIL AND GAS PLATFORMS

Currently, publications concerning the use of ORC systems in the WHR within offshore facilities are limited. Pierobon e Nguyen (2012b) modeled an ORC system for the WHR from the exhaust gases coming from a SGT-500 turbine used in a platform located at North Sea. Their methodology was focused on the working fluid selection of the cycle, in order to obtain a higher power output. The results indicated cyclohexane as the best candidate among four chosen candidates,

which reported a thermal efficiency enhancement of 12.9% considering the combined cycle. Posteriorly Pierobon et al. (2013) conducted an optimization analysis aiming the reduction of the size of the components that make up the same ORC system meeting the maximum thermal efficiency. The results pointed out the acetone and the cyclopentane as two optimal working fluids, the later reporting a greater thermal efficiency.



### 3 METHODOLOGY

In order to investigate the behavior of the operation conditions of the plant, a process simulation is carried out to determine the mass and energy balances of each subsystem involved. This simulation was developed considering the design parameters supplied in its engineering documentation (WASCO, 2012), whose values correspond to the occupation of 100% of the capacity of the plant. Missing information were properly set according to specific literature (MAXWELL, 1968; ARNOLD; STEWART, 2008). The model was developed using two well-known engineering software with two different levels of detailing and different criteria applied; the chosen alternatives were Hysys and Engineering Equation Solver (EES). Specifically, Hysys (or its former version Hysim) has been used in previous works to develop exergy analysis of oil production plants, (*e.g.* Nguyen et al. (2012), Pierobon e Nguyen (2012b), Oliveira e Hombeek (1997)), mainly due to its algorithms for modeling crude oil and its fractions from standardized data. On the other hand, numerous academic studies focused on ORC have been developed different analysis using EES (*e.g.* Li, Wang e Du (2012), Little e Garimella (2011)), because of its capability to work with the thermodynamic properties of common substances as continuous functions, as well as other multi-purpose characteristics. The data calculated using both programs are presented with the purpose of enabling the identification of the differences between the obtained results and to provide a contribution for future works that contemplate the use of Hysys or EES for this type of simulation.

Based on the energy balance of the plant, the heat losses as well the power demand in all operations in the plant were quantified. The possible sources to activate the ORC and its potential of use were identified in accordance with these results. In addition, appropriate exergy balances were developed with the intention of determining the actual potential of utilization of these sources (specifically, the exergy of the waste heat corresponds to the maximum amount theoretically attainable by the ORC) and to identify the operations where an improvement would have a greater impact on the energy efficiency of the plant.

Special attention was taken in the calculation of the exergy using Hysys, mainly due to the coherence required between the method used by this program for modeling the physical properties of crude fractions and the method of estimation of its chemical properties (including its chemical exergy). Considering the basic information commonly used

to characterize a crude oil, a hybrid strategy was adopted integrating previous studies and establishing some assumptions based on available literature. This strategy was developed in the following steps: (i) estimation of the molecular weight distribution and physical properties of crude in accordance with the method proposed by Whitson (1983) and Twu (1984), (ii) estimation of the higher heating value (gross calorific value) of each fraction according Maxwell (1968) data, (iii) estimation of the elemental composition of each fraction using the Boie equation *apud*. Ringen, Lanum e Miknis (1979) and (iv) estimation of the chemical exergy considering each fraction as a liquid technical fuel according the method described by Szargut, Morris e Steward (1988) and Rivero, Rendon e Monroy (1999).

The same operating conditions were used in the EES model, but adopting a simpler strategy to model the crude fractions: physical and chemical properties of whole crude oil were determined using Maxwell (1968) data; then its chemical exergy was approximated to its LHV as mentioned by Rivero, Rendon e Monroy (1999). The main drawback of this methodology is that the mass transfer between the liquid and vapor phases is not quantified due to the omission of the composition and the equilibrium of phases. Another remarkable difference between the models, is that in the case of Hysys, where the crude is modeled as a mixture of several hydrocarbon fractions, the calculation of the total exergy of material streams includes the mixing exergy term –as proposed by Hinderink et al. (1996), in order to incorporate the exergy destruction associated with the entropy generated by mixing. This term was not necessary in the EES model, since the compositions of the material streams remains constant through the plant.

Once the exergy analysis of the plant was completed, the losses and destruction of exergy in each operation were established, so that the energy efficiency of the process scheme can be compared adequately with that incorporating the ORC. In that way, this work proposes the use of three indicators: two related to exergy efficiency and another associated with the energy consumption per volumetric unit of produced oil.

Considering the great variability of the production parameters in this kind of installations, a comparison of the results using the ORC was made along a production profile. This profile is formed by 16 scenarios, and comprises the variation of five parameters independently: (i) oil flow, (ii) production water flow, (iii) well pressure, (iv) injected gas flow and (v) injected water flow.

The incorporation of the ORC system was proposed recovering



waste heat from the exhaust gases coming from the gas turbines and the power generated by this system was discounted from their total load. With the purpose of taking advantage of the current configuration of the plant, the ORC was modeled coupled to the HTF (Heat Transfer Fluid) circulation system (described below). By the other side, cyclopentane was selected as the ORC working fluid based on the results of a recent study focused on the optimization of this cycle (PIEROBON et al., 2013). The operation scheme of the ORC was established based on its vapor saturation curve, as explained in sec. 2.3.2.1.

This methodology contemplates the combination of various procedures in order to obtain a reliable panorama of the energy performance of an oil and gas production platform and its improvement using an innovative technology as the ORC. These procedures were adapted considering a small availability of information about the characterization of the well fluids, a fact that is common in this industry.

## 3.1 OIL CHARACTERIZATION

### 3.1.1 Physical Properties

In order to obtain a reliable simulation of the production plant, an important key is the proper calculation of the thermophysical properties of the crude oil and petroleum fractions. The algorithms of calculation included in Hysys permit to estimate these properties directly from the standard data obtained from laboratory and its method is broadly accepted in the oil industry. On the other hand, Maxwell (1968) is a great compendium of thermophysical and chemical properties based on experimental data of various petroleum fractions with different characteristics, and it can be used as a good reference to easily characterize a crude (or fraction) from basic information. On account of that, this reference was used for the estimation of the thermophysical and chemical properties in the simulation case developed in EES. The comparison of values obtained from these two methods will permit to validate the order of magnitude of the results and to distinguish how the grade of detail used in crude characterization affects its calculated parameters.

### 3.1.1.1 Hysys cases

The algorithm used by Hysys to characterize the crude and its fractions can be outlined as follows (ASPENTECH, 2011):

1. An adjusted TBP curve is generated from two of the following bulk properties of crude (user supplied): (i) standard specific gravity, (ii) Watson UOPK characterization factor and (iii) molecular weight. Hysys uses the methodology proposed by Whitson (1983), where the molar distribution of crude (mole fraction/molecular weight relation) is adjusted as a three-parameter gamma probability function. These parameters are dependent on the molecular weight of crude, which can be calculated from its UOPK factor and its standard specific gravity.
2. From this curve, several pseudocomponents are generated according the following procedure, as explained by Chang, Pashikanti e Liu (2012):
  - The curve is cut into an arbitrary number of intervals in order to define the number of pseudocomponents. The recommended number of intervals can vary from 8 to 30 depending on the boiling point range of the curve.
  - The normal boiling point (NBP) is determined for each interval by equalizing the areas between the TBP curve and a horizontal line representing the NBP temperature. This is shown in Fig. 15, with the gray areas representing the equalized areas.
  - The density distribution of pseudocomponents is calculated assuming a constant UOPK factor throughout the entire boiling range.
3. Main thermophysical properties are calculated for each pseudocomponent from its specific gravity, boiling point and UOPK factor. The models used by Hysys to determine these properties are explained by Chang, Pashikanti e Liu (2012) and are summarized as follows:
  - *Molecular weight and critical properties:* Corresponds to the model proposed by Twu (1984), which uses correlations for the molecular weight, specific gravity and critical properties of a group of pure n-alkanes (  $C_1$  to  $C_{100}$ ) as a reference

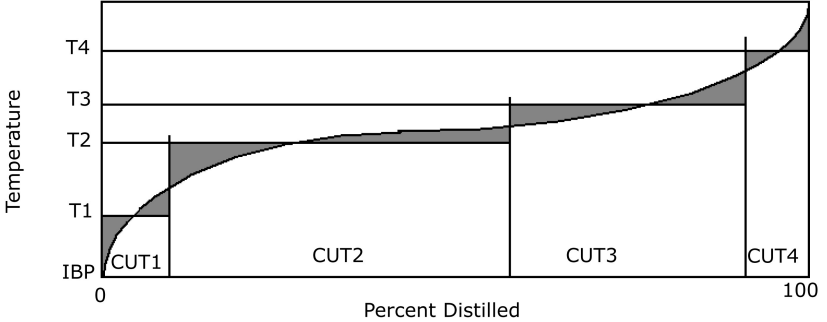


Figure 15 – Determination of the normal boiling point (NBP) of each pseudocomponent (ASPENTECH, 2011).

system. These correlations are adjusted appropriately by the inclusion of a correction term depending on the boiling temperature and specific gravity of each pseudocomponent.

- *Acentric factor*: The expression used in for the calculation of acentric factor is shown in Eq. 3.1.

$$\omega = -\log_{10} \left( P_r^{v*} \right) - 1.0 \quad (3.1)$$

where  $\omega$  corresponds to the acentric factor and  $P_r^{v*}$  corresponds to the reduced pressure at a reduced temperature ( $T_r$ ) equivalent to 0.7.

- *Density (liquid phase)*: Even when Hysys uses an equation of state approach for refinery modeling (*i.e.* Peng-Robinson method), density of each pseudocomponent (liquid) is calculated independently to ensure accurate results. Specifically, the method chosen for the calculation of the density of liquids in the developed model is the Spencer-Danner method with corresponding states liquid density (COSTALD) correction for pressure.
- *Heat capacity (vapor phase)*: represents the vapor heat capacity of the pseudocomponent at a given standard condition. The standard conditions typically refer to 15 °C and 1 atm. The heat capacities of hydrocarbons do not vary significantly over a wide range of temperatures, so very accurate

heat capacities are not necessary for good modeling results. The procedure used by Hysys in this case corresponds to the Lee-Kesler method.

- *Heat capacity (liquid phase):* The method used by Hysys to calculate the heat capacity of pseudocomponents (liquid phase) corresponds to the Lee-Kesler method when  $145 \text{ K} < T < 0.8 T_c$  and a correlation recommended by API when  $T_r < 0.85$ .
- *Thermodynamic model:* The chosen method to model the PVT (Pressure-Volume-Temperature) behavior of the pseudocomponents and their mixtures was the Peng-Robinson EOS (Equation of State). This cubic equation requires three main properties: critical temperature, critical pressure and acentric factor. In general, the interaction parameters for pseudocomponents can be set to 0 without changing model results.

### 3.1.1.2 EES cases

The algorithm implemented in EES incorporates data obtained from Maxwell (1968) depending on the calculation needed to analyze the physical exergy of oil. Basically, the only information needed to the estimation of enthalpy and entropy of oil was a correlation of the specific heat as a function of temperature. Figure 16 reproduces the data found in this reference.

### 3.1.2 Chemical exergy

The calculation of the chemical exergy of oil was carried out based partly on the procedure initially proposed by Szargut, Morris e Steward (1988) and then adjusted by Rivero, Rendon e Monroy (1999) that relates the chemical exergy of oil fractions with their elemental composition and LHV. This procedure considers molecular structures of oil fractions as formed principally by C (carbon), H (Hydrogen), N (Nitrogen), O (Oxygen) and S (sulfur) atoms. Since this information is not commonly available in routine crude analysis (including the crude studied in this work), the incorporation of other techniques was needed in order to estimate adequately these properties from known data. In the case of the heat of combustion, data were obtained from

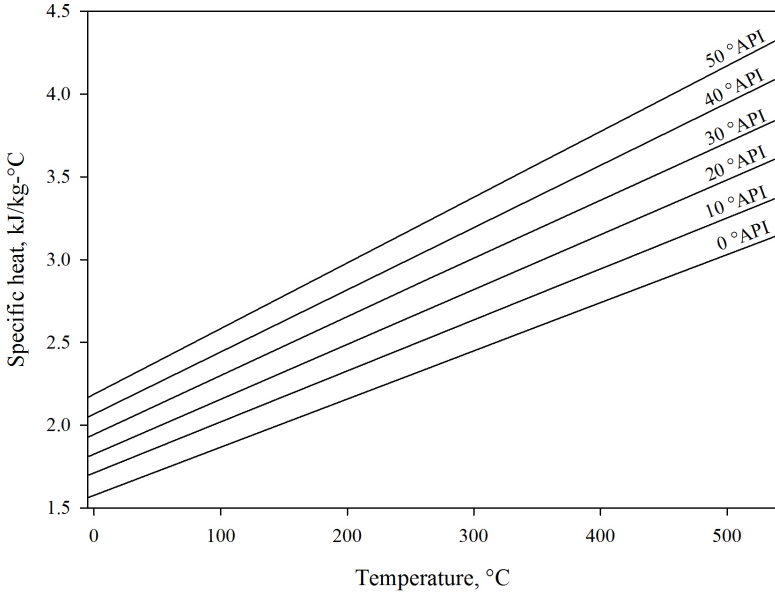


Figure 16 – Specific heat of crude fractions as a function of temperature and its standard specific gravity (MAXWELL, 1968).

Maxwell (1968), where the LHV and HHV can be estimated directly from the specific gravity of the pseudocomponent and its UOPK factor; Fig. 17 reproduces the data for a UOPK factor of 12. On the other hand, the elemental composition was determined using the Boie equation (Eq. 3.2) *apud*. Ringen, Lanum e Miknis (1979) that relates the elemental composition of a crude fraction with its HHV.

$$\begin{aligned}
 HHV_i = & 35170 x_{C,i} + 116252 x_{H,i} + 6280.5 x_{N,i} \\
 & + 10467.5 x_{S,i} - 11095.5 x_{O,i}
 \end{aligned}
 \tag{3.2}$$

where  $HHV_i$  is the higher heating value (kJ/kg) of the pseudocomponent  $i$ .  $x_{C,i}$ ,  $x_{H,i}$ ,  $x_{N,i}$ ,  $x_{S,i}$  and  $x_{O,i}$  correspond to its mass fractions of C, H, N, S and O respectively.

The values of the sulfur and nitrogen content was assumed based

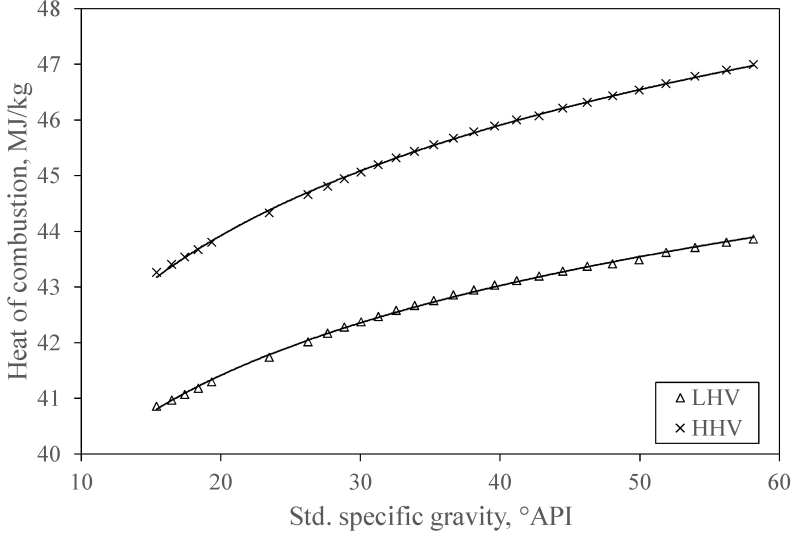


Figure 17 – Heat of combustion of crude fractions as function of its standard specific gravity (MAXWELL, 1968).

on a crude analysis available online (BG Group, 2012), that corresponds to a field located relatively next to the studied platform. These values were assumed constant and oxygen content was adjusted to meet the molecular weight of each pseudocomponent. Once the elemental composition was determined, the correction factor  $\beta$  is calculated using the expression presented by Rivero, Rendon e Monroy (1999) (see Eq. 3.3).

$$\beta_i = 1.0401 + 0.0864 \cdot \frac{x_{H,i}}{x_{C,i}} + 0.0216 \cdot \frac{x_{O,i}}{x_{C,i}} + 0.2169 \cdot \frac{x_S}{x_{C,i}} \cdot \left( 1 - 1.0314 \cdot \frac{x_{H,i}}{x_{C,i}} \right) + 0.0214 \cdot \frac{x_N}{x_{C,i}} \quad (3.3)$$

The specific chemical exergy of each pseudocomponent ( $b_{ch,i}$ ) is then calculated using eq. 3.4.

$$b_{ch,i} = \beta_i \cdot LHV_i \quad (3.4)$$

where  $LHV_i$  corresponds to the lower heating value of pseudocomponent  $i$  (kJ/kg).

The referenced method establishes the specific chemical exergy ( $\bar{b}_{ch}$ ) of a mixture (in molar basis) as the sum of the contribution of each component plus a compositional term, as shown in Eq. 3.5.

$$\bar{b}_{ch,oil} = \sum z_i \cdot \bar{b}_{ch,i} + R T_0 \sum z_i \ln (z_i \cdot \gamma_i) \quad (3.5)$$

where  $\bar{b}_{ch,oil}$  corresponds to the specific chemical exergy of the oil fraction in kJ/kmol.  $z_i$  and  $\gamma_i$  correspond to the molar fraction and activity coefficient of the component  $i$ .

However, in this work the compositional addend was replaced by a term called mixing exergy ( $\Delta_{mix}b$ ) as proposed by Hinderink et al. (1996), which quantifies the effect of the composition over the total exergy of a multicomponent stream. As shown in Eq. 3.6, this term corresponds to the difference between the sum of the exergy contribution of each component and the total exergy of the stream ( $b^m$ ). Its calculation is explained in Sec. 3.3.1.

$$\Delta_{mix}b = b^m - \sum x_i \cdot b_i \quad (3.6)$$

In accordance with this adoption, the specific chemical exergy of crude was defined simply as the sum of the contribution of each component (in mass basis) as shown in Eq. 3.7.

$$b_{ch,oil} = \sum x_i \cdot b_{ch,i} \quad (3.7)$$

In the case where the components are known (*e.g.* methane), the specific chemical exergy was determined from the standard chemical exergy data available in (SZARGUT; MORRIS; STEWARD, 1988). Analogously to eq. 3.7, a more general expression (see Eq. 3.8) was adopted for streams including known components as well as the pseudocomponents.

$$b_{ch} = \sum x_i \cdot b_{ch,i} + \sum x_j \cdot b_{ch,j} \quad (3.8)$$

where  $b_{ch,i}$  and  $b_{ch,j}$  correspond to the specific chemical exergy associated with the pseudocomponents and associated with the known components respectively (kJ/kg).

Appendix B shows the code integrated to Hysys for implementing the calculation of the chemical exergy of each material stream. Conversely, for the cases developed using EES, the specific chemical exergy was approximated to the LHV of whole crude (*i.e.* without considering its composition), accordingly with Rivero, Rendon e Monroy (1999) when no compositional data were available.

## 3.2 PLANT MODELING

### 3.2.1 Plant description

#### 3.2.1.1 Separation plant

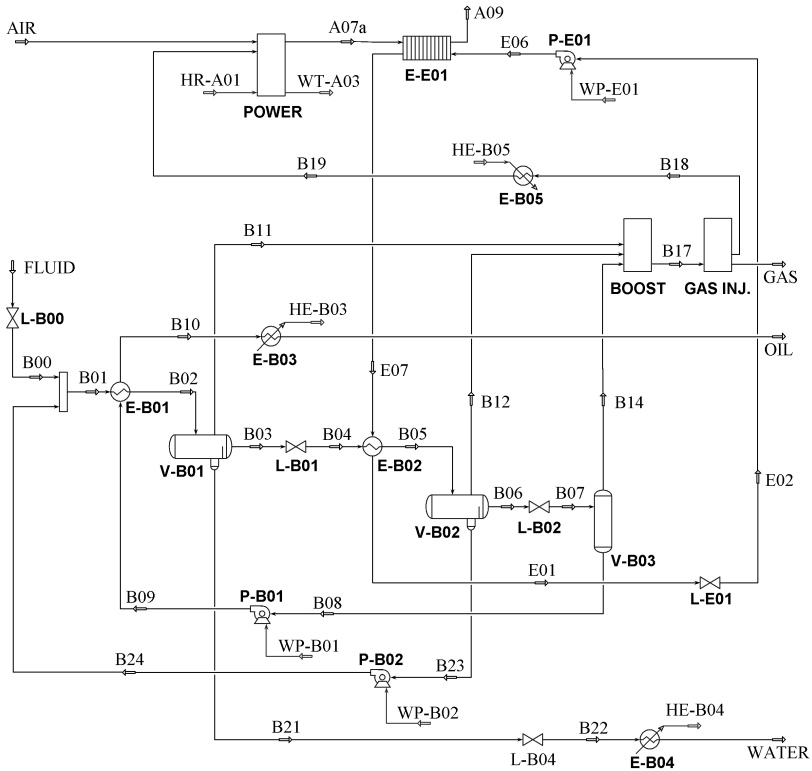


Figure 18 – Basic PFD (Process Flow Diagram) of the separation plant.

As mentioned above, the considered production plant corresponds to an FPSO located at the Santos basin (Brazil). The main purpose of the process is to separate the well fluid into oil, gas and water meeting the specifications for their export/further treatment. Figure 18 presents a simplified scheme of operation, a more detailed scheme is



presented in Appendix A. The well fluid (FLUID) is throttled through a choke (valve L-B00) to meet the pressure level of the first separation stage, which is formed by the heat exchanger E-B01, where the well fluid is preheated with the exported oil stream (B09) and the separator V-B01, where significant amounts of gas (B11) and water (B21) are removed from the oil stream (B03). Next, the oil stream is throttled through valve L-B01 and heated in the heat exchanger E-B02 in order to promote further separation of gas and water in the separator V-B02 (streams B12 and B23 respectively). The heat is supplied to E-B02 by the circulation of a heat transfer fluid (streams E07 and E01), which withdraws heat from the exhaust gases coming from the power generation subsystem through the heat exchanger E-E01. The separation is accomplished with an electrostatic separator for meeting the final specifications of the oil stream (not shown) and a further separation in separator V-B03 at lower pressure. Then, the oil is pumped (P-B01) through E-B01 and dispatched to the tankers (stream OIL), previous cooling with seawater in the cooler E-B02. By the other hand, the water separated in V-B02 (B23) is pumped back (P-B02) and mixed with the inlet wellfluid in order to promote the phases separation prior to the first separation stage. The main production water stream coming from V-B01 is directed to the water treatment system (not shown) to meet the required conditions for its disposal, then is throttled through valve L-B04 and cooled with seawater in cooler E-B04 before being discharged on board.

### 3.2.1.2 Boost system

The gas separated in V-B01, V-B02 and V-B03 is directed to the gas boost subsystem (BOOST), where the streams at lower pressures are compressed up to an intermediate pressure level before being compressed for injection/export in the gas injection subsystem (GAS INJ.). A simplified scheme of the gas boost system is presented in Fig. 19, a more detailed scheme is presented in Appendix A.

The gas coming from V-B03 (B14) is compressed by C-C01 up to second separation stage pressure (stream B12), then both streams are mixed and cooled with seawater through cooler E-C01. The liquids formed by condensation are removed from the gas stream in the separator V-C01 and sent back to V-B03 (B26). Next, the gas stream (C06) is compressed (C-C02) up to an intermediate pressure slightly less than the first separation stage (stream B11) and is cooled with

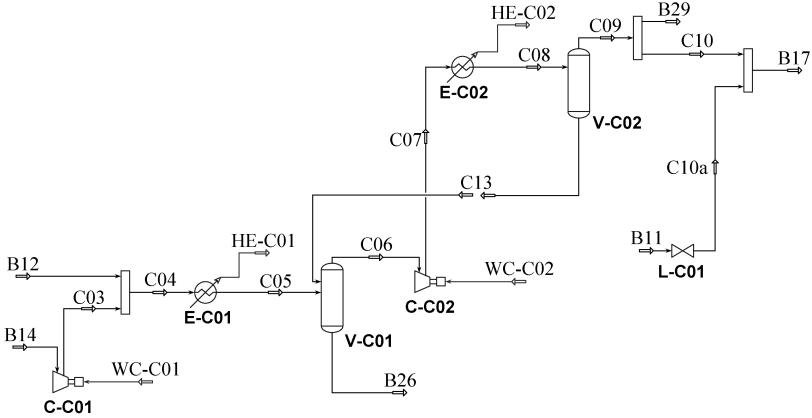


Figure 19 – Basic PFD (Process Flow Diagram) of the boost system.

seawater in E-C02. The condensates separated (V-C02) are returned to V-C01. The boost compression train works recirculating a portion of gas to V-B02 (B29). Then, the gas coming from V-B01 is regulated through valve L-C01 and mixed with the boosted gas (C10).

### 3.2.1.3 Gas injection/export system

The gas stream coming from boost subsystem (B17) is directed to the gas injection system (GAS INJ.), where the gas is compressed and dehydrated in order to meet the requirements to be injected back to the reservoir or sent to onshore facilities via pipeline. A simplified scheme of operation is shown in Fig. 20, a more detailed scheme is presented in Appendix A.

In a similar manner to the boost subsystem, the gas injection train consists of four compression stages (C-D01/C-D02/C-D03/C-D04), each one accomplished with a gas cooling (air coolers F-D01/F-D02/F-D03/F-D04 respectively) and the subsequent separation of condensates, which are returned back to the previous stage (streams B27, D12, D13 and D15 respectively). Before the fourth stage, the dehydration subsystem (DEH) removes the humidity from the gas stream using TEG (triethylene glycol) as absorbent. Fuel gas (stream B18) used in power generation subsystem (POWER) is derived from the dehydrated gas

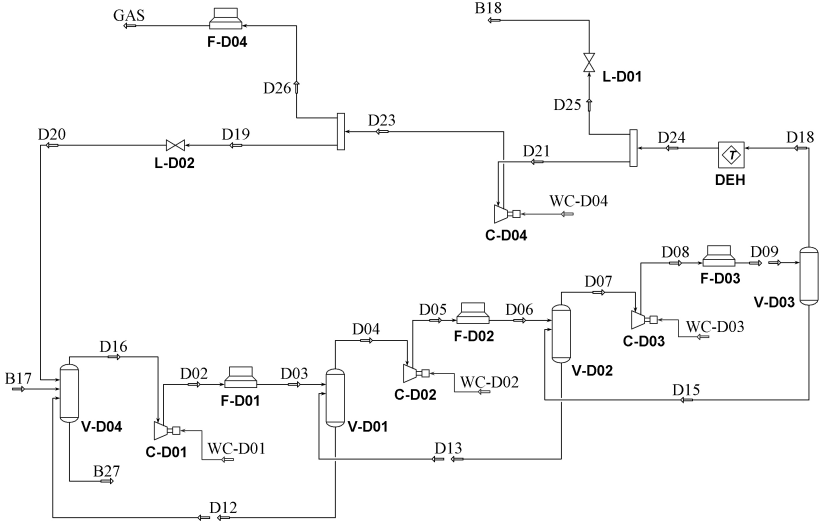


Figure 20 – Basic PFD (Process Flow Diagram) of the gas injection/-export system.

stream (D24). This stream is regulated by the valve L-D01 according to the fuel demand of the gas turbines. A portion of the compressed gas is recirculated to the compression train suction (stream D19), in order to maintain the necessary operating parameters of the equipment. The compressed gas (stream GAS) is then injected into the reservoir or exported via pipeline.

### 3.2.1.4 Power generation system

The required energy for the operation of the plant is supplied by the power generation system, which is formed by two gas turbines Siemens SGT-400 operating at part load. Figure 21 shows the working scheme of these turbines. The power cycle was modeled as two compression stages and a third stage supplying the power to the plant. The operating parameters were adjusted according to the curves provided by supplier (SIEMENS AG, 2009), as shown in Fig. 22.

The maximum output per turbine was limited to 11 MW, such that when the demand of the plant does not exceed this value, only one

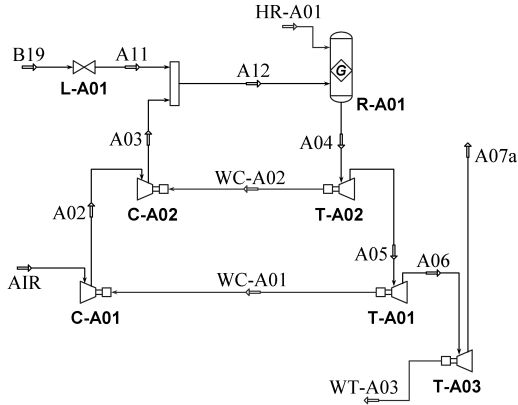


Figure 21 – Basic PFD (Process Flow Diagram) of the power generation system.

turbine is considered in operation. Consequently, when the demanded power in plant exceeds 11 MW, the second turbine enters in operation sharing the 50% of the total load.

### 3.2.1.5 Seawater injection system

On the other side, in order to promote the oil recovery from the reservoir, the analyzed FPSO has a seawater treatment and injection system that is outlined in Fig. 23. A part of the injected water is recirculated to the pump suction to guarantee the minimum flow necessary for the secure operation of the equipment.

Based on the results of previous works (NGUYEN et al., 2012, 2013; VOLDSUND et al., 2010), the following process subsystems were neglected in the plant model, due to their small energy demand when compared to the main operations described above:

- Gas dehydration system.
- Production water treatment.
- Seawater treatment.

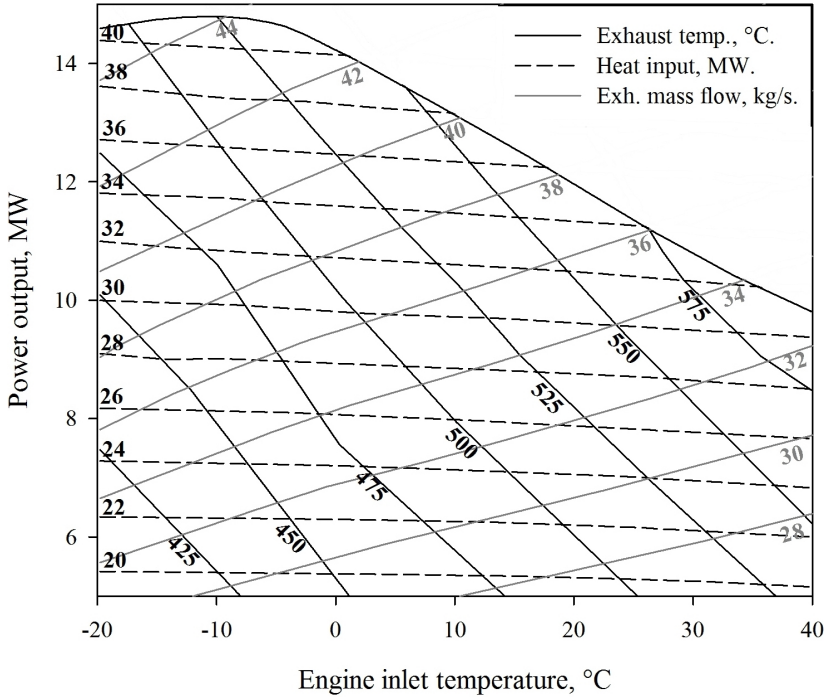


Figure 22 – Operating parameters of gas turbines (SIEMENS AG, 2009).

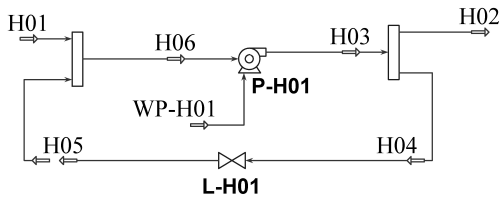


Figure 23 – Basic PFD (Process Flow Diagram) of the water injection system.

### 3.2.2 Input data

Tables 2 through 6 presents the main operation parameters of each subsystem in the plant. As mentioned above, these conditions do not exceed the design constraints of the process reported in this engineering documentation (WASCO, 2012).

Table 2 – Simulation input data for separation plant.

| <b>Parameter</b>              | <b>Units</b>     | <b>Value</b> |
|-------------------------------|------------------|--------------|
| Well pressure                 | <i>kPa</i>       | 3000         |
| Manifold pressure             | <i>kPa</i>       | 1500         |
| Inlet temperature             | $^{\circ}C$      | 55           |
| Inlet vol. Flow - Liq. Phases | $sm^3/day^{(1)}$ | 12800        |
| Gas molar flow                | $Nm^3/day^{(2)}$ | 1500000      |
| BSW                           | %                | 29.7         |
| Oil heating temperature       | $^{\circ}C$      | 81           |
| 3rd stage pressure            | <i>kPa</i>       | 101.3        |
| Oil export temperature        | $^{\circ}C$      | 55           |
| Oil export pressure           | <i>kPa</i>       | 175          |
| Water export temperature      | $^{\circ}C$      | 55           |

<sup>(1)</sup> *Standard cubic meters per day.*

<sup>(2)</sup> *Normal cubic meters per day.*

Table 3 – Simulation input data for boost subsystem.

| <b>Parameter</b>             | <b>Units</b> | <b>Value</b> |
|------------------------------|--------------|--------------|
| Boost discharge pressure     | <i>kPa</i>   | 1300         |
| Compressor adiab. efficiency | %            | 65*          |
| Gas cooling temperature      | $^{\circ}C$  | 40           |
| Boost recycle mass %         | %            | 15           |

*\*Assumed.*

Table 7 summarizes the main assumptions adopted in the developed model. In general, the model considers a steady state of operation (no variations with time) and all the streams and operations meets thermodynamic equilibrium.

Table 4 – Simulation input data for gas injection/export subsystem.

| <b>Parameter</b>             | <b>Units</b> | <b>Value</b> |
|------------------------------|--------------|--------------|
| Gas injection pressure       | <i>kPa</i>   | 20000        |
| Compressor adiab. efficiency | %            | 65           |
| Gas cooling temperature      | $^{\circ}C$  | 40           |
| Injection recycle mass %     | %            | 15           |
| Fuel gas pressure            | <i>kPa</i>   | 1500         |
| Fuel gas temperature         | $^{\circ}C$  | 55           |

Table 5 – Simulation input data for power generation subsystem.

| <b>Parameter</b>          | <b>Units</b> | <b>Value</b> |
|---------------------------|--------------|--------------|
| Inlet air temperature     | $^{\circ}C$  | 25           |
| Inlet air pressure        | <i>kPa</i>   | 101.3        |
| Outlet net power          | <i>MW</i>    | 7.2          |
| Exhaust gases temperature | $^{\circ}C$  | 525.4        |
| Turbine heat input        | <i>MW</i>    | 24.5         |
| Exhaust mass flow         | <i>kg/s</i>  | 30.4         |

Table 6 – Simulation input data for seawater injection subsystem.

| <b>Parameter</b>                 | <b>Units</b>              | <b>Value</b> |
|----------------------------------|---------------------------|--------------|
| Seawater vol. Flow               | <i>sm<sup>3</sup>/day</i> | 12000        |
| Seawater injection pressure      | <i>kPa</i>                | 20000        |
| Injection pump adiab. efficiency | %                         | 75           |
| Seawater injection recycle       | %                         | 15           |

Table 7 – Model assumptions

| <b>Parameter</b>              | <b>Units</b> | <b>Value</b> |
|-------------------------------|--------------|--------------|
| Exchangers $\Delta P$         | <i>kPa</i>   | 50           |
| Pumps adiab. efficiency       | %            | 75           |
| HTF hot temperature           | $^{\circ}C$  | 300          |
| HTF circulating pressure      | <i>kPa</i>   | 1000         |
| E-B02 HTF $\Delta T$          | $^{\circ}C$  | 20           |
| Exhaust gas min. allow. temp. | $^{\circ}C$  | 150          |
| E-B01 pinch point difference  | $^{\circ}C$  | 10           |

### 3.2.2.1 Fluids data

Tables 8 and 9 summarizes the data used for the characterization of the well fluid. These data correspond to the minimal information necessary to characterize the phases (oily phase, aqueous phase and gas phase) conforming the fluid. The aqueous phase was modeled as pure water and a total immiscibility with the oily phase was considered.

Table 8 – Oil characterization parameters

| <b>Parameter</b>             | <b>Units</b>  | <b>Value</b> |
|------------------------------|---------------|--------------|
| Standard density             | $kg/m^3$      | 874.4        |
| Standard density             | $^{\circ}API$ | 30           |
| Watson UOPK                  | –             | 12           |
| Sulphur Content              | $\%wt.$       | 0.362        |
| Nitrogen Content             | $ppm$         | 3136         |
| Viscosity at 100 $^{\circ}F$ | $cP$          | 8            |
| Viscosity at 210 $^{\circ}F$ | $cP$          | 1.5          |

Table 9 – Gas composition

| <b>Component</b> | <b>Mol. Fraction</b> |
|------------------|----------------------|
| CO2              | 0.0516               |
| Nitrogen         | 0.0064               |
| Methane          | 0.7824               |
| Ethane           | 0.0944               |
| Propane          | 0.0412               |
| n-butane         | 0.0152               |
| n-pentane        | 0.0049               |
| n-hexane         | 0.0019               |
| n-heptane        | 0.002                |

Pure substances and their mixtures present within the process were modeled using the PR (Peng-Robinson) equation of state, except for the HTF (dowtherm A), which was modelled using the available information from supplier (DOW Chemical, 2001).

In the same way, the chemical exergy of pure substances involved in the process were assumed as its standard chemical exergy as proposed by Szargut, Morris e Steward (1988), except for the HTF, whose chem-



ical exergy was approximated to its LHV, reported by supplier (DOW Chemical, 2001). The corresponding value is 36,05 MJ/kg.

### 3.2.3 EES case

Appendix C presents the model developed in EES. As mentioned above, its conception was simpler than the model done using Hysys (described in this section). The comparison of results using both models can be used to examine the influence of the detailing level in the calculation of the exergy efficiency of the plant.

### 3.2.4 Production parameters profiles

With the aim of analyzing the influence of the main production variables over the impact of an integrated ORC in the studied FPSO, different profiles were proposed. As shown in Fig. 24, these profiles were developed in 16 scenarios such that each variable could be analyzed separately. As mentioned above, the chosen variables were: (i) oil flow varying from 800 up to 9000 standard  $\text{m}^3/\text{d}$ , (ii) Gas flow varying from 1.5 up to 2 million of  $\text{Nm}^3/\text{d}$ , (iii) production water flow, varying from 200 up to 4000 standard  $\text{m}^3/\text{d}$ , (iv) seawater flow varying from 12000 up to 18000 standard  $\text{m}^3/\text{d}$  and (v) well pressure varying from 3000 down to 1500 kPa. As stated earlier, the standard conditions for liquid volumetric flow are referred to  $T=15^\circ\text{C}$  and  $P=101.325$  kPa. Similarly, the gas volumetric flow ( $\text{Nm}^3/\text{d}$ ) is referred at normal conditions ( $T=0^\circ\text{C}$  and  $P=101.325$  kPa).

## 3.3 EXERGY ANALYSIS

### 3.3.1 Exergy calculation

As previously mentioned, the formulation adopted for the calculation of total exergy of the material streams within the process corresponds to that proposed by Hinderink et al. (1996). The specific exergy of a multicomponent stream ( $b$ ) is expressed as shown in Eq. 3.9.

$$b = b_{chem} + b_{phys} + \Delta_{mix}b \quad (3.9)$$

where  $b_{chem}$ ,  $b_{phys}$  and  $\Delta_{mix}b$  correspond to the specific chem-

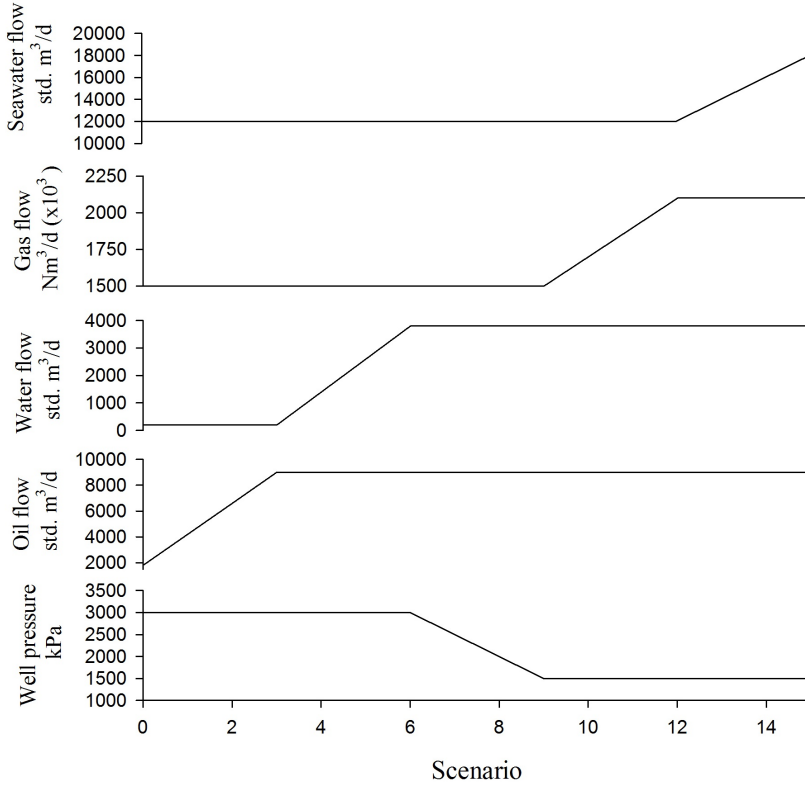


Figure 24 – Analyzed production profiles.

ical exergy, the specific physical exergy and the mixing exergy respectively. Eq. 3.8 is used for the calculation of  $b_{chem}$ , as explained in Sec. 3.1.2. By other side, the Eq. 3.10 is used for the calculation of  $b_{phys}$ , as explained by Szargut, Morris e Steward (1988).

$$b_{phys} = \Delta h - T_0 \Delta s \quad (3.10)$$

where  $\Delta h = h - h^o$  and  $\Delta s = s - s^o$ , considering  $h$  and  $s$  as the current specific enthalpy and the specific entropy of the stream respectively. On the other hand,  $h^o$  and  $s^o$  correspond to the specific enthalpy and specific entropy of the stream evaluated at dead state conditions, which were defined at  $T_0 = 25 \text{ }^\circ\text{C}$  and  $P_0 = 101.325 \text{ kPa}$ .

Appendix B shows the code developed for implementing the calculation of the physical exergy of a material stream using Hysys. This code was developed based on the work of Abdollahi-Demneh et al. (2011).

Eq. 3.11 presents the calculation of  $\Delta_{mix}b$ , which represents the exergy destroyed due to the entropy generation during a non-ideal mixing process at isothermal and isobaric conditions. This term is commonly negative and its use permits to isolate the net effect of a separation process over the exergy flow associated with a multicomponent stream (HINDERINK et al., 1996).

$$\Delta_{mix}b = \Delta_{mix}h - T_0 \Delta_{mix}s \quad (3.11)$$

considering  $\Delta_{mix}h = h^m - \sum x_i h_i$  and  $\Delta_{mix}s = s^m - \sum x_i s_i$ , where  $h^m$  and  $s^m$  correspond to the molar enthalpy and the molar entropy of the mixture respectively.  $h_i$  and  $s_i$  are the molar enthalpy and the molar entropy of the component  $i$  at the same conditions of the mixture respectively. Appendix B shows the code integrated to Hysys for implementing the calculation of the mixing exergy of each material stream. Adopting this procedure, Eq. 3.9 for calculation of the total exergy of a multicomponent stream is reformulated as shown in Eq. 3.12.

$$b = \sum x_i b_{chem,i} + ((h - h^o) - T_0 (s - s^o)) + \left( (h^m - \sum x_i h_i) - T_0 (s^m - \sum x_i s_i) \right) \quad (3.12)$$

### 3.3.2 Plant exergy balances

Appendix D presents the formulation of the exergy balance for each equipment conforming the plant. Exergy losses ( $B_L$ ) are associated with those material and energy streams that are not part of the desired product of the plant/subsystem. Conversely, destroyed exergy ( $B_D$ ) is associated with the entropy generation (irreversibility) present in each process. Eq. 3.13 presents the relation between the destruction of exergy and the entropy generated during a non-reversible operation (CENGEL; BOLES, 2010). Given that Hysys calculates the entropy of the material streams directly according to the chosen thermodynamic package and by other side the implementation of the exergy calculation must be done through a programming block, this expression can be useful

to check the consistency of obtained data. Values of  $B_D$  obtained from the exergy balance of each equipment must match with that calculated using the entropy values reported by Hysys.

$$B_D = T_0 \cdot S_{gen} \quad (3.13)$$

where

$$S_{gen} = (S_{out} - S_{in}) - \sum \frac{Q}{T}$$

### 3.3.3 Exergy and energy efficiency indicators

#### 3.3.3.1 Overall indicators

Given the scheme of operation of the whole plant shown in Fig. 18, the desired effects of the process can be divided in the following items:

- Remove water and gas incorporated together with the oil in the inlet fluid stream.
- Compress the gas stream for further use.
- Pump the seawater to be injected into the reservoir.

As it can be inferred from previous works (HINDERINK et al., 1996; SILVA et al., 2012), the decrease of the mixing term in Eq. 3.9 also represents a chemical exergy increment when conceived as (RIVERO; RENDON; MONROY, 1999). This increase of exergy constitutes the main effect (product) of separation process when considering a mixture and its components at equilibrium (SILVA, 2008).

Adopting the concept presented by Bejan (1996), the exergy associated with the entire product (or effect) of the plant ( $B_P$ ) was expressed by the sum of the exergy effects related to the above-mentioned items, as shown in Eq. 3.14.

$$B_P = \Delta B_{mix} + \Delta B_{phys,GAS} + \Delta B_{phys,SEA} \quad (3.14)$$

considering

$$\Delta B_{mix} = \Delta_{mix} B_{FLUID} - (\Delta_{mix} B_{OIL} + \Delta_{mix} B_{GAS})$$

where  $\Delta_{mix}B_i = m_i \Delta_{mix}b_i$  is the exergy of mixing of stream  $i$  (*i.e.* streams named *FLUID*, *OIL* and *GAS* in the model scheme –see Fig. 18); here  $m_i$  corresponds to its mass flow. Analogously,

$$\begin{aligned}\Delta B_{phys,GAS} &= m_{GAS} b_{phys,GAS} - (m_{B11} b_{phys,B11} \\ &\quad + m_{B12} b_{phys,B12} + m_{B14} b_{phys,B14}) \\ \Delta B_{phys,SEA} &= m_{H02} \cdot b_{phys,H02} - m_{H01} \cdot b_{phys,H01}\end{aligned}$$

Considering that a great extent of the exergy contained in the streams of interest (*i.e.* oil, gas and injected water streams) are supplied initially with the inlet streams, the consumed exergy  $B_F$  was expressed as the sum of  $B_P$  and the difference between the exergy associated with inlet streams ( $B_{in}$ ) and the exergy associated with product streams ( $B_{PS}$ ). Eq. 3.15 presents the exergy indicator chosen to evaluate the performance of the plant.

$$\eta_{II} = \frac{B_P}{B_F} \quad (3.15)$$

considering  $B_F = B_P + (B_{in} - B_{PS})$  and

$$\begin{aligned}B_{in} &= B_{FLUID} + B_{AIR} + B_{H01} \\ B_{PS} &= B_{OIL} + B_{GAS} + B_{H02}\end{aligned}$$

As mentioned in previous works (SILVA et al., 2012; SILVA, 2008), another exergy indicator that can be used for this kind of processes is the degree of perfection  $\eta_P$ . This index was defined by Szargut, Morris e Steward (1988) and relates the exergy of the products of interest leaving the system ( $B_{PS}$ ) and the inlet exergy ( $B_{in}$ ) as shown in Eq. 3.16.

$$\eta_P = \frac{B_{PS}}{B_{in}} \quad (3.16)$$

Alternatively, with the aim to demonstrate the energy efficiency in terms that can be associated with production variables, this study propose the indicator  $\lambda$  that represents the energy consumption per standard cubic meter of exported oil. This indicator is presented in Eq. 3.17. It can be easily converted to fuel gas consumption or to energy consumption expressed in BOE (barrels of oil equivalent<sup>1</sup>) per volumetric unit of produced oil.

---

<sup>1</sup>The BOE is a unit of energy based on the approximate energy released by burning one barrel of crude oil and it is equivalent to about 1.7 MWh.

$$\lambda = \frac{m_{B18} \cdot LHV_{B18}}{v_{OIL}} \quad (3.17)$$

where  $v_{OIL}$  corresponds to the standard volumetric flow of produced oil in  $\text{m}^3/\text{s}$ .

### 3.3.3.2 Subsystems indicators

Analogously,  $B_{P,i}$  was defined for each subsystem  $i$  in order to obtain the exergy indicators  $\eta_{p,i}$  and  $\Phi_i$  associated with each process. As shown in Eq. 3.18,  $\Phi_i$  corresponds to the second law efficiency ( $\eta_{II,i}$ ) but formulated using the irreversibility ( $B_{D,i}$ ) and the exergy losses ( $B_{L,i}$ ) calculated for each process. In that way, Tab. 10 shows the formulation of  $B_{P,i}$  for each subsystem. Evidently, the value of  $\Phi$  for the entire plant must be equal to  $\eta_{II}$  (explained in the previous section) to be coherent with the definition presented by Bejan (1996).

$$\Phi_i = \frac{B_{P,i}}{B_{P,i} + B_{L,i} + B_{D,i}} \quad (3.18)$$

here  $B_{F,i} = B_{P,i} + B_{L,i} + B_{D,i}$ .

## 3.4 ORC MODELING

### 3.4.1 fluid selection

As explained in Sec. 2.3.2, numerous works had analyzed different ORC working fluids candidates with the purpose of determining the best candidate taking into account different fluid characteristics as the slope of the vapor saturation curve, critical properties, enthalpy of vaporization, density, specific heat and others related to environmental aspects as ODP (ozone depletion potential) or GWP (global warming potential)(CHEN; GOSWAMI; STEFANAKOS, 2010; BAO; ZHAO, 2013). This work is focused on the use of cyclopentane as working fluid based on the results of a recent study (PIEROBON et al., 2013), where cyclopentane was indicated as the best option when accounting the ORC power output and the size of ORC equipment as choosing criteria. Despite its flammable and toxicological characteristics, it is important to remark that the plant already deals with this type of substances (*i.e.* hydrocarbons) in its main processes and it would be

Table 10 – Subsystems exergy product definition.

| <b>System</b>   | <b>Streams</b> |          |          |          |
|---|----------------|----------|----------|----------|
| Separation plant  | <i>i</i>       | <i>j</i> |          |          |
|   |                | OIL      | FLUID    |          |
|   |                | B11      | A07a     |          |
|   |                | B13      | A07b     |          |
|   |                | B15      | B18      |          |
|   |                | B20a     | B26      |          |
|   |                | B20b     | B27      | B29      |
|   |                |          |          |          |
| Gas turbines  | <i>i</i>       |          |          |          |
| $\sum_i W_i$  | WT-A03a        |          |          |          |
|   | WT-A03b        |          |          |          |
| Gas boost system  | <i>i</i>       | <i>j</i> | <i>k</i> | <i>m</i> |
| $B_P = \sum_i B_{phys,i} - \sum_j B_{phys,j}$                                       | C10            | B13      | B16      | B11      |
|   | B29            | B15      | B29      | B13      |
| $+ \sum_k \Delta_{mix} B_k - \sum_m \Delta_{mix} B_m$                               |                |          |          | B15      |
| Gas injection system  |                |          | <i>i</i> | <i>j</i> |
| $B_P = \sum_i \Delta_{mix} B_i + B_{phys,i} - \sum_j \Delta_{mix} B_j + B_{phys,j}$ |                |          | GAS      | B17      |
|   |                |          | B18      |          |
| Seawater injection system   | <i>i</i>       | <i>j</i> |          |          |
| $B_P = \sum_i B_{phys,i} - \sum_j B_{phys,j}$                                       | H02            | H01      |          |          |
| ORC system  | <i>i</i>       |          |          |          |
| $W_i$   | WT-F01         |          |          |          |

not necessary to make important modifications due to safety issues. Table 11 summarizes the main properties of this substance.

Table 11 – Main physical properties of the cyclopentane

| <b>Property</b>                    | <b>Units</b>        | <b>Value</b> |
|------------------------------------|---------------------|--------------|
| Molecular wt.                      |                     | 70.14        |
| Critical temperature               | °C                  | 234          |
| Critical pressure                  | <i>kPa</i>          | 4506         |
| $\xi$                              | J/kg-K <sup>2</sup> | 1.04         |
| Type of T-s vapor saturation curve |                     | Dry          |
| Freezing point                     | °C                  | -93          |
| Autoignition temperature           | °C                  | 361          |

### 3.4.2 Configuration

The operation scheme of the ORC working with cyclopentane is determined by the slope of its saturated vapor line in the T-s diagram. Since this slope is positive (as seen in Tab. 11), the expansion process (F10 – F11 in Fig. 10 – Sec. 2.3) results in an overheated vapor stream at the turbine outlet. This means that the incorporation of an intermediate regenerator (E-F04) is convenient in order to take some advantage of the remaining energy associated with this stream.

It can be noted that superheating of vapor at turbine inlet (E-F01) is not necessary theoretically. However, this study contemplates a slight superheating of vapor in order to avoid any condensation at the turbine intake.

### 3.4.3 Integration with plant model and parameters of operation

In accordance with previous works focused on the exergy analysis of oil and gas production platforms, the most appropriate use of ORC systems in these installations consist in recovering exergy from the exhaust gases coming from gas turbines or from processes associated with combustion (PIEROBON; NGUYEN, 2012a; NGUYEN et al., 2013). Considering the operation scheme of the analyzed FPSO, this study proposes the integration of the ORC within the existing HTF circuit,



in order to take some advantage and reduce the number of modifications to the operating scheme of existing installations. The ORC was located downstream of exchanger E-B02 (HTF side) at the valve L-E01 position.

Evidently, when the ORC is integrated within the model, a relationship is established between the amount of energy taken from exhaust gases, the HTF mass flow rate, HTF temperature levels and the ORC system performance. This correlation makes necessary to update their corresponding values in order to take an acceptable advantage. Likewise, the internal parameters of the ORC that influence directly its output (*e.g.* evaporation temperature, working fluid mass flow, temperature of condensation, etc.) must be adjusted properly according to established criteria. In that way, Tab. 12 presents the assumptions used in this paper for the variables affecting the ORC performance.

Table 12 – ORC parameters and assumptions

| <b>Parameter</b>                       | <b>Units</b> | <b>Value</b> |
|--|--------------|--------------|
| Condensation pressure                  | <i>kPa</i>   | 110          |
| HTF maximum temperature                | °C           | 300          |
| Regenerator pinch point                | °C           | 5            |
| Superheating                           | °C           | 1            |
| Expander adiabatic efficiency          | %            | 65           |
| Pump adiabatic efficiency              | %            | 75           |
| Economizer pinch point                 | °C           | 5            |
| Heat exchangers $\Delta P$ (tubeside)  | <i>kPa</i>   | 50           |
| Heat exchangers $\Delta P$ (shellside) | <i>kPa</i>   | 25           |

Particularly, the evaporation temperature of cyclopentane within the cycle was analyzed varying it from an established minimum temperature (180 °C) up to its critical temperature. This was done with the aim of finding an appropriate evaporation temperature at which the flow rate and rejected heat were reduced in each scenario.

Considering a centralized power distribution (*i.e.* all the power demand of the plant is supplied by only one power distribution system), the power generated by the ORC was subtracted from the total power demand and the remainder was supplied by existing turbines. These assumptions together with the turbines operation configure the calculation algorithm for each scenario, as presented in Fig. 25. The nomenclature used in this figure is listed as follows:

- *Processes:*

A.–Update overall mass and energy balances.

B.–Calculate operation parameters of 2 turbines.

C.–Calculate operation parameters of 1 turbine.

D.–Calculate operation parameters of ORC.

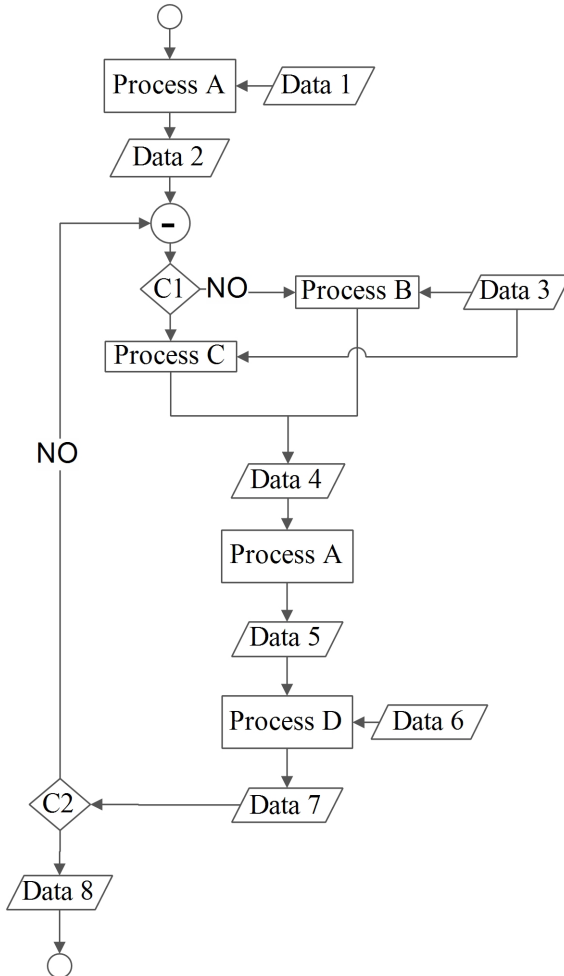


Figure 25 – Model general algorithm.

- *Data:*
  1. Operation parameters of the plant (*e.g.* BSW, GOR, etc.).
  2. Power demand of the plant.
  3. Air temperature and pressure.
  4. Exhaust gases flow and temperature.
  5. Exergy for activate the ORC.
  6. ORC parameters (*e.g.*  $T_{ev}$ , PPDs, etc.).
  7. ORC output.
  8. Model results (*e.g.* exergy flows, heat flows, etc.).
  
- *Conditions:*
  - C1. Is the total power demand less than 11 MW?.
  - C2. All material and energy balances converged?.



## 4 RESULTS

### 4.1 OIL CHARACTERIZATION

Appendix E summarizes the results about the oil characterization. Despite its importance for obtaining accurate results, this information was compiled in a separate section because it is not considered as a fundamental part within the aims of the present work.

### 4.2 MODEL DEVELOPMENT

The mass and energy balances of the plant enable the quantification of the power requirements as well as the heat rejected in each operation involved in the process. Although currently there are no data available from field to corroborate the model, the comparison with the results of previous studies can give an idea about the size of the plant and the consistency of the model. Particularly, the platform analyzed by Nguyen et al. (2012) has a similar configuration to that studied in this work. Table 13 presents some results for both models developed (using Hysys and EES) together with the results obtained from this reference. As stated above, the great variability of the well fluid properties and production characteristics from field to another make each installation unique and this fact makes difficult the validation of the results of a plant model with the data from another.

By the other hand, the power consumption breakdown (presented in Tab. 14), indicates how the energy is distributed among the subsystems and the load of each one within the entire system. Particularly, the injection operations (*i.e.* gas and seawater) presented a value far above from that reported to the separation plant. In general, the results obtained using EES were appreciably smaller than those using Hysys, except for the gas boosting where the gas compressed had a lower molecular weight in the EES case. The power distribution (as percentages) is presented in Tab. 15, which is practically in accordance with those reported by Nguyen et al. (2012). Analogously, Fig. 26 exhibits the results obtained by both models. Considering the differences about the size of the plants, the proportion and the conditions of the oil, gas and water flows as well as the subsystems considered in the models, the results obtained here are noticeably in line with the model developed for the platform located at North Sea.

Table 13 – Comparison of mass and energy balances of models.

| Parameter                                       | Nguyen, 2012 | This work |           |
|---|--------------|-----------|-----------|
|   |              | EES       | Hysys     |
| Platform localization                           | North Sea    | Brazil    | Brazil    |
| <i>Considered Operations</i>                    |              |           |           |
| Production manifolds                            | yes          | no        | yes       |
| Crude oil separation                            | yes          | yes       | yes       |
| Oil pumping and export                          | yes          | yes       | yes       |
| Oil heating by furnace                          | no           | no        | no        |
| Gas re-compression (boost)                      | yes          | yes       | yes       |
| Gas dehydration                                 | yes          | no        | no        |
| Gas injection/exportation                       | yes          | yes       | yes       |
| Wastewater treatment                            | yes          | no        | no        |
| Seawater injection                              | yes          | yes       | yes       |
| Power generation                                | yes          | yes       | yes       |
| Recycling streams                               | yes          | no        | yes       |
| <i>Size of the plant</i>                        |              |           |           |
| Oil produced, $\text{sm}^3/\text{h}$            | 156-457      | 375       | 75-375    |
| Gas produced, $10^3 \cdot \text{Nm}^3/\text{h}$ | 190-320      | 63.5      | 62.5-87.5 |
| Water produced, $\text{sm}^3/\text{h}$          | 50-123       | 158.3     | 8.3-158.3 |
| Seawater injected, $\text{sm}^3/\text{h}$       | 900-2900     | 500       | 500-750   |
| Seawater inj. Pressure, MPa                     | 11.5         | 20        | 20        |
| Gas export pressure, MPa                        | 15-25        | 20        | 20        |
| Power demand, MW                                | 18-23.5      | 13        | 14.2-20.6 |
| Separation stages                               | 4            | 3         | 3         |
| <i>Fluid parameters</i>                         |              |           |           |
| Oil spec. Gravity, °API                         | 39.9         | 30        | 30        |
| <i>Software</i>                                 |              |           |           |
|   | Aspen plus   | EES       | Hysys     |
|   | Hysys        |           |           |
|   | DNA          |           |           |

Table 14 – Power consumption per subsystem, kW.

| System                     | Value      |              |
|----------------------------|------------|--------------|
|                            | <i>EES</i> | <i>Hysys</i> |
| Oil pumping and export     | 20.1       | 151.6        |
| Gas re-compression (boost) | 358.8      | 317.4        |
| Gas injection/exportation  | 8908       | 9531.1       |
| Seawater injection         | 3685.2     | 4568.9       |

Table 15 – Power supply distribution, %.

| System                     | Nguyen, 2012 | This work  |              |
|----------------------------|--------------|------------|--------------|
|                            |              | <i>EES</i> | <i>Hysys</i> |
| Oil pumping and export     | 0.98-3.1     | 0.15       | 1.04         |
| Gas re-compression (boost) | 4.74-9.8     | 2.77       | 2.18         |
| Gas injection/exportation  | 51.37-64.46  | 68.67      | 65.42        |
| Seawater injection         | 29.79-38.79  | 28.41      | 31.36        |

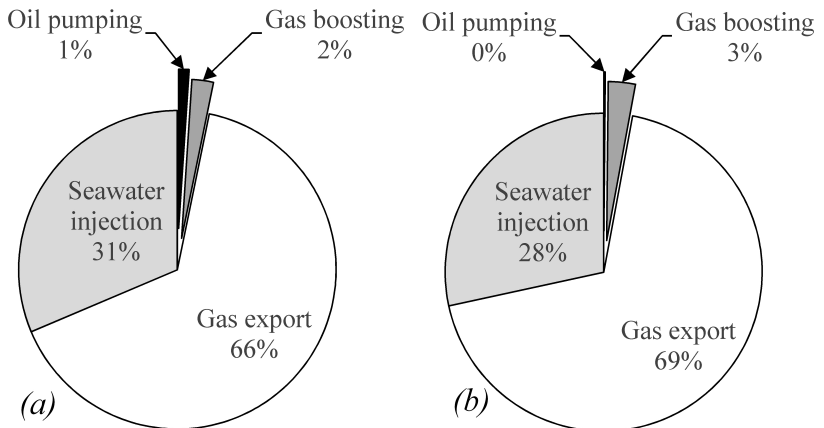


Figure 26 – Power supply distribution for: (a)-Hysys model and (b)-EES model.

Another result coming from the energy balance of the plant is the rejected heat breakdown, which enabled the identification of the

main heat sources that can be used to activate the ORC system. As can be seen in Tab. 16, the power generation system is responsible for over the half of the total heat rejection in the plant (see also Fig. 27). Here, the largest heat discharge to the atmosphere corresponds to the exhaust gas stream, which has a calculated temperature of 471 °C. It can be inferred that this heat source is the most suitable to activate the ORC.

Table 16 – Rejected heat per subsystem, kW.

| System             | <i>EES</i>   |          | <i>Hysys</i> |          |
|--------------------|--------------|----------|--------------|----------|
|                    | <i>Value</i> | <i>%</i> | <i>Value</i> | <i>%</i> |
| Separation plant   | 2994         | 7.90     | 3029         | 7.61     |
| Gas turbines*      | 25066        | 66.12    | 22656        | 56.94    |
| Gas boost system   | 436          | 1.15     | 694          | 1.74     |
| Gas injection      | 9412         | 24.83    | 13407        | 33.70    |
| Seawater injection | 0            | 0.00     | 0            | 0.00     |
| Total              | <i>37909</i> |          | <i>39786</i> |          |

\*With a min. allowed temp. of 150 °C for exhaust gases.

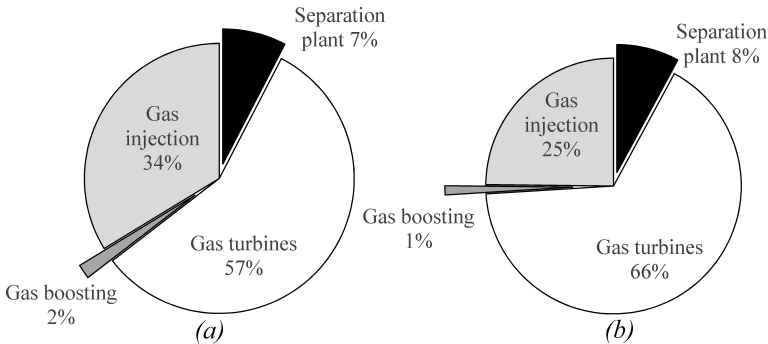


Figure 27 – Rejected heat distribution for: (a)-Hysys model and (b)-EES model.

Detailed results of mass and energy balances (accounting for each



equipment separately) are presented in Appendix C. Examining these results for the Hysys case, a minor imbalance of 22 kg/h was identified within the power generation system. This imbalance was caused by the omission of the traces of pseudocomponents in the fuel gas stream, with the aim to enable the calculation sequence of the Gibbs reactors simulating the combustor chambers of the turbines. Since the data of the Gibbs energy of formation ( $\Delta_f G^\circ$ ) of the pseudocomponents are unknown, the internal algorithm of calculation does not attain a minimum Gibbs free energy for the combustion reaction ( $\Delta_r G^\circ$ ) and the composition of the products cannot be determined. Given that the amount of pseudocomponents in the fuel gas is negligible (most of them have a high molecular weight) and according to Hinderink et al. (1996) the estimation of their  $\Delta_f G^\circ$  may result in an inconsistent set of standard chemical exergies, their mass fractions were approximated to 0. Future work should include an appropriate procedure to estimate the  $\Delta_r G^\circ$  of a hydrocarbon pseudocomponent combustion adequately.

## 4.3 EXERGY ANALYSIS

### 4.3.1 Exergy balance

As mentioned earlier, the exergy balance of the plant enables the recognition of the processes with greatest exergy destruction as well as the quantification of the losses discharged to the atmosphere. By means of this analysis, it is possible to establish the reference case and the parameters of comparison in order to demonstrate the effect of the ORC system along the proposed production profile. In a similar way to mass and energy balances, Tab. 17 and Tab. 18 presents the results of the exergy balances obtained using Hysys and EES. Given that the existing WHR system recovers part of the energy associated to exhaust gases and is considered part of the separation plant, the exergy losses associated with this stream are not accounted for in the power generation system, but in the separation plant. Detailed results (balances per equipment) are presented in Appendix D. Due to the mass flow imbalance previously discussed for the power generation system, a difference of 271 kW was identified in its exergy balance. Considering the magnitude of the involved flows and the high specific exergy value of the fuel gas stream, this value represents a minor deficit in the exergy calculations and is not significant for the analysis of the performance of the plant.

Table 17 – Exergy losses per subsystem, kW.

| System           | Value          |                |
|------------------|----------------|----------------|
|                  | <i>EES</i>     | <i>Hysys</i>   |
| Separation plant | 20062.8        | 16968.2        |
| Gas turbines     | 1006.3         | 758.3          |
| Gas boost        | 83.4           | 104.2          |
| Gas injection    | 1590.3         | 1981.2         |
| <i>Total</i>     | <i>22742.7</i> | <i>19811.9</i> |

Likewise the results obtained by Nguyen et al. (2012), the greatest exergy losses are associated with the exhaust gases coming from gas turbines. Similarly, when the combustor chambers in the power generation subsystem are not considered, the largest exergy destruction takes place in separation plant (mainly caused by pressure reduction in manifold) and in the gas injection compressors. This observation is in accordance with the previous analysis carried out by Nguyen et al. (2013) and Voldsund et al. (2010) for fixed platforms in North Sea.

Table 18 – Exergy destruction rate per subsystem, kW.

| System                    | Value          |                |
|---------------------------|----------------|----------------|
|                           | <i>EES</i>     | <i>Hysys</i>   |
| Separation plant          | 2064.5         | 3879.9         |
| Gas turbines              | 17345.6        | 19795.1        |
| Gas boost system          | 95.2           | 309.6          |
| Gas injection system      | 2713.3         | 3592.6         |
| Seawater injection system | 933.4          | 1313.8         |
| <i>Total</i>              | <i>23152.0</i> | <i>28891.1</i> |

The Sankey diagram is a graphical representation of any type of flow or transfers (*e.g.* material, energy, exergy, emissions, costs, etc.) through a series of processes, in which the width of the arrows is shown proportionally to the flow quantity. In this case, this diagram is used to visualize the relation between the exergy flows within the plant and the proportion of their magnitudes (commonly called Grassmann diagram when refers to exergy flows). From the Grassmann diagram for the Hysys case displayed in Fig. 28 it can be seen that the exergy bal-

ance is largely dominated by exergy associated with the oil and gas streams when compared with the others associated with their processing. This behavior is related with the high specific chemical exergy associated with these streams. Given that any improvement in the energy efficiency of the plant would modify the rest of the streams, it appears that the shape and the proportion of this diagram are unlikely to change. Subsequently, it is reasonable that an exergy performance indicator for this type of installations were process-oriented and represents how far a process is from ideality. In that way, exergy flows should not be considered entirely as exergy products or fuels in order to avoid values too high or too low for performance indicators.

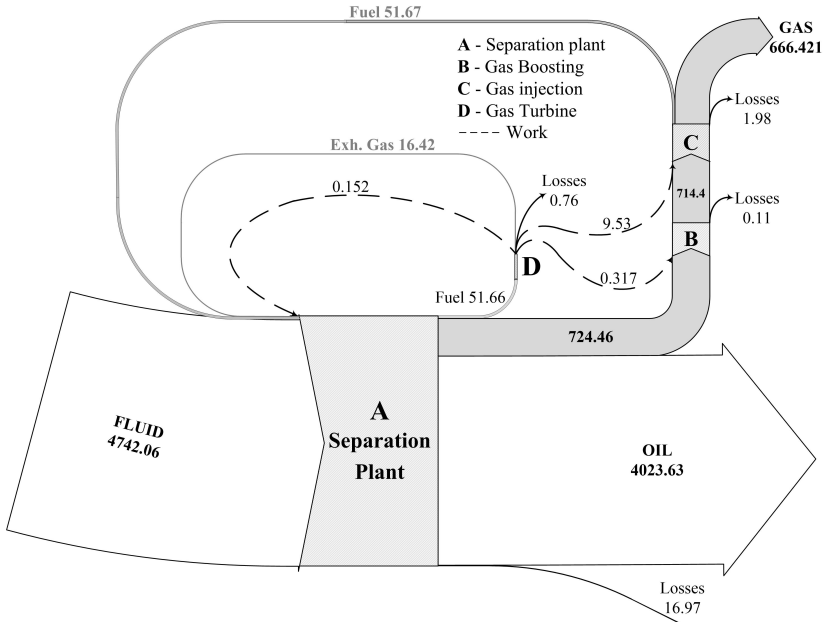


Figure 28 – Simplified Grassmann diagram of the plant, exergy flows in MW.

Analogously to the energy balances of the plant, the individual contribution of each system in the total exergy destruction of the plant can be calculated using the Eq. 4.1 and can serve for comparison with previous studies. In that way, Tab. 19 presents the corresponding data of the present work together with those reported by Nguyen et al.

(2012). Distributions of the destroyed exergy and exergy losses for both models are exhibited in Figs. 29 and 30 respectively. Additionally, data obtained considering only the separation plant, the gas boosting and the gas injection were compared with those reported by Voldsund et al. (2010) (see Tab. 20). The exergy destruction sharing displayed values very close to the data obtained by the first reference, especially for the case developed in Hysys. However, in the second comparison the values shown a considerable discrepancy with the data published. This can be associated with the great difference between the operation conditions and the fact that the inlet manifold (where a sudden expansion of well fluid occurs) is not considered by the author. By other side, concerning the exergy losses that take place in the plant (see Tab. 21), results suggest that the exergy losses sharing is associated directly with the production parameters of the plant.

$$y_{D,i} = \frac{B_{D,i}}{\sum B_{D,i}} \quad y_{L,i} = \frac{B_{L,i}}{\sum B_{L,i}} \quad (4.1)$$

Table 19 – Exergy destruction rate distribution.

| <b>System</b>             | <b><math>y_{D,i}</math></b> | <b>This work</b> |              |
|---------------------------|-----------------------------|------------------|--------------|
|                           | <i>Nguyen, 2012</i>         | <i>EES</i>       | <i>Hysys</i> |
| Separation plant          | 0.16-0.18                   | 0.089            | 0.134        |
| Gas turbines              | 0.65-0.68                   | 0.749            | 0.685        |
| Gas boost system          | 0.033-0.042                 | 0.004            | 0.011        |
| Gas injection system      | 0.076-0.101                 | 0.117            | 0.124        |
| Seawater injection system | 0.03-0.035                  | 0.040            | 0.045        |

Table 20 – Exergy destruction rate distribution (only separation and gas processes).

| <b>System</b>        | <b><math>y_{D,i}</math></b> | <b>This work</b> |              |
|----------------------|-----------------------------|------------------|--------------|
|                      | <i>Voldsund, 2010</i>       | <i>EES</i>       | <i>Hysys</i> |
| Separation plant     | 0.23                        | 0.424            | 0.499        |
| Gas boost system     | 0.11                        | 0.020            | 0.040        |
| Gas injection system | 0.66                        | 0.557            | 0.462        |

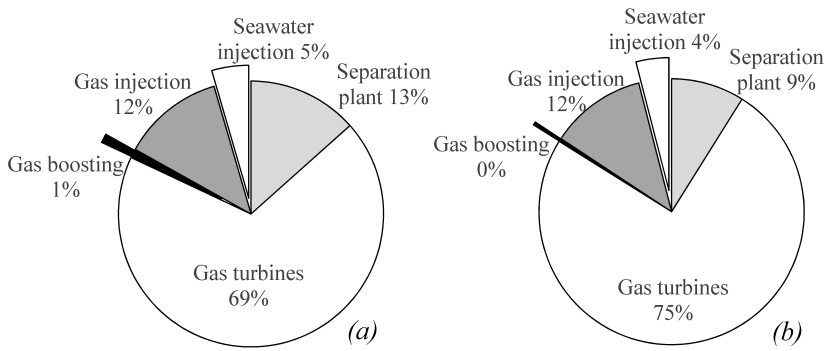


Figure 29 – Exergy destruction rate distribution for: (a)-Hysys model and (b)-EES model.

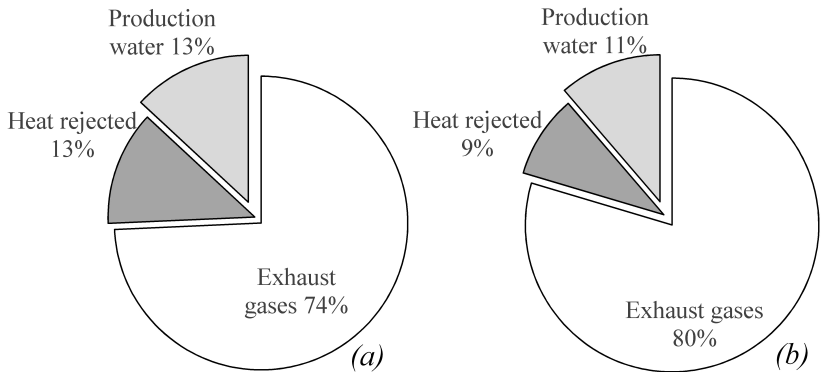


Figure 30 – Exergy losses distribution for: (a)-Hysys model and (b)-EES model.

Table 21 – Exergy losses distribution.

| System           | $y_{L,i}$           | This work  |              |
|------------------|---------------------|------------|--------------|
|                  | <i>Nguyen, 2012</i> | <i>EES</i> | <i>Hysys</i> |
| Exhaust gases    | 0.914               | 0.796      | 0.743        |
| Cooling water    | 0.065               | 0.091      | 0.126        |
| Flared gases     | 0.012               | 0.000      | 0.000        |
| Production water | 0.009               | 0.113      | 0.131        |

### 4.3.2 Exergy performance

From the definition of the exergy performance indicators presented in Sec. 3.3.3.2, it is possible to demonstrate how the consumed exergy is effectively transferred to obtain the desired effect (or products) of the plant. Tabs. 22 and 23 summarize the data related to the exergy performance obtained from models developed using Hysys and EES respectively. Particularly, the formulation presented in Eq. 4.2 was applied to the exergy balance obtained with the EES model in order to obtain comparable data. Despite compositional changes were not taken into account, there is a change in the mixing term due to the phase separation. As pointed by Silva et al. (2012), this term corresponds to the main product of separation processes.

$$\Delta_{mix}B_j = n_j \left( R T_0 \sum z_i \ln (z_i \cdot \gamma_i) \right) \quad (4.2)$$

where  $n_j$  corresponds to the molar flow of stream  $j$  in kmol/s and  $\gamma_i$  (*i.e.* activity coefficient of component  $i$ ) were approximated to 1.  $\Delta_{mix}B_j$  is given in kJ/s.

Figures 31 and 32 display the exergy efficiencies ( $\eta_p$  and  $\Phi$  respectively) for each subsystem obtained by both models. Regarding the degree of thermodynamic of perfection, the system with the worst performance within the processing plant (*i.e.* without considering the combustor chambers) corresponds to the seawater injection system followed by the gas injection for both models. This behavior is related to the proportion between the outlet exergy and the unused exergy (*i.e.* losses or destruction) by the operation; the lower the outlet exergy magnitude, worse the exergy performance is. Thus, for processes with outlets with high exergy content (*e.g.* gas streams) an amount of unused exergy does not have a significant impact over  $\eta_p$ . While pro-

Table 22 – Exergy performance indicators by system - Hysys model.

| <b>System</b>             | $\eta_p$      | $\Phi$       |
|---------------------------|---------------|--------------|
| Separation plant          | 0.9957        | 0.008        |
| Gas turbines              | 0.2808        | 0.281        |
| Gas boost system          | 0.9957        | 0.030        |
| Gas injection system      | 0.9919        | 0.403        |
| Seawater injection system | 0.8857        | 0.553        |
| Whole plant               | <i>0.9897</i> | <i>0.124</i> |

Table 23 – Exergy performance indicators - EES model

| <b>System</b>             | $\eta_p$      | $\Phi$       |
|---------------------------|---------------|--------------|
| Separation plant          | 0.9953        | 0.004        |
| Gas turbines              | 0.2563        | 0.256        |
| Gas boost system          | 0.9958        | 0.504        |
| Gas injection system      | 0.9943        | 0.517        |
| Seawater injection system | 0.9120        | 0.747        |
| Whole plant               | <i>0.9901</i> | <i>0.137</i> |

cesses with products with relatively low exergy content (*e.g.* seawater streams) have a  $\eta_p$  more sensible to their unused exergy.

By other side, considering the exergy indicator  $\Phi$  for each subsystem within the processing plant, the separation plant appears with the lowest exergy performance. This is related with the exergy-dissipative operations (*i.e.* pressure reduction, mixing and recirculation) that dominate the separation plant. Analogously, it can be inferred that the discrepancies between the values reported by the models are associated with the recirculation modeling. While in EES model these streams were not considered, in Hysys were considered as exergy losses for each specific operation.

Particularly for the gas turbines, the value of  $\eta_p$  equals the  $\Phi$  value. This is related to the power produced by this system and the performance reported for the equipment. The difference between the reported values from both models corresponds to the operation point of turbines. While the power required by the plant in EES was 12.97 MW, the power requirement in Hysys was 14.57 MW.

Regarding the overall exergy performance, the results were consistent for both models. EES reports higher performance indicators,

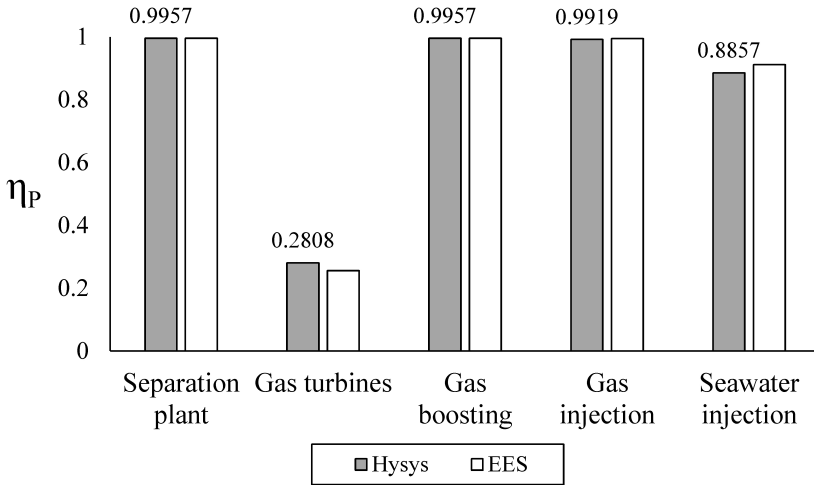


Figure 31 – Exergy efficiencies ( $\eta_p$ ) for Hysys and EES models.

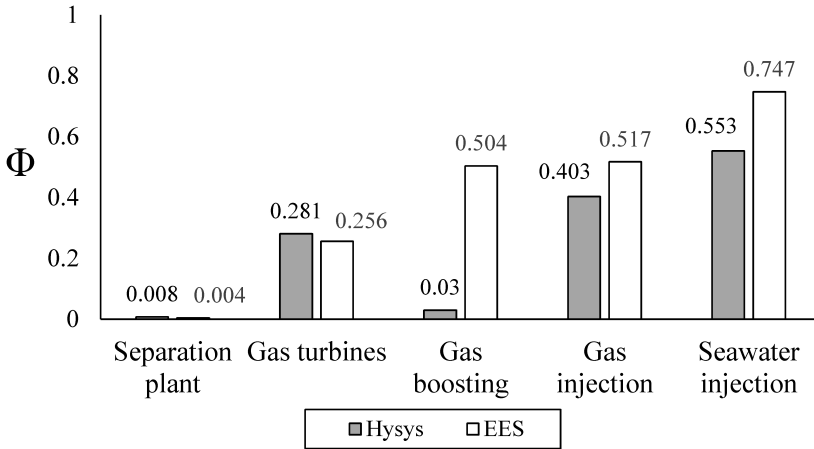


Figure 32 – Exergy efficiencies ( $\Phi_p$ ) for Hysys and EES models.



probably associated with the calculation of the specific chemical exergy of the oil streams for  $\eta_p$  and with the calculation of mixing exergy for  $\Phi$ . In the first case, the sum of component contributions to obtain  $b_{ch,oil}$  (Hysys case) was greater than the calculation of this considering the oil as a unique substance (EES case). Consequently, this affects directly the ratio between the outlet exergy and unused exergy (thus  $\eta_p$ ). By other side, considering that the oily and aqueous phases were treated as pure substances in EES (*i.e.*  $\Delta_{mix}B_j = 0$ ), the mixing term difference between products and inlets was greater than that reported using Hysys.

#### 4.4 ORC COUPLED TO THE PLANT

There are multiple considerations and variables to define in order to model adequately the operation of the ORC and its incorporation to an existing system. Given the extensive literature dedicated to explore the performance of this system and the focus of this work, the ORC modeled to be included into the studied plant was defined based on previous studies that indicate cyclopentane as the best choice when there is a comprise between performance, compactness and economic revenue (PIEROBON et al., 2013; LAI; WENDLAND; FISCHER, 2011). However, the integration of the cycle still has various degrees of freedom to adjust its service within the plant. As can be deduced from the information presented in Sec. 3.4.3, following criteria were applied in the Hysys model with the purpose of reducing conveniently the number of degrees of freedom when calculating the performance of the integrated ORC.

- The maximum HTF temperature was set to 300°C (stream E07).
- The mass flow of HTF is calculated to meet a pinch point of 10°C in the heat exchanger E-E01.
- The ORC working fluid flow and HTF outlet temperature (stream E02) are updated to meet the pinch point restrictions of the heat exchangers within the ORC system.
- A superheating of 1°C was set at E-F01 (ORC subsystem).
- A pinch point of 5°C was set for the regenerator E-F04.
- The evaporator pinch point is updated to meet a minimum approach of 5 °C between the cyclopentane temperature profile and the HTF temperature profile.

- The ORC output is subtracted from total plant demand, and the operation conditions of gas turbines are updated according to this value.

With the adoption of these criteria, the ORC system is modeled completely defining only the evaporation temperature at E-F02. In that way, a set of 20 temperatures ranging from 180°C up to 235.5°C were run in order to examine the behavior of the energy and exergy parameters of the cycle and choose a convenient evaporation temperature. As it can be seen in Fig. 33, the examined parameters were: (i) cyclopentane mass flow, (ii) ORC exergy performance, (iii) Total rejected heat and (iv) ORC output.

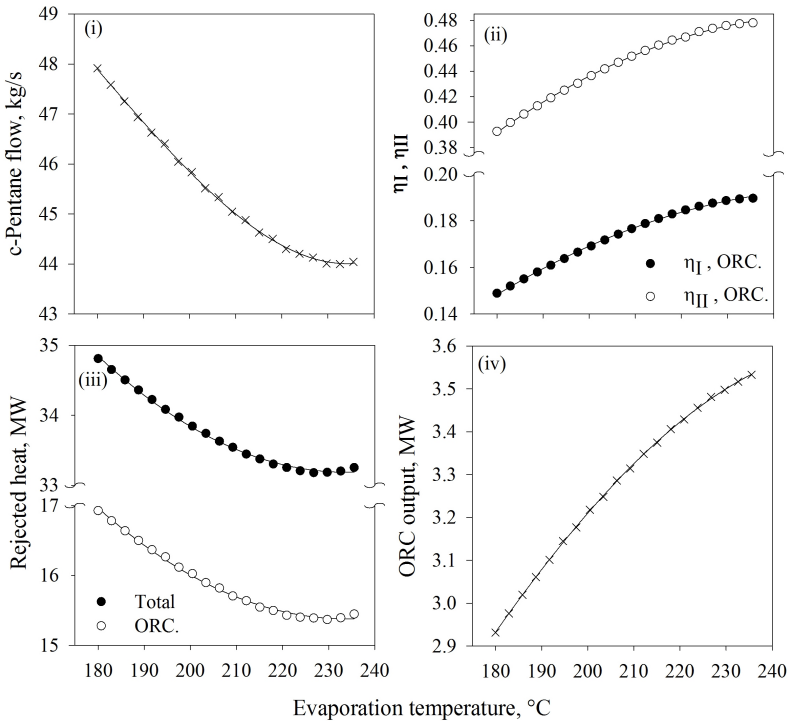


Figure 33 – Variation of (i) cyclopentane mass flow, (ii) ORC performance, (iii) Rejected heat and (iv) ORC output with the evaporation temperature of cyclopentane.

An inspection of the figures on the left side indicates a local minimum of the working fluid mass flow and the plant rejected heat in the proximity of its critical point ( $226.8^{\circ}\text{C}$ ). Conversely, the performance and the output of the cycle demonstrate a continuous increase with the evaporation temperature ( $T_{ev}$ ). This behavior apparently refutes the results obtained by Declaye (2009) described previously in Sec. 2.3.2.2. However, as explained by Invernizzi, Iora e Silva (2007), when the critical temperature ( $T_c$ ) of the working fluid is lower than that of the heat source (as in this case), the resulting optimum  $T_{ev}$  is very close to its  $T_c$ . On the contrary, if  $T_c$  is higher than the maximum temperature of the heat source (as ketone in the example earlier shown), optimum  $T_{ev}$  should be determined in order to maximize the ORC output.

In order to investigate the behavior of the curves shown previously, an examination of the ORC operation conditions and the HTF outlet temperature was carried out. An inspection of Fig. 34 indicates a local maximum of HTF outlet temperature ( $T_{E02}$ ) close to the  $T_{ev}$  where the heat rejected by the plant reported a minimum.

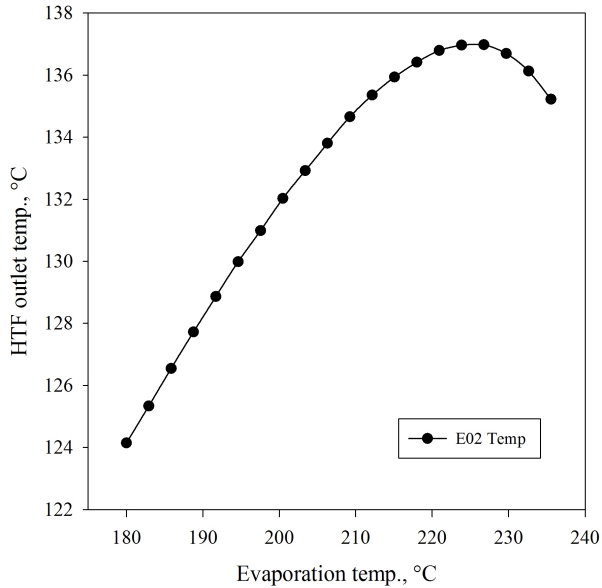


Figure 34 – Variation of the HTF outlet temperature and HTF mass flow with the evaporation temperature of cyclopentane.

Analogously, operation conditions of the cycle using the minimum and the maximum evaporation temperatures ( $180^{\circ}\text{C}$  and  $235.6^{\circ}\text{C}$  respectively) were compared with those calculated with a  $T_{\text{ev}} = 226.8^{\circ}\text{C}$  in the T-s diagram. As can be seen from Fig. 35(i), the higher the  $T_{\text{ev}}$ , the larger the  $\Delta P$  in the expander and the higher the temperature of the expander outlet (stream F11). Consequently, there is an increment of the ORC output (see Fig. 33(iv)) with the simultaneous reduction of its heat input, inherent to the load reduction in gas turbines (see Fig. 36). As the heat input decreases, the working fluid mass flow should be reduced to meet the energy balance of the cycle components with the established constraints (see Fig. 33(i)). As illustrated in Fig. 36, the increase of ORC output simultaneously with the decrease of the cyclopentane mass flow implies a rise in its specific work.

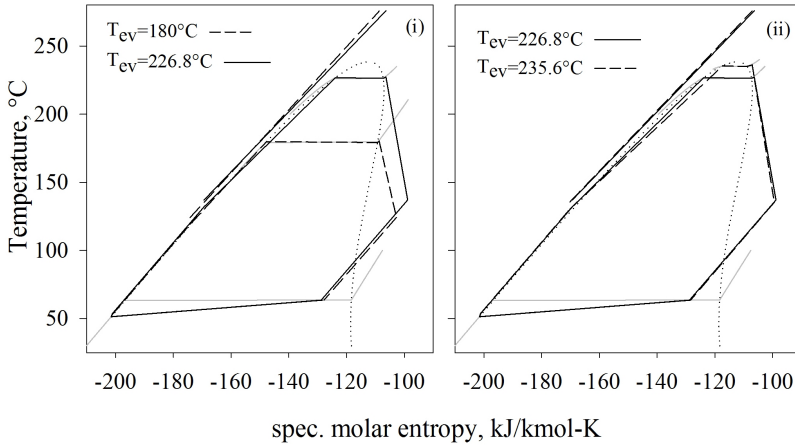


Figure 35 – T-s diagram of the ORC at different evaporation temperatures.

Taking into account the temperature rise at the expander outlet, the heat capacity flows and the PPD constraints for E-F03 (economizer) and E-F04 (regenerator), an increase of  $T_{\text{ev}}$  results in an increase of  $T_{\text{E02}}$ . As this temperature increases, the HTF temperature difference at E-E01 decreases and its circulating mass flow should be increased in order to meet the energy balance of the equipment with its specified PPD.

By other side, the behavior of the results suggests that there is a maximum  $T_{\text{E02}}$  (see Figs 34 and 35(ii)) reported at a  $T_{\text{ev}}$  in the prox-

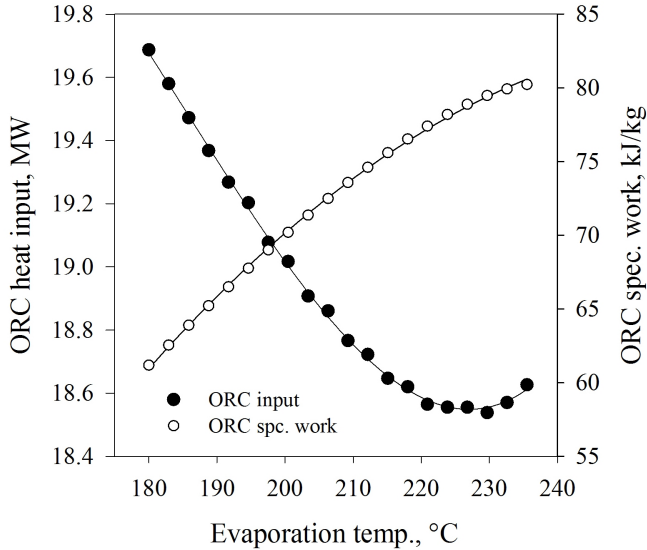


Figure 36 – Variation of ORC input and cyclopentane specific work with the evaporation temperature.

imity of  $226.8^{\circ}\text{C}$  in which the cyclopentane mass flow and the rejected heat display a minimum value (see Fig 33(i)-(iii)). It could be inferred that the location of this point is influenced by the performance of the cycle together with the gas turbines operation, which is determined by the whole plant demand.

In this way, the ORC working  $T_{\text{ev}}$  was set at the temperature that reports the minimum mass flow and rejected heat among the 20 analyzed temperatures (from  $180^{\circ}\text{C}$  up to  $235.6^{\circ}\text{C}$ ) in each analyzed scenario. For this case a  $T_{\text{ev}}$  of  $226.8^{\circ}\text{C}$  was set for the ORC system, which reports an output of 3.48 MW.

With the aim of showing the effect that the ORC has over the operation of the plant, a comparison of some key parameters is presented in Tab. 24. In general, the inclusion of the ORC within the plant has a positive impact over its performance. The improvement of thermal efficiency of the power generation and the reduction of the heat rejection of the plant were remarkable, although fuel savings and reduction of  $\text{CO}_2$  emissions are the most interesting improvements environmentally and economically speaking. Concerning the exergy performance

indicators, the operation of the ORC system has a greater impact over the chosen  $\eta_{II}$ , which would be the most appropriate to demonstrate its influence over the plant performance.

Table 24 – Effect of the ORC integration over some production parameters of the plant

| Parameter                                      | Base   | Base +ORC | % Diff. |
|--|--------|-----------|---------|
| Power demand, kW                               | 14459  | 14821     | 2.50    |
| Heat rejected, kW                              | 39662  | 33177     | -16.35  |
| Fuel consumption, $10^3 \text{ Nm}^3/\text{d}$ | 106.2  | 90.4      | -14.93  |
| $\lambda$ , MJ/m <sup>3</sup> oil              | 19.44  | 16.54     | -14.93  |
| Exhaust mass flow, kg/s                        | 60.85  | 56.31     | -7.45   |
| Thermal efficiency                             | 0.2946 | 0.3550    | 20.50   |
| $\eta_P$                                       | 0.9897 | 0.9913    | 0.16    |
| $\eta_{II}$                                    | 0.1250 | 0.1461    | 16.91   |

## 4.5 PRODUCTION PARAMETER PROFILES

Given the chosen performance indicators and based on the obtained results concerning the integration of the ORC within the plant, an analysis of the behavior of the plant performance when varying production parameters is done by comparing the base case with that with the ORC incorporated. These results can bring a better understanding of the effect of the ORC over the performance of the plant under changing operation conditions, which is the most common situation in this type of installation. As described earlier in Sec. 3.2.4, the performance of the plant was evaluated along an arbitrary production profile formed by 16 cases varying 5 production parameters separately, such that each parameter was modified (increased or reduced) independently along 4 cases. Table 25 presents the chosen production parameters together with their variation ranges and associated cases. The base case analyzed in previous sections corresponds to the case N° 6.

### 4.5.1 ORC working $T_{ev}$ establishment

Prior to the evaluation of the production profile, it is necessary to establish the ORC working  $T_{ev}$  in each scenario. In that way, Tab. 26

Table 25 – Production parameters profiles.

| Parameter  | Range         | Cases   | Behavior  |
|--|---------------|---------|-----------|
| Produced oil, m <sup>3</sup> /d                    | 1800 - 9000   | 0 - 3   | increased |
| Production water, m <sup>3</sup> /d                | 200 - 3800    | 3 - 6   | increased |
| Well pressure, kPa                                 | 1500 - 3000   | 6 - 9   | decreased |
| Gas injected, 10 <sup>6</sup> · Nm <sup>3</sup> /d | 1.5 - 2.1     | 9 - 12  | increased |
| Seawater injected, m <sup>3</sup> /d               | 12000 - 18000 | 12 - 15 | increased |

presents the selected temperatures using the criterion described in the previous section. By the other side, Fig. 37 displays the curves of the total rejected heat as a function of ORC  $T_{ev}$  for some reference scenarios with the aim of illustrating the adopted method and show the local minimum found in each case.

Table 26 – ORC  $T_{ev}$  chosen for each case.

| Case | $T_{ev}$ | Min. Heat, kW |
|------|----------|---------------|
| 0    | 226.8    | 32097         |
| 1    | 229.7    | 32383         |
| 2    | 226.8    | 32658         |
| 3    | 229.7    | 32929         |
| 4    | 229.7    | 33028         |
| 5    | 229.7    | 33118         |
| 6    | 226.8    | 33177         |
| 7    | 229.7    | 33180         |
| 8    | 229.7    | 33183         |
| 9    | 229.7    | 33180         |
| 10   | 229.7    | 36085         |
| 11   | 229.7    | 38961         |
| 12   | 226.8    | 41829         |
| 13   | 226.8    | 41829         |
| 14   | 226.8    | 43042         |
| 15   | 229.7    | 43641         |

As can be seen, the minimum heat rejected by the plant is apparently located at a  $T_{ev}$  between 223.8 and 232.6 °C independently the operation conditions of the plant (the values found for  $T_{ev}$  were 226.8 °C in some cases and 229.7 °C in the others). This range is relatively wide (8.8 °C) and it is not possible to conclude where the minimum

is located because the number of points within the analyzed  $T_{ev}$  range were not enough to obtain a narrower range for its location. An algorithm of optimization can be applied in further analysis in order to calculate its value with more accuracy and determine if it is constant independently to the operation parameters of the plant.

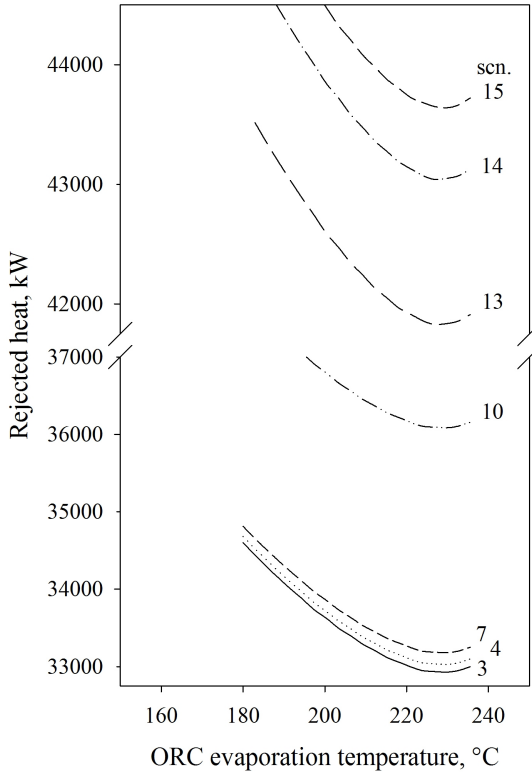


Figure 37 – Total rejected heat vs. ORC  $T_{ev}$  for selected scenarios.

#### 4.5.2 Influence of production parameters over the plant performance

Concerning the power plant demand, it can be seen in Fig. 38(i) that is widely dominated by the injection of gas and seawater. The



reduction of well pressure evidently has no effect over the power supply to the plant and the pumping work (produced oil and production water) is not appreciable when compared with the injection processes. By the other hand, the integration of the ORC system gives a slight increase of power demand due to its pumping work. Analogously, the rejected heat presents a great dependence with the operation that reports the larger energy consumption, which is logical since the greater demand, the higher the power generated by the gas turbines, thus more is the fuel burned and the exhaust gases rejected. The rejection of heat is notably reduced by the ORC integration, a reduction of about 15.4-18.5% is reported along the entire production profile. Evidently, an increase of the work supplied by the ORC implies a reduction of the waste heat of the plant.

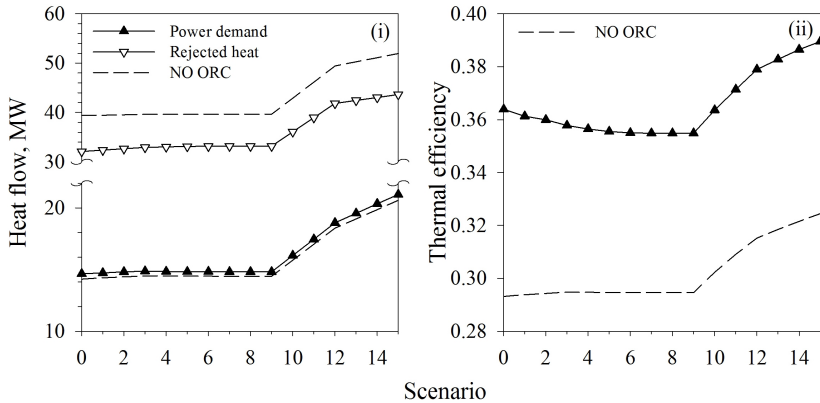


Figure 38 – Total rejected heat (i), power demand (i) and thermal efficiency of power generation (ii) profiles.

By other side, the thermal efficiency of the power generation within the plant is presented in Fig. 38(ii). Initially for cases 0 to 3, there is a little increase in thermal efficiency when the ORC is not included. However, the opposite is found when this system is operating. This behavior could be associated with the heat withdrawal in the heat exchanger E-B02: as the oil or water flow increases, the heat transferred to the well fluid in this equipment also increases. Thus, the exergy transferred by the HTF for activating the ORC diminish with the inherent decrease in ORC output (as illustrated in Fig. 39).

Analogously to the power demand and rejected heat, the thermal

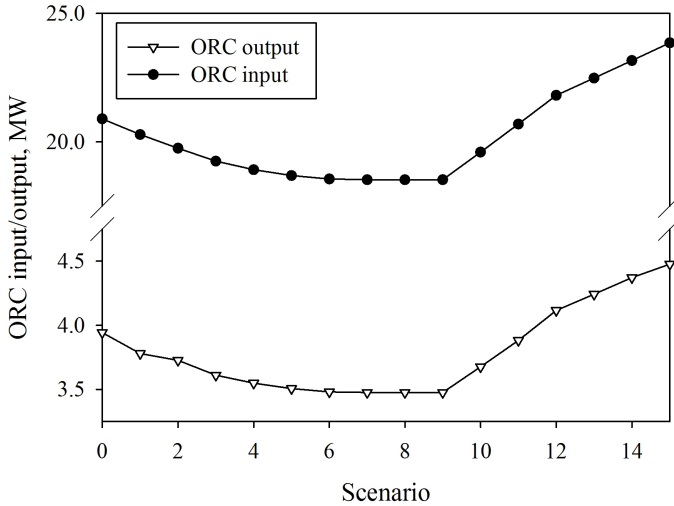


Figure 39 – ORC input and output, MW.

efficiency of the plant is strongly influenced by the injection of gas and seawater processes. Also considering that the inherent efficiency of the gas turbines increases as their load increases, a notable enhancement of about 20-24.4% is obtained along the entire profile when applying the ORC system for WHR.

The degree of thermodynamic perfection  $\eta_P$  together with the proposed indicator  $\lambda$  are particularly influenced by the quantity of the produced oil in the plant (see Fig. 40(i)). It is likely that this behavior is linked with the great exergy content of oil and to the rapid decrease of the ratio between the consumed energy and oil production respectively. The influence of the other parameters over  $\eta_P$  and  $\lambda$  is illustrated in Fig. 40(ii), where the first three cases were omitted. An increase in the production water flow reduces marginally  $\eta_P$ , which is associated with the inherent increase of the exergy losses. While it practically has no effect over the  $\lambda$  value. A similar situation is reported for the well pressure, but its decrease slightly improves the value of  $\eta_P$  evidently due to the reduction of the exergy destroyed at inlet manifolds (represented by valve L-B00).

By the other hand, the injection of gas and water has a greater impact over these indicators. It seems that the increase of gas and water flows implies a decrease of  $\eta_P$ , and an increase in  $\lambda$ . It could

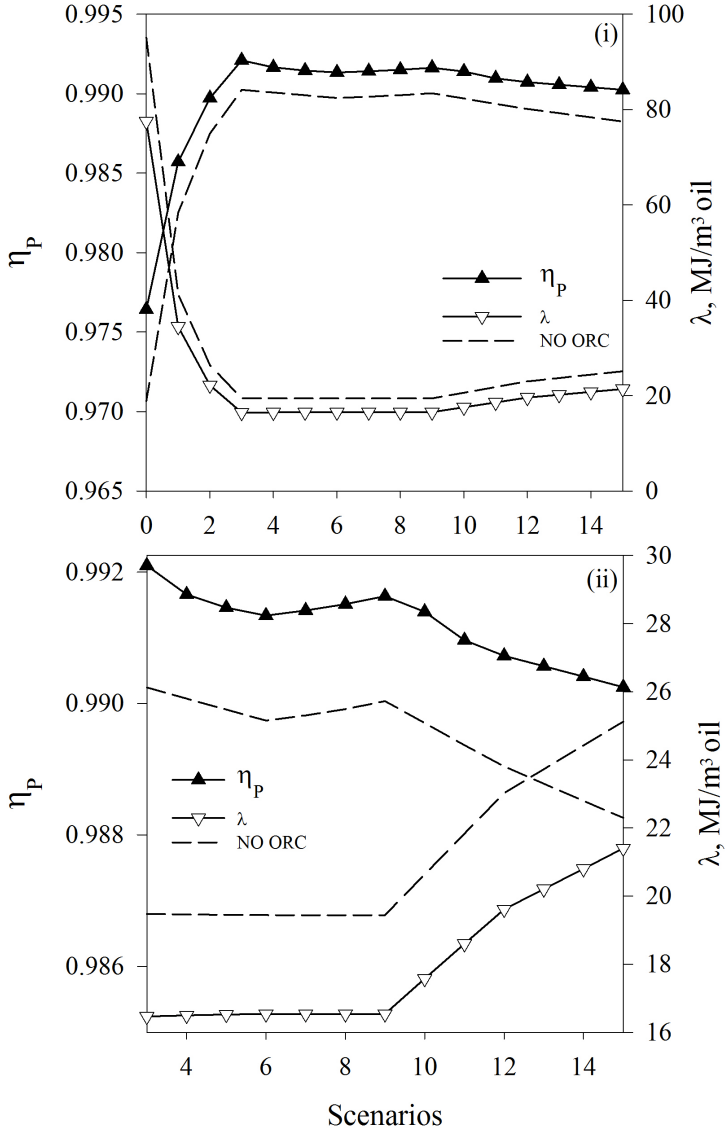


Figure 40 –  $\eta_P$  and  $\lambda$ : (i) for cases 0 through 15 and (ii) for cases 3 through 15.

be linked to the greater exergy losses rejection in the injection systems and the increment of the energy consumption respectively. Anew, the application of ORC seems to be favorable for the performance of the plant independently of the operation conditions. The improvement was around 0.15-0.59% and 15.8-18.4% for  $\eta_P$  and  $\lambda$  respectively.

In general, the exergy performance indicator  $\eta_{II}$  exhibits a greater variation along the production profile than  $\eta_P$  and  $\lambda$  (see Fig. 41). As it can be seen in Fig. 41(i), the shape of the curve for the plant with the ORC incorporated is approximately the same as that displayed in the base case. However, this graph was split into case groups depending on the varying parameter in order to obtain a better resolution. First, it seems that the behavior of  $\eta_{II}$  displays the same effect that  $\eta_I$  in the first three cases (see Fig. 41(ii)), where the decrease of the performance efficiency is related to the amount of heat withdrawn by the HTF to activate the ORC. However, between the third and fourth case, there is a sudden rise in the  $\eta_{II}$  value. The causes of this behavior are not clear, but it can be attributable to the simultaneous influence of the separation addend (which is increasing) and the decline of ORC output on the indicator  $\eta_{II}$ . In the same way, the behavior of  $\eta_{II}$  with respect to the production water flow and well pressure can be seen in Fig. 41(iii) and (iv) respectively. While the increase of the production water flow results in a decrease of the exergy efficiency due clearly to the growth of the exergy losses associated with this stream, a reduction of well pressure prior to manifold valves demonstrate an improvement of  $\eta_{II}$ . It could be linked to the reduction of the destroyed exergy at this point.

By other side, the rise of the injected gas and seawater flows increments the value of the overall  $\eta_{II}$ . It could be explained by the increment of the ratio between the product exergy and the consumed exergy as the gas or seawater flow increases in each subsystem. In addition, the ORC contribution seems to be uniform along these profiles as illustrated in Figs. 41(v) and 41(vi).

With the purpose of comparing the influence of the analyzed production parameters over the exergy efficiency of the plant and contrast it with that using the coupled ORC, an influence factor  $f$  is introduced for each segment shown in Fig. 41 using the following expression:

$$f = \left| \frac{\Delta\eta_{II}}{\Delta A_n} \right| \quad (4.3)$$

where  $A_n$  corresponds to the normalized production parameter

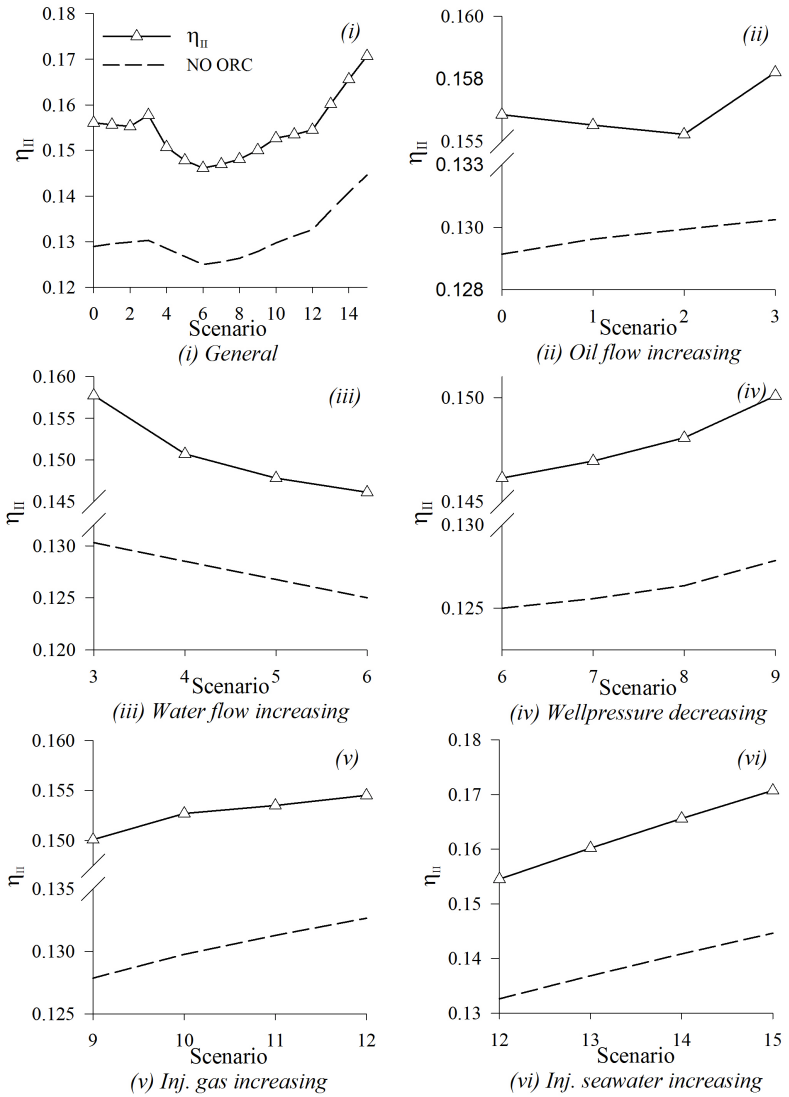


Figure 41 –  $\eta_{II}$  variation along the production profile.

(i.e.  $\Lambda$  represents the oil flow, well pressure, water flow, etc.). As can be seen from Fig. 42(i), the amount of injected seawater seems to be the variable with the greatest weight over the exergy indicator  $\eta_{II}$  (i.e. a variation of seawater flow results in a greater variations of  $\eta_{II}$  when compared with the other parameters), independently to the variation of the other production parameters. In contrast, the produced oil has the lowest influence over this indicator when no ORC is used and its impact presents a slight decline as this flow increases. By other side, the effect of the injected gas increase and the production water decrease is intermediate and presents a minimal drop as the injected gas increases while the effect of the production water seems to be constant. Analogously, the influence of the well pressure over  $\eta_{II}$  appears to be greater as its value decreases.

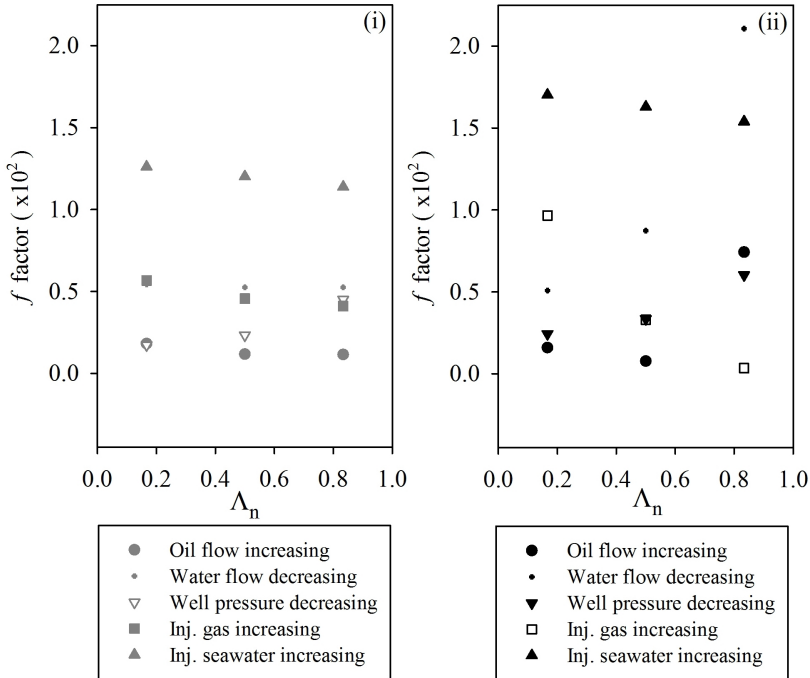


Figure 42 – Influence factor  $f$  for each production parameter. (i) current configuration, (ii) ORC integrated.

It can be inferred from Fig. 41 that the improvement of  $\eta_{II}$  of

the plant using the ORC was around 14-17% along the entire profile. Despite its contribution apparently was uniform in whole the range, data presented in Fig. 42(ii) suggest that the impact of the production parameters over the plant performance using the ORC was altered when compared with the current configuration. The increase of  $\eta_{II}$  is dominated principally by the amount of injected water, except when the flow of production water approaches its minimum value (point at upper right corner). Analogously, as the injected gas flow and well pressure increase, their impact over the exergy performance decrease. The influence of oil flow along the profile is not very clear probably due to the simultaneous effect of the ORC output and the separation addend in the definition of  $\eta_{II}$ . A further analysis can be conducted in order to analyze the impact of these parameters separately over the exergy performance as defined in this work.

#### 4.5.3 Influence of the production parameters over ORC performance

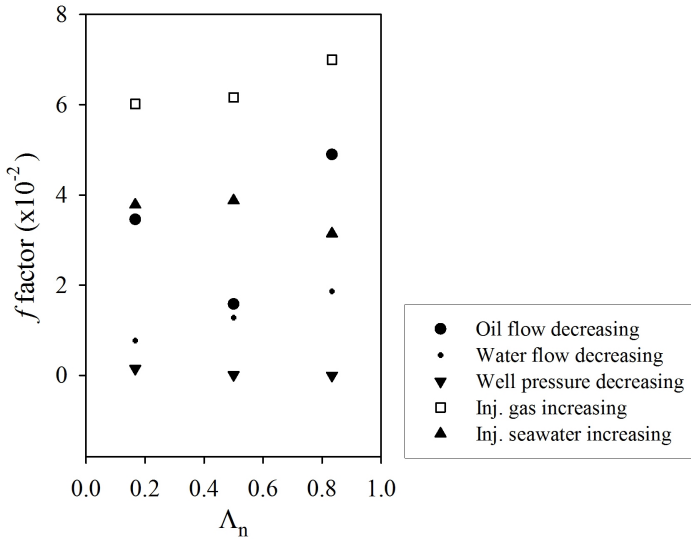


Figure 43 – Influence factor  $f$  for each production parameter applied in the ORC performance.

As mentioned earlier, when an ORC system is used as WHR system, it is more advantageous to obtain a greater output than a greater efficiency. Consequently, the variable analyzed to determine the influence of the production parameters over the performance of this system was its power output (as illustrated in Fig. 39). In general, it was found that the oil and water flows have a negative impact over the ORC input. As mentioned previously, the greater the fluid flow, the lower the amount of heat for activating the ORC; thus the lower its output. Analogously, well pressure has no practical effect over the ORC output and the injection of gas and seawater dominates noticeably the performance of this system. Evidence for this is presented in Fig. 43, where the influence factor introduced previously was applied to the ORC output.

As noted earlier, the parameter with the greatest influence over ORC performance is the gas injection/export followed by the seawater injection, except when the oil flow is low enough to promote the amount of heat transferred to the ORC (a situation that is unlike given the main purpose of the plant). This tendency is evidently caused by the power consumed by both injection operations. The greater the amount of gas (or water) to be injected, greater the required power of the plant and more gas is burned in turbines, which produce more exhaust gases; thus more available heat to activate the cycle. In contrast, although the effect of the reduction of water flow increases along the profile, this is not enough to overcome the effect of the injection processes. As predicted before, the effect of the reduction of well pressure has no inference over the performance of ORC.



## 5 DISCUSSION

Previous works focused on the implementation of ORC technology for WHR in offshore platforms have demonstrated its usefulness under specified conditions in particular platforms (LARSEN *et al.*, 2013; PIEROBON; NGUYEN, 2012b; PIEROBON *et al.*, 2013). However, these studies have not considered the inherent variation in the platform process conditions along its lifespan and by the other side, the exergy analysis for identifying the operations that more strongly demote the efficiency of a process has not been fully adopted in this type of industry. In that way, this work implements the exergy analysis approach to examine the effect of an ORC over the performance of a Brazilian FPSO under varying production conditions.

The adopted procedure dealt with the adequate exergy calculation of petroleum fractions and their mixtures as well as the formulation of an appropriate performance indicator associated with the main tasks of the plant. The calculation routines were implemented using two computer programs: Hysys and EES. Particularly, the most significant simplifications were applied to the EES algorithm and the results demonstrated a good agreement for both models concerning the overall plant efficiency. However, there were discrepancies when analyzing the efficiency of plant subsystems, apparently caused mainly by the omission of recycle streams in the EES routine.

When the procedure for oil characterization were assuming a group of pseudocomponents, it is recommended to incorporate the calculation of chemical exergy of these hypothetical compounds together with their Gibbs free energy ( $\Delta_f G^o$ ), in order to avoid uncertainties when a chemical reaction were carrying out within the model. However, it is important to emphasize the fact that all the exergy balances done in this work were corroborated using the relation between the generated entropy  $S_{gen}$  and the destroyed exergy  $B_D$  (see Sec. 3.3.2), showing a good agreement.

Analogously, the ORC system was modeled attached to the existing HTF circuit, taking part of the exergy of the exhaust gases coming from the gas turbines in order to produce additional power. The ORC working fluid chosen was the cyclopentane and its evaporation temperature was set aiming a minimum amount of rejected heat. Next, the complete model (plant + ORC) was compared with the current configuration through a hypothetical profile, varying (i) the produced oil flow, (ii) the production water flow, (iii) the well pressure, (iv) the gas in-

jected and (v) the seawater injected flow, within the design constraints of the plant.

Evaluation of the power demand, total rejected heat and thermal efficiency of the plant indicates a wide influence of the amount of gas and seawater injected back to the reservoir. This observation is in agreement with previous studies (NGUYEN et al., 2013; VOLDSUND et al., 2010) and is associated with the increase of burned gas (thus the exhaust gases) and the rise of the power load at gas turbines. Particularly, the ORC output and its contribution is influenced by the oil and production water flows. It must be related with the amount of heat withdrawn from the HTF in heat exchanger E-B02. The greater the oil (or water) flow, the lesser the available heat to activate the ORC. In the same way, the injection of gas and water appear to have the greatest effect over the performance indicators  $\eta_P$  and  $\lambda$  when the oil flow is not considered.

The use of the degree of thermodynamic perfection  $\eta_P$ , was compared with another exergy indicator  $\eta_{II}$ . Although the behavior of the results was similar, the figures obtained using  $\eta_{II}$ , make more evident the effect of the variation of the plant operation conditions over its performance.

Obtained results show that the ORC integration has a substantial contribution to the performance of the plant and its magnitude remains approximately homogeneous along the entire profile. A comparison of the influence of the production parameters over the exergy efficiency pointed the seawater injection flow out as the parameter with the greatest impact over the indicator when the ORC is not installed. However, the incorporation of the ORC demonstrates an increase of the influence of the other parameters; especially of the production water flow. By other side, the production variable that affects more markedly the ORC output is the injected gas flow, which is directly associated with the increment of the exergy carried to the ORC.

The data presented in this work are in line with previous studies focused on the exergy analysis of offshore platforms and the use of ORC the system for improving their energetic performance. Additionally, a primary comparison of the incidence of chosen production variables was carried out, demonstrating that their impact over the plant performance depends basically on their magnitude. Particularly in this case, the water injection flow was identified as the most dominant variable determining the performance of the plant. It could be associated with the fact that this operation has the best performance among the sub-systems of the plant and has the second largest power demand within

the plant. Although this observation corresponds to the analyzed plant specifically, this type of comparison offers a wider panorama concerning to what parameter is strongly-affecting the energy performance of the plant at given circumstances. In the same way, this approach may be used to analyze other types of production platforms with different configurations and processes involved. For example, for oils that have high salt content where a secondary "washing" stage is included, the exergy contribution of the salt content should be considered at inlet stream(s) and its separation must be evident in the performance indicator. Another case can be the case of heavy crudes or with trend to form emulsions, where more heating is needed to perform the separation of the water from the oil; here the exergy indicator proposed in this work could be strongly influenced by the amount of heat involved in the separation stage (as anticipated in the work of Oliveira e Hombeek (1997)).

Analogously, the performance of the ORC system was evaluated together with the variation of the production parameters of the plant. This innovative approach can bring a better idea of the most appropriate size of the ORC system when applied to this type of installations, which would not be necessarily one with the optimal size under a specific condition, but one that best fulfills the plant requirements and constraints along its lifespan.

The understanding of the behavior of the performance of the plant with variable production conditions –as proposed in this study, could have an important contribution concerning the analysis of actual production profiles and the establishment of the actual convenience of an ORC system given an actual production forecast. In that way, it would be necessary a validation of the proposed methodology with known profiles (record) of plants already established. Further analysis can be conducted considering performance, control and economic optimization strategies, fluid selection and more detailed comparison of the production variables aiming the fabrication and installation of suitable ORC systems in this industry.



## 6 CONCLUSION

The present work demonstrated the advantage of implementing an ORC as WHR system in an existing offshore platform under variable production conditions. It was found that the ORC has a positive impact over the performance of the plant independently of their operation conditions and its contribution seems to be homogeneous and not very influenced by production parameters of the plant. Specifically, it was reported an improvement of 14-17% in the exergy performance indicator and a reduction of 15.8-18.4% for the fuel consumption. These figures evidently imply a reduction of the environmental impact of the plant, proved by the inherent reduction of exhaust gases emissions and the reduction of rejected heat to the atmosphere (calculated as 15.4-18.5% based on current conditions). It would be interesting to complement these results with an economic analysis (*i.e.* costs assessment, payback period, etc.) aiming the feasibility of implementation of this system. By other side, a comparison of the influence of the production parameters over the performance of the analyzed plant indicated the gas and seawater injection as the most influencing operations over the exergy performance of the plant.

The main contribution of the present work consists in a procedure that considers variable operation parameters along the plant lifespan, aiming a wider panorama for exergy analysis and the application of ORC (or other technologies) systems in existing installations subject to large variations in their process conditions. Additionally, its application could offer a better understanding of the features that more strongly demote their efficiency under particular circumstances.

Regarding the modeling of the plant, qualitatively it was found that overall performance can be directly estimated omitting the composition analysis of the petroleum. However, when assessing the individual performance of the equipment (or subsystems) of the plant, it is strongly recommended to consider the composition of the petroleum since it affects importantly the exergy indicators, especially when a separation of phases are involved. In that way, the approach proposed in this work can be useful for selecting an adequate software depending on the required level of detailing. Analogously, when all the data of the plant were available, it is advisable to develop and corroborate the model, including all the components of the plant aiming additional applications for the unused exergy. For more advanced studies, it is desirable to give the same thermodynamic basis for the calculation of

chemical exergy and the composition of petroleum fractions (avoiding the use of empirical expressions), in such a way that discrepancies when considering chemical reactions are prevented.

It is recommended to develop a supplementary optimization algorithm aiming the most suitable  $T_{ev}$  for the ORC, meeting the maximum exergy efficiency of the plant. Nevertheless, the results of the present work constitute a reference basis for further analysis focused on the optimization of the project taking into account the minimization of the volume and cost of ORC components such that it fulfills the process requirements along a variable production profile. By other side an environmental impact analysis (*e.g.* LCA or exergo-environmental analysis) could be useful in order to demonstrate and justify the integration of this type of technologies beyond economic issues.

In order to promote the application of this type of technologies, the examination of commercially available equipment would be advantageous, such that the ORC modelling corresponds to real cycles and can address the choice of actual alternatives.

## REFERENCES

- ABDOLLAHI-DEMNEH, F. et al. Calculating exergy in flowsheeting simulators: A HYSYS implementation. *Energy*, Elsevier Ltd, v. 36, n. 8, p. 5320–5327, ago. 2011.
- ARNOLD, K.; STEWART, M. *Surface Production Operations: Design of Oil Handling Systems and Facilities*. 3. ed. Burlington: Gulf Professional, 2008. 722 p.
- ASPENTECH. *Aspen HYSYS: Simulation Basis Guide*. Burlington: [s.n.], 2011. 570 p.
- BAO, J.; ZHAO, L. A review of working fluid and expander selections for organic Rankine cycle. *Renewable and Sustainable Energy Reviews*, Elsevier, v. 24, p. 325–342, ago. 2013.
- BARTON, C. M. An overview of offshore concepts. In: *Expanding Facilities Knowledge Workshop*. Houston, TX: SPE, 2009. 195 Slides.
- BCS. *Waste Heat Recovery: Technology and Opportunities in U.S. Industry*. [S.l.]: DOE, 2008. 112 p.
- BEJAN, A. *Thermal Design and Optimization*. USA: Wiley, 1996. 532 p.
- BG Group. *Lula Crude Oil Assay*. 2012. <<http://www.bg-group.com/CrudeOilAssays/Brazil/Pages/Lula.aspx>>.
- BOTHAMLEY, M. Offshore processing options for oil platforms. In: *Proceedings of SPE Annual Technical Conference*. Houston, TX: SPE, 2004. p. 17.
- BRANCHINI, L.; PASCALE, A. d. D.; PERETTO, A. Systematic comparison of ORC configurations by means of comprehensive performance indexes. *Applied Thermal Engineering*, v. 61, n. 2, p. 129–140, nov. 2013.
- BRUNO, J. C. et al. Modelling and optimisation of solar organic rankine cycle engines for reverse osmosis desalination. *Applied Thermal Engineering*, v. 28, n. 17-18, p. 2212–2226, 2008.
- BULLER, A. T. Oil and gas technologies. In: *Technology Guide*. Berlin: Springer, 2009. cap. 8, p. 318–323.

CENGEL, Y.; BOLES, M. *Thermodynamics - An engineering approach*. [S.l.]: McGraw-Hill, 2010. 881 p.

CHANG, A.; PASHIKANTI, K.; LIU, Y. Characterization , Physical and Thermodynamic Properties of Oil Fractions. In: *Refinery Engineering: Integrated Process Modeling and Optimization*. [S.l.]: Wiley, 2012. cap. 1, p. 1–56.

CHEN, H.; GOSWAMI, D. Y.; STEFANAKOS, E. K. A review of thermodynamic cycles and working fluids for the conversion of low-grade heat. *Renewable and Sustainable Energy Reviews*, Elsevier Ltd, v. 14, n. 9, p. 3059–3067, 2010.

CRAGER, B. Floating production systems for offshore oil and gas fields. In: *Expanding Facilities Knowledge Workshop*. Houston, TX: SPE, 2010. 47 slides.

DECLAYE, S. *Design , optimization and modeling of an organic Rankine cycle for waste heat recovery*. 92 p. Thesis (Graduação) — University of Liege, Liège, 2009.

DENG, J.; WANG, R.; HAN, G. A review of thermally activated cooling technologies for combined cooling, heating and power systems. *Progress in Energy and Combustion Science*, v. 37, n. 2, p. 172–203, abr. 2011.

DOW Chemical. *Dowtherm A product information*. [S.l.], 2001.

GORDON, B. Floating Production, Storage and Offloading (FPSO) Facilities. In: *Lillehammer Energy Claims Conference*. Lillehammer: CCSL, 2012. 30 slides.

GRIP, C. et al. Possibilities and problems in using exergy expressions in process integration. In: *Proceedings of Renewable Energy Congress*. Linköping, Sweden: Linköping University, 2011. p. 1605–1612.

HEBERLE, F.; PREIBINGER, M.; BRÜGGEMANN, D. Advanced ORC fluid research for cycle efficiency improvement. In: *International Symposium on Advanced Waste Heat Valorisation Technologies*. Kortrijk: [s.n.], 2012. 26 Slides.

HINDERINK, A. P. et al. Exergy analysis with a flowsheeting simulator -I. Theory; calculating exergies of material streams. *Chemical Engineering Science*, v. 51, n. 20, p. 4693–4700, 1996.



- HUNG, T. et al. A study of organic working fluids on system efficiency of an ORC using low-grade energy sources. *Energy*, Elsevier Ltd, v. 35, n. 3, p. 1403–1411, 2010.
- IEA. *Combined heat and power: Evaluating the benefits of greater global investment*. Paris: OECD/IEA, 2008. 39 p.
- IEA. *World energy outlook*. Paris: OECD/IEA, 2012. 668 p.
- INVERNIZZI, C.; IORA, P.; SILVA, P. Bottoming micro-Rankine cycles for micro-gas turbines. *Applied Thermal Engineering*, v. 27, n. 1, p. 100–110, jan. 2007.
- KINNEY, B. Field development options / selection strategy. In: *Expanding Facilities Knowledge Workshop*. Houston, TX: SPE, 2012. 78 slides.
- KOCAMAN, A. Offshore Concept Selection. In: *Expanding Facilities Knowledge Workshop*. Houston, TX: SPE, 2008. 72 slides.
- LAI, N. A.; WENDLAND, M.; FISCHER, J. Working fluids for high-temperature organic Rankine cycles. *Energy*, Elsevier Ltd, v. 36, n. 1, p. 199–211, 2011.
- LARSEN, U. et al. Design and optimisation of organic Rankine cycles for waste heat recovery in marine applications using the principles of natural selection. *Energy*, Elsevier Ltd, p. 1–10, abr. 2013.
- LI, Y.-R.; WANG, J.-N.; DU, M.-T. Influence of coupled pinch point temperature difference and evaporation temperature on performance of organic Rankine cycle. *Energy*, v. 42, n. 1, p. 503–509, jun. 2012.
- LITTLE, A. B.; GARIMELLA, S. Comparative assessment of alternative cycles for waste heat recovery and upgrade. *Energy*, v. 36, n. 7, p. 4492–4504, 2011.
- LUDENA, C.; MIGUEL, C. de; SCHUSCHNY, A. Climate change and reduction of CO<sub>2</sub> emissions. *Environment and development series*, CEPAL, n. 150, p. 47, 2012.
- MAHONEY, C. N. 2013 deepwater solutions & records for concept selection. *Offshore Magazine*, WoodGroup Mustang, 2013.
- MAHONEY, C. N.; KITHAS, K. 2013 Worldwide survey of floating production, storage and offloading (FPSO) units. *Offshore Magazine*, WoodGroup Mustang, Houston, 2013.

MAXWELL, J. B. *Data Book on Hydrocarbons: Application to Process Engineering*. Malabar: Krieger, 1968. 259 p.

NGUYEN, T.-V. et al. Exergetic assessment of energy systems on North Sea oil and gas platforms. *Energy*, Elsevier, p. 1–14, 2013.

NGUYEN, T. van et al. Modelling and analysis of offshore energy systems on North Sea oil and gas platforms. In: *Proceedings of the 53rd SIMS conference on Simulation and Modelling*. Reykjavik: [s.n.], 2012. p. 16.

OLIVEIRA, S. de; HOMBEECK, M. van. Exergy analysis of petroleum separation processes in offshore platforms. *Energy Conversion Management*, v. 38, n. 15, p. 1577–1584, 1997.

PIEROBON, L. et al. Multi-objective optimization of organic Rankine cycles for waste heat recovery : Application in an offshore platform. *Energy*, Elsevier, v. 58, n. 1, p. 538–549, 2013.

PIEROBON, L.; NGUYEN, T. van. Technologies for waste heat recovery in offshore applications. In: *Energieffektivisering for fremtiden*. Lyngby: [s.n.], 2012. Poster.

PIEROBON, L.; NGUYEN, T. van. Waste heat recovery for offshore application. In: *1st International Symposium on Advanced Waste Heat Valorisation Technologies*. Kortrijk, Poland: [s.n.], 2012. Poster.

QUOILIN, S. et al. Working fluid selection and operating maps for Organic Rankine Cycle expansion machines. In: *International Compressor Engineering Conference*. Purdue: [s.n.], 2012.

RINGEN, S.; LANUM, J.; MIKNIS, F. P. Calculating heating values from elemental compositions of fossil fuel. *Fuel*, v. 58, p. 69–71, 1979.

RIVERO, R.; RENDON, C.; MONROY, L. The exergy of crude oil mixtures and petroleum fractions : calculation and application. *International Journal of Applied Thermodynamics*, v. 2, n. 3, p. 115–123, 1999.

SHIMAMURA, Y. FPSO / FSO : state of the art. *Journal of Marine Science and Technology*, v. 7, p. 59–70, 2002.

SIEMENS AG. *SGT-400 Industrial Gas Turbine*. Houston, TX, 2009. 4 p. <<http://www.energy.siemens.com/>>.

SILVA, J. A. da et al. On the exergy determination for petroleum fractions and separation processes efficiency. In: *14th Brazilian Congress of Thermal Sciences and Engineering*. Rio de Janeiro: ABCM, 2012. v. 0, n. 1.

SILVA, M. V. da. *Eficiência exergética de unidades estacionárias de produção de petróleo*. 152 p. Thesis (Master degree) — COPPE-UFRJ, Rio de Janeiro, 2008.

SIMMONS, M. R. Has oil and gas collapse sealed fate of peak oil? In: *Gulf Coast Chapter - PF&C Study Group Meeting*. Houston, TX: SPE, 2009. 50 slides.

SZARGUT, J.; MORRIS, D. R.; STEWARD, F. R. The exergy concept and exergy losses. In: *Exergy analysis of thermal, chemical, and metallurgical processes*. [S.l.]: Hemisphere, 1988. cap. 1, p. 332.

TCHANCHE, B. F. et al. Low-grade heat conversion into power using organic Rankine cycles - A review of various applications. *Renewable and Sustainable Energy Reviews*, Elsevier, v. 15, n. 8, p. 3963–3979, 2011.

TWU, C. H. An internally consistent correlation for predicting the critical properties and molecular weights of petroleum and coal-tar liquids. *Fluid Phase Equilibria*, Elsevier, v. 16, n. 2, p. 137–150, 1984.

VOLDSUND, M. et al. Exergy analysis of the oil and gas separation processes on a North sea oil platform. In: *Proceedings of the 23rd International Conference on Efficiency, Cost, Optimization, Simulation and Environmental Impact of Energy Systems*. Lausanne: [s.n.], 2010. p. 303–310.

WASCO. *Process description FPSO Cidade de Itajaí*. Singapore, 2012. 23 p.

WATSON, K.; NELSON, E. F. Improved methods for approximating critical and thermal properties of petroleum fractions. In: *Symposium on physical properties of hydrocarbon mixtures*. Washington: ACS, 1933. p. 880–887.

WHITSON, C. H. Characterizing Hydrocarbon Plus Fractions. *SPE Journal*, v. 23, n. 4, p. 683–694, 1983.

WILKINSON, R. *Speaking oil & gas*. Australia: BHP, 2006. 194 p.



## **APPENDIX A – Hysys model nomenclature**



## A.1 NOMENCLATURE

This appendix presents the full scheme used in Hysys to simulate the plant (see Sec. A.2) and the nomenclature is introduced in order to improve the understanding of the model. In that way, Tab. 27 lists all the items included within the PFD (Process Flow Diagram) together with their used symbols and acronyms. Here, the letter *S* refers to the subsystem wherein the equipment or stream is: **A**– power generation subsystem, **B**– separation plant, **C**– boost compression subsystem, **D**– gas injection/export subsystem, **E**– HTF circuit, **F**– ORC subsystem and **H**– seawater injection subsystem. In the case of work and heat flows, the letter *Z* refers to the associated equipment and correspond to the letter that identifies it (i.e. bold letters in acronym column). For example HE-B05 identifies the heat flow (H) associated with the heater (E) E-B05, which is part of the separation subsystem (B). *00* refers to the item numeration.

Table 27 – PFD nomenclature.

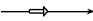


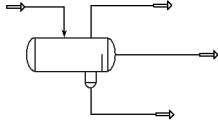

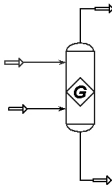
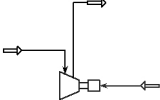
| Item                  | Figure  | Acronym                |
|-----------------------|---|------------------------|
| Material stream       |    | <i>S00</i>             |
| Heat flow             |    | <b>H</b> Z- <i>S00</i> |
| Work flow             |    | <b>W</b> Z- <i>S00</i> |
| Three phase separator |   | <b>V</b> - <i>S00</i>  |
| Air cooler            |  | <b>F</b> - <i>S00</i>  |
| Combustor             |  | <b>R</b> - <i>A00</i>  |
| Compressor            |  | <b>C</b> - <i>S00</i>  |

Table 27 – PFD nomenclature (*cont.*).

| Item           | Figure | Acronym      |
|----------------|--------|--------------|
| Cooler         |        | <b>E-S00</b> |
| Expander       |        | <b>T-S00</b> |
| Heat exchanger |        | <b>E-S00</b> |
| Heater         |        | <b>E-S00</b> |
| Mixer          |        | <b>M-S00</b> |
| Pump           |        | <b>P-S00</b> |
| Recycle        |        | <b>R-S00</b> |
| Separator      |        | <b>V-S00</b> |
| Subsystem      |        | As named.    |
| Tee            |        | <b>Y-S00</b> |
| Valve          |        | <b>L-S00</b> |



## A.2 PROCESS FLOW DIAGRAMS

Figures 44 through 49 present the process flow diagrams of the separation plant and its subsystems, including secondary streams as recycles and condensates separated from gas streams. Second turbine is also shown together with the split of fuel gas stream (B18) and the mixing of the exhaust gas streams (A07a and A07b).

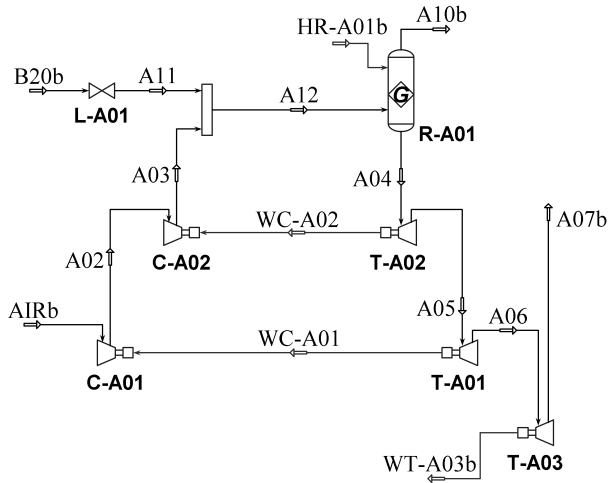


Figure 44 – Process flow diagram of a power subsystem turbine (A).

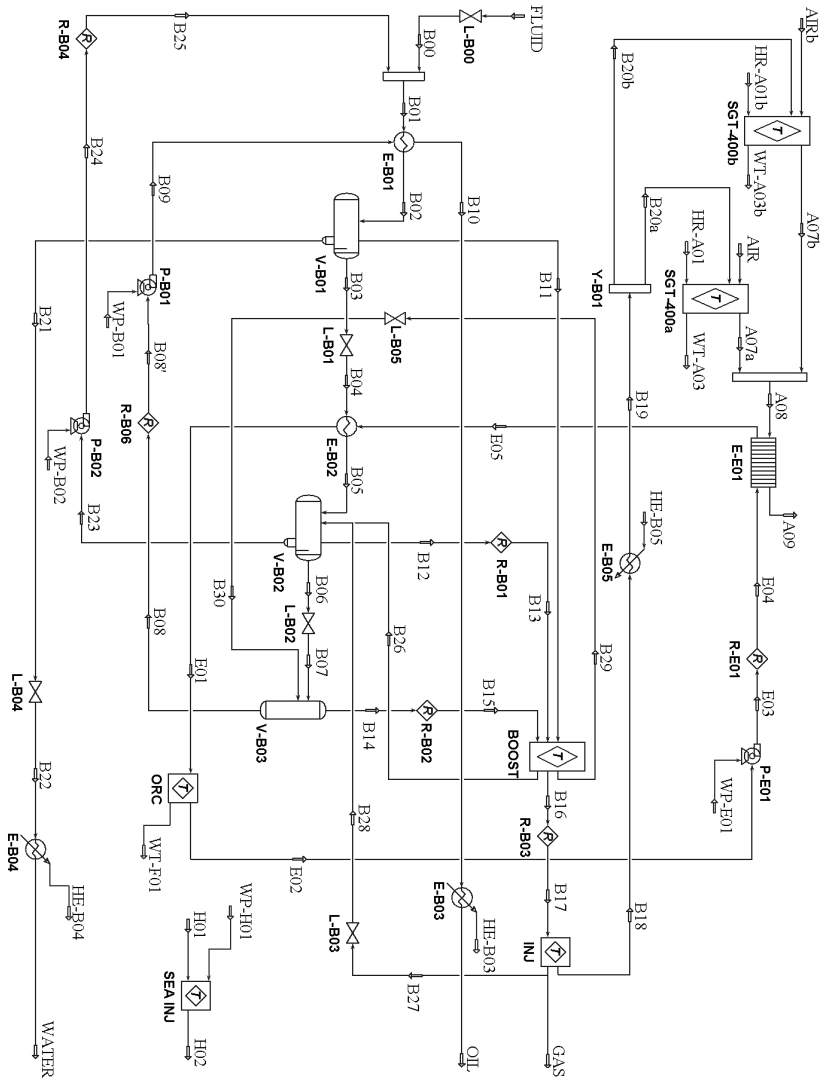


Figure 45 – Process flow diagram of the separation plant (B).

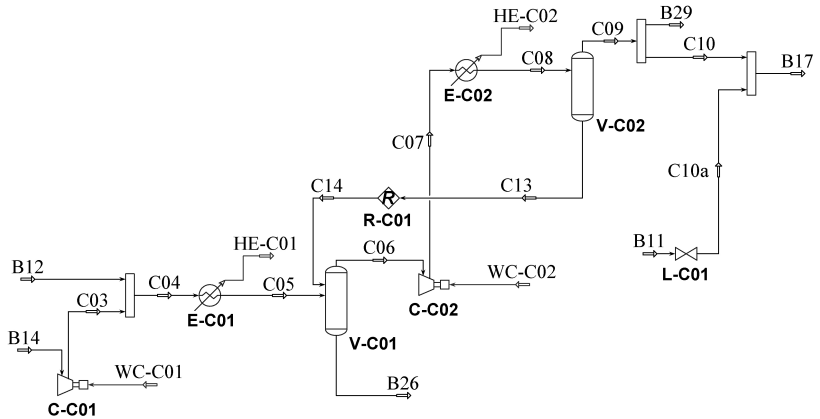


Figure 46 – Process flow diagram of gas boosting subsystem (C).

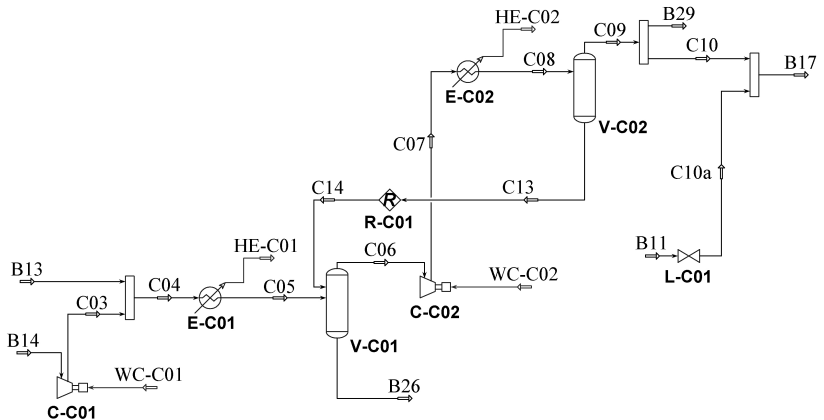


Figure 47 – Process flow diagram of gas injection/export subsystem (D).

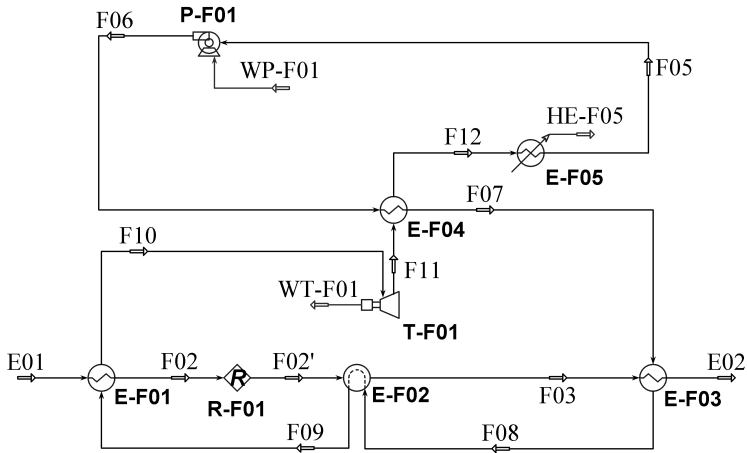


Figure 48 – Process flow diagram of ORC subsystem (F).

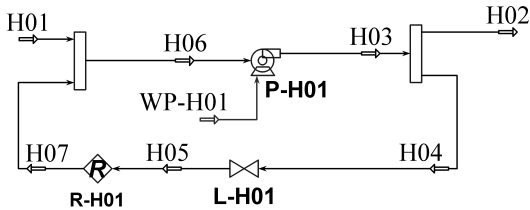


Figure 49 – Process flow diagram of seawater injection subsystem (H).

## APPENDIX B – Hysys code



## B.1 INTRODUCTION

Within the calculation subroutines of Hysys, the calculation of the exergy associated to a stream is not included. Consequently, it was necessary to incorporate a programming code in order to call the values calculated by the software (e.g. enthalpy, entropy, etc.) and create new functions to perform the exergy calculation. In accordance with the proposed methodology, it was necessary to calculate the physical, the chemical and the mixing exergy separately to obtain the overall exergy flow of a stream. The following sections present the code incorporated within the program to execute these routines.

On the other hand, in order to run the cases it was necessary to create a code to combine adequately the calculation of the operation conditions of the power subsystem, the separation plant and the ORC subsystem simultaneously in order to attain the overall model convergence. This code is presented in Sec. B.7.

## B.2 SET DEAD STATE FOR ALL THE STREAMS

### B.2.1 Temperature

```

Sub VariableChanged ()
  On Error GoTo errorHandler
  Dim MS As Streams
  Dim ST As ProcessStream
  Dim X As InternalVariableWrapper
  Dim T0 As Double
  T0=activevariablewrapper.Variable.GetValue()
  Set MS=activeobject.Flowsheet.MaterialStreams
  For Each ST In MS
    Set X=ST.GetUserVariable("AmbTemp")
    X.Variable.SetValue(T0)
  Next ST
  ErrorHandler:
End Sub

```

### B.2.2 Pressure

```

Sub VariableChanged ()

```

```

On Error GoTo errorHandler
Dim MS As Streams
Dim ST As ProcessStream
Dim X As InternalVariableWrapper
Dim P0 As Double
P0=activevariablewrapper.Variable.GetValue()
Set MS=activeobject.Flowsheet.MaterialStreams
For Each ST In MS
Set X=ST.GetUserVariable("AmbPress")
X.Variable.SetValue(P0)
Next ST
ErrorHandler:
End Sub

```

### B.3 PHYSICAL EXERGY

```

Sub PostExecute()
On Error GoTo ErrorHandler
Dim Stream As Fluid
Dim Exergy As RealVariable
Set Stream = ActiveObject.DuplicateFluid
Set Pure = ActiveObject.DuplicateFluid
Set Exergy = ActiveVariableWrapper.Variable
Set X=activeobject.GetUserVariable("AmbTemp")
T0=X.Variable.GetValue()
Set X=activeobject.GetUserVariable("AmbPress")
P0=X.Variable.GetValue()
Set T=activeobject.Temperature
Set P=activeobject.Pressure

If (Stream.VapourFraction.IsKnown And Stream.
    Pressure.IsKnown And Stream.MolarFlow.IsKnown
    And T0<>(-32767+273.15) And Stream.
    MolarFractions.IsKnown(0)) Then
Dim compounds As HYSYS.Components
Dim comp As HYSYS.Component
Dim MassFrac As Variant
Dim MassPure As Variant
Dim compH,compH0, comE As Double
Dim compS,compS0,compE As Double
MassFrac =Stream.MassFractionsValue

```



```

MassPure=Pure.MassFractionsValue
Set compounds = Stream.Components
Set Pures = Pure.Components
comE=0

For var = 0 To compounds.Count-1
  For i = 0 To Pures.Count-1
    MassPure(i)=0
  Next i
  MassPure(var)=1
  Pure.MassFractionsValue=MassPure
  If Pure.TPFlash(Pure.TemperatureValue,Pure.
    PressureValue)=fsFlashOK Then
    compH=Pure.MassEnthalpy.GetValue("kJ/kg")
    compS=Pure.MassEntropy.GetValue("kJ/kg-C")
    Pure.Temperature.SetValue(T0,"C")
    Pure.Pressure.SetValue(P0,"kPa")
    Pure.TPFlash()
    compH0=Pure.MassEnthalpy.GetValue("kJ/kg")
    compS0=Pure.MassEntropy.GetValue("kJ/kg-C")
    compE=(compH-compH0)-(T0+273.15)*(compS-compS0)
    comE=comE+MassFrac(var)*compE
    Pure.Temperature.SetValue(T,"C")
    Pure.Pressure.SetValue(P,"kPa")
  End If
Next var
  Exergy.SetValue(comE*Stream.MassFlow.GetValue("kg/
    s"),"kJ/s")
Else
  Exergy.Erase()
  ErrorHandler:
End If
End Sub

```

#### B.4 CHEMICAL EXERGY

```

'Chemical Exergy With Heat Flow Unit
Sub PostExecute()
On Error GoTo ErrorHandler
Dim Stream As Fluid
Dim Exergy As RealVariable

```

```

Set Stream = ActiveObject.DuplicateFluid
Set Exergy = ActiveVariableWrapper.Variable
If (Stream.VapourFraction.IsKnown And Stream.
    Pressure.IsKnown And Stream.MolarFlow.IsKnown
    And T0<>(-32767+273.15) And Stream.
    MolarFractions.IsKnown(0)) Then
    Dim Comps As HYSYS.Components
    Dim Comp As HYSYS.Component
    Dim MolFrac As Variant
    Dim Comchem As Double
    MolFrac =Stream.MolarFractionsValue
    Set Comps = Stream.Components
    Comchem=0
    For var = 0 To Comps.Count-1
        Set Comp = Comps.Item(var)
        If MolFrac(var)=0 Then
            Comchem=Comchem+MolFrac(var)*Comp.
                GetUserProperty("Mol_Chm_Ex.")
        Else
            Comchem=Comchem+MolFrac(var)*Comp.
                GetUserProperty("Mol_Chm_Ex.")'+MolFrac(var)
                *Log(MolFrac(var))
        End If
    Next var
    Exergy.SetValue(Comchem*Stream.MolarFlow.GetValue(
        "kgmole/s"), "kJ/s")
Else
    Exergy.Erase()
    ErrorHandler:
End If
End Sub

```

## B.5 MIXING EXERGY

```

Sub PostExecute()
On Error GoTo ErrorHandler
Dim Stream As Fluid
Dim Exergy As RealVariable
Set Stream = ActiveObject.DuplicateFluid
Set Pure = ActiveObject.DuplicateFluid
Set Exergy = ActiveVariableWrapper.Variable

```

```

Set X=activeobject.GetUserVariable("AmbTemp")
T0=X.Variable.GetValue()

If (Stream.VapourFraction.IsKnown And Stream.
    Pressure.IsKnown And Stream.MolarFlow.IsKnown
    And T0<>(-32767+273.15) And Stream.
    MolarFractions.IsKnown(0)) Then
Dim Comps As HYSYS.Components
Dim Comp As HYSYS.Component
Dim MassFrac As Variant
Dim MassPure As Variant
Dim ComH As Double
Dim ComS As Double
MassFrac =Stream.MassFractionsValue
MassPure=Pure.MassFractionsValue
Set Comps = Stream.Components
Set Pures = Pure.Components
ComH=0
ComS=0

For var = 0 To Comps.Count-1
    For i = 0 To Pures.Count-1
        MassPure(i)=0
    Next i
    MassPure(var)=1
    Pure.MassFractionsValue=MassPure
    If Pure.TPFlash(Pure.TemperatureValue, Pure.
        PressureValue)=fsFlashOK Then
        ComH=ComH+MassFrac(var)*Pure.MassEnthalpy.
            GetValue("kJ/kg")*Stream.MassFlow.GetValue("
            kg/s")
        ComS=ComS+MassFrac(var)*Pure.MassEntropy.
            GetValue("kJ/kg-C")*Stream.MassFlow.GetValue
            ("kg/s")
    End If
Next var
DeltaH=Stream.MassFlow.GetValue("kg/s")*Stream.
    MassEnthalpy.GetValue("kJ/kg")-ComH
DeltaS=Stream.MassFlow.GetValue("kg/s")*Stream.
    MassEntropy.GetValue("kJ/kg-C")-ComS
DeltaE=DeltaH-(T0+273.15)*DeltaS

```

```

    Exergy.SetValue(DeltaE,"kJ/s")
Else
    Exergy.Erase()
    ErrorHandler:
End If
End Sub

```

## B.6 OVERALL EXERGY

```

Sub PostExecute()
    On Error GoTo ErrorHandler
    Set Stream = ActiveObject.DuplicateFluid
    Dim Exergy As RealVariable
    Set Exergy = ActiveVariableWrapper.Variable
    chem=activeobject.GetUserVariable("Chemical_Exergy")
    phys=activeobject.GetUserVariable("Physical_exergy")
    mix=activeobject.GetUserVariable("Mixing_Exergy").
    Variable.GetValue()
    If (Stream.VapourFraction.IsKnown And Stream.
    Pressure.IsKnown And Stream.MolarFlow.IsKnown
    And T0<>(-32767+273.15) And Stream.
    MolarFractions.IsKnown(0)) Then
    Exergy.SetValue(chem+phys+mix)
Else
    Exergy.Erase()
    ErrorHandler:
End If
End Sub

```

## B.7 INTEGRATION CODE

### B.7.1 Base case (without ORC integrated)

```

Sub Main
    Dim hyCase As SimulationCase
    Dim hySS As SpreadsheetOp
    Dim a As Variant
    a=0.01

```

```

'define spreadsheets
Set hyCase = ActiveCase
Set inputs = hyCase.Flowsheet.Operations.Item("
    INPUTS-B00")
Set outputs=hyCase.Flowsheet.Operations.Item("
    OUTPUTS-B00")
Set results = hyCase.Flowsheet.Operations.Item("
    RESULTS")
On Error GoTo errorhandler
For i= 1 To 16
    'stop solver
    hyCase.Solver.CanSolve=False
    'change variables
    inputs.Cell(1,25).CellValue=results.Cell(i,1).
        CellValue 'fluid flow
    inputs.Cell(1,26).CellValue=results.Cell(i,2).
        CellValue 'BSW
    inputs.Cell(1,13).CellValue=results.Cell(i,3).
        CellValue 'Gas flow
    inputs.Cell(1,6).CellValue=results.Cell(i,4).
        CellValue 'Pressure
    inputs.Cell(1,21).CellValue=results.Cell(i,5).
        CellValue 'Injected water
    'If inputs.Cell(1,15).ImportedVariable.CanModify=
        True Then
    'inputs.Cell(1,15).ImportedVariable.Erase
    'Else
    'inputs.Cell(1,0).ImportedVariable.Erase
    'End If
    'If results.Cell(i,4).CellValue<1500 Then
    'inputs.Cell(1,0).CellValue=0
    'inputs.Cell(1,8).CellValue=inputs.Cell(1,15).
        CellValue-50
    'Else
    'inputs.Cell(1,15).CellValue=1500
    'End If
    'start solver
    hyCase.Solver.CanSolve=True
    'adjust turbine parameters
    point_1:
    If Abs(inputs.Cell(1,1).CellValue -inputs.Cell

```

```

(4,27).CellValue)<a And Abs(inputs.Cell(1,2).
CellValue-inputs.Cell(4,28).CellValue)<a And
Abs(inputs.Cell(1,3).CellValue-inputs.Cell
(4,29).CellValue)<a Then
'MsgBox "OK"
Else
hyCase.Solver.CanSolve=False
inputs.Cell(1,1).CellValue=inputs.Cell(4,27).
CellValue 'exhaust temperature
inputs.Cell(1,2).CellValue=inputs.Cell(4,28).
CellValue 'exhaust mass flow
inputs.Cell(1,3).CellValue=inputs.Cell(4,29).
CellValue 'Heat load
hyCase.Solver.CanSolve=True
If hyCase.Solver.IsSolving=False Then GoTo
point_1
End If
'obtain results
'hyCase.Solver.CanSolve=False
results.Cell(i,7).CellValue=outputs.Cell(3,24).
CellValue 'eta_p
results.Cell(i,8).CellValue=outputs.Cell(3,25).
CellValue 'eta_II
results.Cell(i,9).CellValue=outputs.Cell(3,26).
CellValue 'Xi
results.Cell(i,10).CellValue=outputs.Cell(3,27).
CellValue 'exhaust mass flow
results.Cell(i,11).CellValue=outputs.Cell(3,28).
CellValue 'fuel consumption
results.Cell(i,12).CellValue=outputs.Cell(3,29).
CellValue 'eta-I, turb
results.Cell(i,13).CellValue=outputs.Cell(1,20).
CellValue 'y-L SGT-400a
results.Cell(i,14).CellValue=outputs.Cell(1,21).
CellValue 'y-L SGT-400b
results.Cell(i,15).CellValue=outputs.Cell(1,22).
CellValue 'y-L BOOST
results.Cell(i,16).CellValue=outputs.Cell(1,23).
CellValue 'y-L GAS INJ
results.Cell(i,17).CellValue=outputs.Cell(1,24).
CellValue 'y-L E-B03

```

```

results . Cell ( i , 18 ) . CellValue = outputs . Cell ( 1 , 25 ) .
    CellValue 'y-L E-B04
results . Cell ( i , 19 ) . CellValue = outputs . Cell ( 1 , 26 ) .
    CellValue 'y-L A09
results . Cell ( i , 20 ) . CellValue = outputs . Cell ( 1 , 27 ) .
    CellValue 'y-L WATER
results . Cell ( i , 21 ) . CellValue = outputs . Cell ( 3 , 0 ) .
    CellValue 'Rejected heat
results . Cell ( i , 22 ) . CellValue = outputs . Cell ( 3 , 1 ) .
    CellValue 'Power demand
results . Cell ( i , 23 ) . CellValue = outputs . Cell ( 3 , 2 ) .
    CellValue 'Total exergy losses
Next i
MsgBox "OK"
errorhandler :
End Sub

```

### B.7.2 Cases with ORC integrated

```

Sub Main
Dim hyCase As SimulationCase
Dim a As Variant
a=0.01
'define spreadsheets
Set hyCase = ActiveCase
Set inputs = hyCase.Flowsheet.Operations.Item("
    INPUTS-B00")
Set outputs=hyCase.Flowsheet.Operations.Item("
    OUTPUTS-B00")
Set results = hyCase.Flowsheet.Operations.Item("
    RESULTS")
Set ORC=hyCase.Flowsheet.Operations.Item("ORC_
    MASTER")
On Error GoTo errorhandler
For i= 16 To 16
    hyCase.Solver.CanSolve=False 'stop solver
    'change plant variables
    inputs . Cell ( 1 , 25 ) . CellValue = results . Cell ( i , 1 ) .
        CellValue 'fluid flow
    inputs . Cell ( 1 , 26 ) . CellValue = results . Cell ( i , 2 ) .
        CellValue 'BSW

```

```

inputs . Cell (1,13) . CellValue=results . Cell (i,3) .
    CellValue 'Gas flow
inputs . Cell (1,21) . CellValue=results . Cell (i,5) .
    CellValue 'Injected water
inputs . Cell (1,6) . CellValue=results . Cell (i,4) .
    CellValue 'Pressure
'If inputs . Cell (1,15) . ImportedVariable . CanModify=
    True Then
'inputs . Cell (1,15) . ImportedVariable . Erase
'Else
'inputs . Cell (1,0) . ImportedVariable . Erase
'End If
'If results . Cell (i,4) . CellValue<1500 Then
'inputs . Cell (1,0) . CellValue=0
'inputs . Cell (1,8) . CellValue=inputs . Cell (1,15) .
    CellValue-50
'Else
'inputs . Cell (1,15) . CellValue=1500
'End If
'change ORC variables
For j= 20 To 20
    ORC . Cell (1,0) . CellValue=ORC . Cell (j,20) .
        CellValue 'ORC evaporation temp
        'start solver
    hyCase . Solver . CanSolve=True
        'adjust turbine parameters
    point_1 :
    If Abs(inputs . Cell (1,1) . CellValue -inputs . Cell
        (4,26) . CellValue)<a And Abs(inputs . Cell
        (1,2) . CellValue-inputs . Cell (4,27) . CellValue
        )<a And Abs(inputs . Cell (1,3) . CellValue-
        inputs . Cell (4,28) . CellValue)<a And Abs(
        inputs . Cell (4,24) . CellValue-inputs . Cell
        (6,6) . CellValue)<a Then
        'MsgBox "OK"
    Else
        hyCase . Solver . CanSolve=False
        inputs . Cell (1,1) . CellValue=inputs . Cell (4,26) .
            CellValue 'exhaust temperature
        inputs . Cell (1,2) . CellValue=inputs . Cell (4,27) .
            CellValue 'exhaust mass flow

```



```

inputs . Cell (1,3) . CellValue=inputs . Cell (4,28) .
    CellValue 'Heat load
inputs . Cell (4,24) . CellValue=inputs . Cell (6,6) .
    CellValue
hyCase . Solver . CanSolve=True
If hyCase . Solver . IsSolving=False Then GoTo
    point_1
End If
'obtain ORC results
ORC . Cell (j,21) . CellValue=ORC . Cell (3,4) .
    CellValue 'ORC Exergy Losses
ORC . Cell (j,22) . CellValue=ORC . Cell (3,5) .
    CellValue 'ORC Rejected Heat
ORC . Cell (j,23) . CellValue=ORC . Cell (3,6) .
    CellValue 'ORC Power
ORC . Cell (j,24) . CellValue=ORC . Cell (3,7) .
    CellValue 'ORC Exergy Destruction
ORC . Cell (j,25) . CellValue=ORC . Cell (1,10) .
    CellValue 'E-F01 y_D
ORC . Cell (j,26) . CellValue=ORC . Cell (1,11) .
    CellValue 'E-F02 y_D
ORC . Cell (j,27) . CellValue=ORC . Cell (1,12) .
    CellValue 'E-F03 y_D
ORC . Cell (j,28) . CellValue=ORC . Cell (1,13) .
    CellValue 'E-F04 y_D
ORC . Cell (j,29) . CellValue=ORC . Cell (1,14) .
    CellValue 'P-F01 y_D
ORC . Cell (j,30) . CellValue=ORC . Cell (1,15) .
    CellValue 'T-F01 y_D
ORC . Cell (j,31) . CellValue=ORC . Cell (1,16) .
    CellValue 'etha_I ,ORC
ORC . Cell (j,32) . CellValue=ORC . Cell (1,18) .
    CellValue 'etha_II ,ORC
ORC . Cell (j,33) . CellValue=ORC . Cell (3,0) .
    CellValue 'ORC Evaporation pinch
ORC . Cell (j,34) . CellValue=ORC . Cell (3,1) .
    CellValue 'ORC Economizer pinch
ORC . Cell (j,35) . CellValue=ORC . Cell (3,2) .
    CellValue 'ORC Pressure
ORC . Cell (j,36) . CellValue=ORC . Cell (3,3) .
    CellValue 'ORC mass flow

```

ORC. Cell(j,37).CellValue=ORC. Cell(3,17).  
     CellValue *'ORC input*  
 ORC. Cell(j,38).CellValue=ORC. Cell(1,5).  
     CellValue *'HTF mass flow*  
     *'obtain PLANT results*  
     *'Consolidate table*  
 ORC. Cell(j,40).CellValue=outputs. Cell(3,24).  
     CellValue *'eta\_p*  
 ORC. Cell(j,41).CellValue=outputs. Cell(3,25).  
     CellValue *'eta\_II*  
 ORC. Cell(j,42).CellValue=outputs. Cell(3,26).  
     CellValue *'Xi*  
 ORC. Cell(j,43).CellValue=outputs. Cell(3,27).  
     CellValue *'exhaust mass flow*  
 ORC. Cell(j,44).CellValue=outputs. Cell(3,28).  
     CellValue *'fuel consumption*  
 ORC. Cell(j,45).CellValue=outputs. Cell(3,29).  
     CellValue *'eta\_I, turb*  
 ORC. Cell(j,46).CellValue=outputs. Cell(1,20).  
     CellValue *'y-L SGT-400a*  
 ORC. Cell(j,47).CellValue=outputs. Cell(1,21).  
     CellValue *'y-L SGT-400b*  
 ORC. Cell(j,48).CellValue=outputs. Cell(1,22).  
     CellValue *'y-L BOOST*  
 ORC. Cell(j,49).CellValue=outputs. Cell(1,23).  
     CellValue *'y-L GAS INJ*  
 ORC. Cell(j,50).CellValue=outputs. Cell(1,24).  
     CellValue *'y-L E-B03*  
 ORC. Cell(j,51).CellValue=outputs. Cell(1,25).  
     CellValue *'y-L E-B04*  
 ORC. Cell(j,52).CellValue=outputs. Cell(1,26).  
     CellValue *'y-L A09*  
 ORC. Cell(j,53).CellValue=outputs. Cell(1,27).  
     CellValue *'y-L WATER*  
 ORC. Cell(j,54).CellValue=outputs. Cell(1,28).  
     CellValue *'y-L ORC*  
 ORC. Cell(j,55).CellValue=outputs. Cell(3,0).  
     CellValue *'Rejected heat*  
 ORC. Cell(j,56).CellValue=outputs. Cell(3,1).  
     CellValue *'Power demand*  
 ORC. Cell(j,57).CellValue=outputs. Cell(3,2).

```
        CellValue 'Total exergy losses
    Next j
    k=i-1
    MsgBox("copy_to_excel"&k&"_iteration")
    Stop
Next i
errorhandler:
End Sub
```



## **APPENDIX C – EES case development**



## C.1 INTRODUCTION

This appendix summarizes the development of the model using the software EES (Engineering Equation Solver). In general, this model takes the same inputs of that developed using Hysys. However, its approach is simpler and is based on various simplifying assumptions. The purpose of this development is to offer a comparison framework to the model developed in Hysys and investigate how the level of detailing of the model affect the pretended results of the simulations. Following sections present the main assumptions adopted and the results obtained using this program.

## C.2 ASSUMPTIONS

The main assumptions adopted in the development of the model are listed as follows:

- Continuous operation, with constant conditions (steady state regime).
- Constant thermophysical properties of oil during the separation processes.
- The power generation system is modeled as one turbine operating in accordance with the data reported for the SGT-400 model (Its parameters are adjusted to represent both existing turbines).
- Gases are considered ideal.
- There are no interfacial or chemical interactions between the fluid phases (*i.e.* oil, gas and water).
- Constant composition of the associated gas through the whole process. This implies that the saturation of the gas stream with water is neglected and gas dehydration is discarded.

The last two assumptions cause the well fluid to be modeled as the sum of three unmixed flows (*i.e.* oil, gas and water), which physically does not represent adequately the equilibrium between phases and cause the separation stages to be unnecessary hypothetically. However, considering that all hydrocarbons entering the plant are recognized either as a product or as consumed fuel within the process, the results related to the overall behavior of the plant may be comparable with those calculated by a detailed model.

C.3 SCHEME OF OPERATION

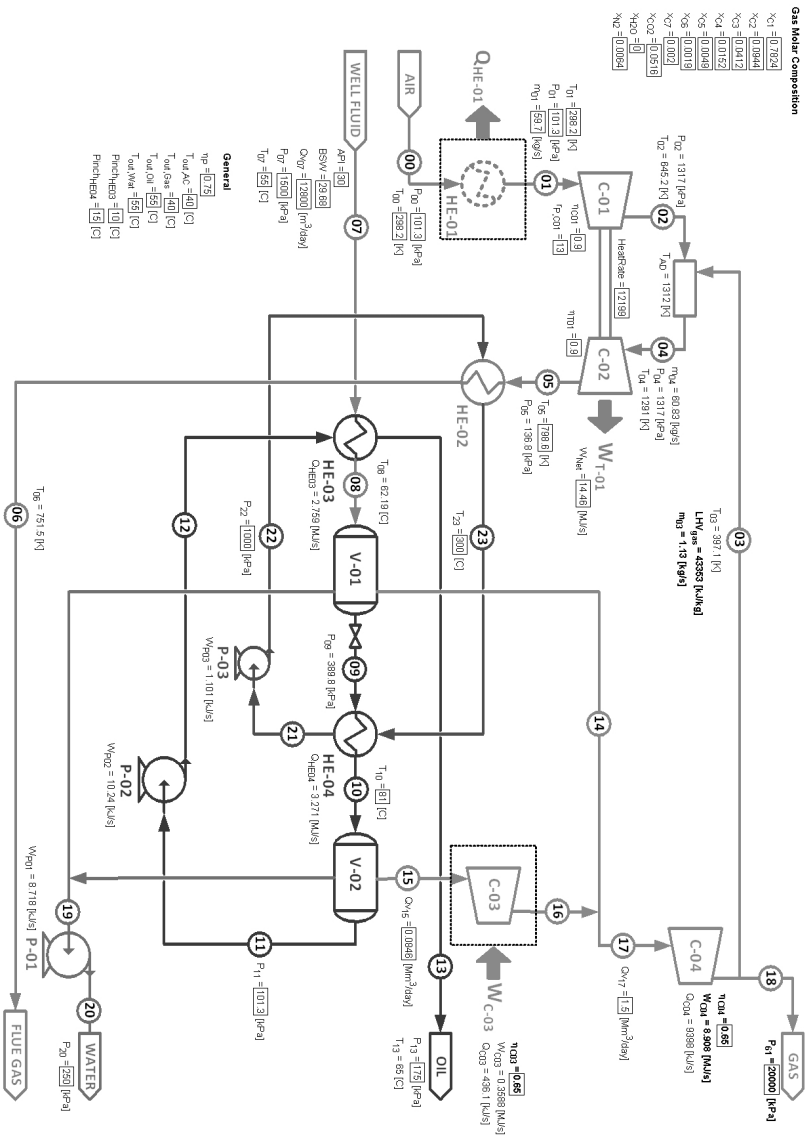


Figure 50 – Scheme of operation of EES model.



Figure 50 presents the scheme of operation considered in the model developed using EES. Analogously, Figs. 51 and 52 show the schemes contemplated for the gas boosting system and gas injection/-export respectively.

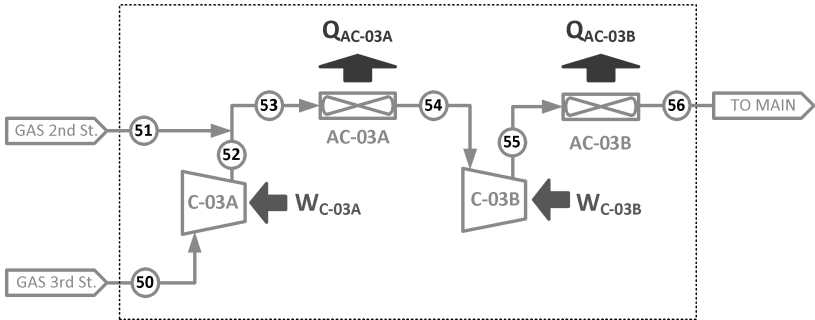


Figure 51 – Scheme of operation of gas boost system in EES model.

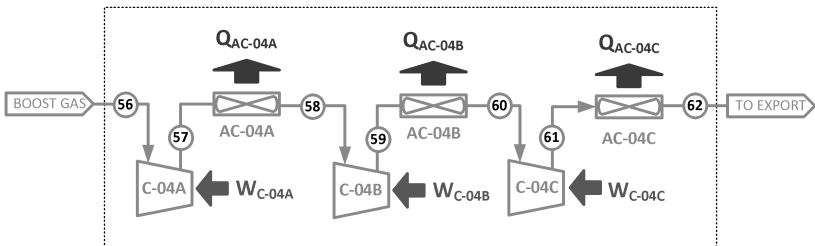


Figure 52 – Scheme of operation of gas injection/export system in EES model.

#### C.4 SOLUTION

The following list presents the values obtained for variables calculated by the model (as reported in the program) .

$$AO = 7.100 \times 10^{-13}$$

$$\beta = 7.089$$

$$B_{00} = 2.8001 \text{ [MJ/s]}$$

$$API = 30$$

$$BSW = 29.68$$

$$B_{01} = 2.8001 \text{ [MJ/s]}$$

|                                    |                              |
|------------------------------------|------------------------------|
| $B_{02} = 22.5130$ [MJ/s]          | $B_{03} = 47.8084$ [MJ/s]    |
| $B_{03A} = 70.2451$ [MJ/s]         | $B_{04} = 54.4178$ [MJ/s]    |
| $B_{05} = 19.2869$ [MJ/s]          | $B_{06} = 17.2914$ [MJ/s]    |
| $B_{07} = 4618.9236$ [MJ/s]        | $B_{08} = 4619.2034$ [MJ/s]  |
| $B_{09} = 3910.6909$ [MJ/s]        | $B_{10} = 3911.1328$ [MJ/s]  |
| $B_{11} = 3869.0674$ [MJ/s]        | $B_{12} = 3869.0755$ [MJ/s]  |
| $B_{13} = 3868.6933$ [MJ/s]        | $B_{14} = 705.5958$ [MJ/s]   |
| $B_{17} = 747.7656$ [MJ/s]         | $B_{19} = 2.5892$ [MJ/s]     |
| $B_{20} = 2.5957$ [MJ/s]           | $B_{21} = 0.0951$ [MJ/s]     |
| $B_{22} = 0.0959$ [MJ/s]           | $B_{23} = 1.2936$ [MJ/s]     |
| $B_{50} = 12.6575$ [MJ/s]          | $B_{51} = 29.3320$ [MJ/s]    |
| $B_{52} = 12.7281$ [MJ/s]          | $B_{53} = 42.0524$ [MJ/s]    |
| $B_{54} = 42.0253$ [MJ/s]          | $B_{55} = 42.2273$ [MJ/s]    |
| $B_{56} = 42.1709$ [MJ/s]          | $B_{57} = 750.0633$ [MJ/s]   |
| $B_{58} = 749.3655$ [MJ/s]         | $B_{59} = 751.4806$ [MJ/s]   |
| $B_{60} = 751.0196$ [MJ/s]         | $B_{61} = 753.1346$ [MJ/s]   |
| $B_{61A} = 704.9931$ [MJ/s]        | $B_{62} = 704.5616$ [MJ/s]   |
| $B_{70} = 6.924$ [MJ/s]            | $B_{71} = 9.676$ [MJ/s]      |
| $B_{ch,03} = 47.4641$ [MJ/s]       | $B_{ch,07} = 4613$ [MJ/s]    |
| $B_{ch,08} = 4613$ [MJ/s]          | $B_{ch,09} = 3910$ [MJ/s]    |
| $B_{ch,10} = 3910$ [MJ/s]          | $B_{ch,11} = 3868$ [MJ/s]    |
| $B_{ch,12} = 3868$ [MJ/s]          | $B_{ch,13} = 3868$ [MJ/s]    |
| $B_{ch,14} = 700.7$ [MJ/s]         | $B_{ch,17} = 742.5$ [MJ/s]   |
| $B_{ch,50} = 12.65$ [MJ/s]         | $B_{ch,51} = 29.22$ [MJ/s]   |
| $B_{ch,52} = 12.65$ [MJ/s]         | $B_{ch,53} = 41.88$ [MJ/s]   |
| $B_{ch,54} = 41.88$ [MJ/s]         | $B_{ch,55} = 41.88$ [MJ/s]   |
| $B_{ch,56} = 41.88$ [MJ/s]         | $B_{ch,57} = 742.5$ [MJ/s]   |
| $B_{ch,58} = 742.5$ [MJ/s]         | $B_{ch,59} = 742.5$ [MJ/s]   |
| $B_{ch,60} = 742.5$ [MJ/s]         | $B_{ch,61} = 742.5$ [MJ/s]   |
| $B_{ch,61A} = 695.1$ [MJ/s]        | $B_{ch,62} = 695.1$ [MJ/s]   |
| $B_{ch,out,Oil} = 3868.282$ [MJ/s] | $B_{ch,wat} = 0.05$ [MJ/s]   |
| $B_{Out,Oil} = 3868.5176$ [MJ/s]   | $B_{out,Wat} = 2.462$ [MJ/s] |
| $B_{ph,03} = 0.3443$ [MJ/s]        | $B_{ph,07} = 5.908$ [MJ/s]   |
| $B_{ph,08} = 6.188$ [MJ/s]         | $B_{ph,09} = 0.5299$ [MJ/s]  |
| $B_{ph,10} = 0.9718$ [MJ/s]        | $B_{ph,11} = 0.7855$ [MJ/s]  |
| $B_{ph,12} = 0.7936$ [MJ/s]        | $B_{ph,13} = 0.4114$ [MJ/s]  |
| $B_{ph,14} = 4.938$ [MJ/s]         | $B_{ph,17} = 5.229$ [MJ/s]   |
| $B_{ph,50} = 0.00267$ [MJ/s]       | $B_{ph,51} = 0.1078$ [MJ/s]  |
| $B_{ph,52} = 0.0733$ [MJ/s]        | $B_{ph,53} = 0.1733$ [MJ/s]  |
| $B_{ph,54} = 0.1463$ [MJ/s]        | $B_{ph,55} = 0.3482$ [MJ/s]  |
| $B_{ph,56} = 0.2919$ [MJ/s]        | $B_{ph,57} = 7.526$ [MJ/s]   |

$$\begin{aligned}
B_{ph,58} &= 6.829 \text{ [MJ/s]} & B_{ph,59} &= 8.944 \text{ [MJ/s]} \\
B_{ph,60} &= 8.483 \text{ [MJ/s]} & B_{ph,61} &= 10.6 \text{ [MJ/s]} \\
B_{ph,61A} &= 9.92 \text{ [MJ/s]} & B_{ph,62} &= 9.489 \text{ [MJ/s]} \\
B_{ph,out,Oil} &= 0.2358 \text{ [MJ/s]} & CO &= 0.07378 \\
\Delta P_{HE02,cool} &= 50 \text{ [kPa]} & \Delta P_{P04} &= 19900 \text{ [kPa]} \\
\Delta P_{HE04,hot} &= 50 \text{ [kPa]} & \eta_{2nd} &= 0.9901 \\
Diff &= 20.09 & \eta_{C01} &= 0.9 \\
\eta_{Bray} &= 0.2849 & \eta_{C04} &= 0.65 \\
\eta_{C03} &= 0.65 & \eta_{T01} &= 0.9 \\
\eta_P &= 0.75 & E_{02} &= 20698 \text{ [kJ/s]} \\
E_{01} &= 2.904 \text{ [kJ/s]} & E_{03A} &= 66443 \text{ [kJ/s]} \\
E_{03} &= 45745 \text{ [kJ/s]} & E_{05} &= 31281 \text{ [kJ/s]} \\
E_{04} &= 64946 \text{ [kJ/s]} & E_{07} &= 4592011 \text{ [kJ/s]} \\
E_{06} &= 28010 \text{ [kJ/s]} & E_{09} &= 3.915 \times 10^6 \text{ [kJ/s]} \\
E_{08} &= 4.595 \times 10^6 \text{ [kJ/s]} & E_{11} &= 3.878 \times 10^6 \text{ [kJ/s]} \\
E_{10} &= 3.918 \times 10^6 \text{ [kJ/s]} & E_{13} &= 3.875 \times 10^6 \text{ [kJ/s]} \\
E_{12} &= 3.878 \times 10^6 \text{ [kJ/s]} & E_{17} &= 713423 \text{ [kJ/s]} \\
E_{14} &= 673225 \text{ [kJ/s]} & E_{20} &= 6838 \text{ [kJ/s]} \\
E_{19} &= 6833 \text{ [kJ/s]} & E_{22} &= 844.8 \text{ [kJ/s]} \\
E_{21} &= 844 \text{ [kJ/s]} & E_{50} &= 12170 \text{ [kJ/s]} \\
E_{23} &= 4115 \text{ [kJ/s]} & E_{52} &= 12261 \text{ [kJ/s]} \\
E_{51} &= 28105 \text{ [kJ/s]} & E_{54} &= 40198 \text{ [kJ/s]} \\
E_{53} &= 40366 \text{ [kJ/s]} & E_{56} &= 40198 \text{ [kJ/s]} \\
E_{55} &= 40466 \text{ [kJ/s]} & E_{58} &= 712733 \text{ [kJ/s]} \\
E_{57} &= 716516 \text{ [kJ/s]} & E_{60} &= 712733 \text{ [kJ/s]} \\
E_{59} &= 715640 \text{ [kJ/s]} & E_{61A} &= 669895 \text{ [kJ/s]} \\
E_{61} &= 715640 \text{ [kJ/s]} & E_{D,03A} &= 0.07633 \text{ [MJ/s]} \\
E_{62} &= 667174 \text{ [kJ/s]} & E_{D,53} &= 0.007765 \text{ [MJ/s]} \\
E_{D,17} &= 0.001194 \text{ [MJ/s]} & E_{D,AC03A} &= 0.02705 \text{ [MJ/s]} \\
E_{D,61A} &= 0.3331 \text{ [MJ/s]} & E_{D,AC04A} &= 0.6977 \text{ [MJ/s]} \\
E_{D,AC03B} &= 0.05634 \text{ [MJ/s]} & E_{D,AC04C} &= 0.4315 \text{ [MJ/s]} \\
E_{D,AC04B} &= 0.461 \text{ [MJ/s]} & E_{D,C03A} &= 0.02017 \text{ [MJ/s]} \\
E_{D,C01} &= 0.9827 \text{ [MJ/s]} & E_{D,C04A} &= 0.7954 \text{ [MJ/s]} \\
E_{D,C03B} &= 0.06605 \text{ [MJ/s]} & E_{D,C04C} &= 0.7924 \text{ [MJ/s]} \\
E_{D,C04B} &= 0.7924 \text{ [MJ/s]} & E_{D,Gas} &= 4.149 \text{ [MJ/s]} \\
E_{D,Comb} &= 15.83 \text{ [MJ/s]} & E_{D,HE02} &= 0.7978 \text{ [MJ/s]} \\
E_{D,HE01} &= 0 \text{ [MJ/s]} & E_{D,HE04} &= 0.7566 \text{ [MJ/s]} \\
E_{D,HE03} &= 0.1024 \text{ [MJ/s]} & E_{D,HE,Wat} &= 0.1335 \text{ [MJ/s]} \\
E_{D,HE,OIL} &= 0.1757 \text{ [MJ/s]} & E_{D,Mix,Comb} &= 14.41 \text{ [MJ/s]} \\
E_{D,HTF} &= 0.0002865 \text{ [MJ/s]} & E_{D,P01} &= 0.002198 \text{ [MJ/s]} \\
E_{D,Oil} &= 1.44 \text{ [MJ/s]} & & 
\end{aligned}$$

$E_{D,P02} = 0.002085$  [MJ/s]  
 $E_{D,Sea} = 0.933$  [MJ/s]  
 $E_{D,V01} = 0.3275$  [MJ/s]  
 $E_{D,Wat} = 2.598$  [MJ/s]  
 $E_{Out,Oil} = 3873079$  [kJ/s]  
 $HeatRate = 12637$   
 $H_{00} = 2.904$  [kJ/s]  
 $H_{02} = 20698$  [kJ/s]  
 $H_{03A} = 16260$  [kJ/s]  
 $H_{05} = -18.87$  [kJ/s]  
 $H_{06A} = -42.47$  [MJ/s]  
 $h_{07,gas} = -4374$  [kJ/kg]  
 $h_{07,wat} = 231.5$  [kJ/kg]  
 $h_{08,gas} = -4359$  [kJ/kg]  
 $h_{08,wat} = 261.5$  [kJ/kg]  
 $H_{10} = 5251$  [kJ/s]  
 $H_{13} = 6471$  [kJ/s]  
 $H_{17} = -71658$  [kJ/s]  
 $H_{21} = 844$  [kJ/s]  
 $H_{51} = -2793$  [kJ/s]  
 $H_{53} = -3912$  [kJ/s]  
 $H_{55} = -3812$  [kJ/s]  
 $H_{57} = -68565$  [kJ/s]  
 $H_{59} = -69441$  [kJ/s]  
 $H_{61} = -69441$  [kJ/s]  
 $H_{62} = -67724$  [kJ/s]  
 $H_{out,Wat} = 10124$  [kJ/s]  
 $LHV_{Oil} = 42380$  [kJ/kg]  
 $Mm_{Fuel} = 21.21$   
 $m_{02} = 57.6$  [kg/s]  
 $m_{03A} = 58.65$  [kg/s]  
 $m_{05} = 58.65$  [kg/s]  
 $m_{07} = 151.6$  [kg/s]  
 $m_{09} = 92.2$  [kg/s]  
 $m_{11} = 91.28$  [kg/s]  
 $m_{13} = 91.28$  [kg/s]  
 $m_{15} = 0.9266$  [kg/s]  
 $m_{19} = 43.93$  [kg/s]  
 $m_{21} = 7.5$  [kg/s]  
 $m_{23} = 7.5$  [kg/s]  
 $m_{51} = 0.6466$  [kg/s]

$E_{D,Pow} = 36.44$  [MJ/s]  
 $E_{D,T01} = 1.466$  [MJ/s]  
 $E_{D,V02} = 0.07591$  [MJ/s]  
 $e_f = 45528$  [kJ/s]  
 $E_{Out,Wat} = 5518$  [kJ/s]  
 $HO = 0.2521$   
 $H_{01} = 2.904$  [kJ/s]  
 $H_{03} = -4439$  [kJ/s]  
 $H_{04} = 14.79$  [kJ/s]  
 $H_{06} = -22.14$  [MJ/s]  
 $H_{07} = -56746$  [kJ/s]  
 $h_{07,Oil} = 54.12$  [kJ/kg]  
 $H_{08} = -53987$  [kJ/s]  
 $h_{08,Oil} = 67.27$  [kJ/kg]  
 $H_{09} = 1980$  [kJ/s]  
 $H_{12} = 9230$  [kJ/s]  
 $H_{14} = -67578$  [kJ/s]  
 $H_{20} = 11444$  [kJ/s]  
 $H_{23} = 4115$  [kJ/s]  
 $H_{52} = -1119$  [kJ/s]  
 $H_{54} = -4080$  [kJ/s]  
 $H_{56} = -4080$  [kJ/s]  
 $H_{58} = -72348$  [kJ/s]  
 $H_{60} = -72348$  [kJ/s]  
 $H_{61A} = -65002$  [kJ/s]  
 $H_{out,Oil} = 4797$  [kJ/s]  
 $LHV_{gas} = 43353$  [kJ/kg]  
 $Mm_{Ex} = 28.56$   
 $m_{01} = 57.6$  [kg/s]  
 $m_{03} = 1.05$  [kg/s]  
 $m_{04} = 58.65$  [kg/s]  
 $m_{06} = 58.65$  [kg/s]  
 $m_{08} = 151.6$  [kg/s]  
 $m_{10} = 92.2$  [kg/s]  
 $m_{12} = 91.28$  [kg/s]  
 $m_{14} = 15.5$  [kg/s]  
 $m_{17} = 16.43$  [kg/s]  
 $m_{20} = 43.93$  [kg/s]  
 $m_{22} = 7.5$  [kg/s]  
 $m_{50} = 0.28$  [kg/s]  
 $m_{52} = 0.28$  [kg/s]

$$m_{53} = 0.9266 \text{ [kg/s]}$$

$$m_{55} = 0.9266 \text{ [kg/s]}$$

$$m_{57} = 16.43 \text{ [kg/s]}$$

$$m_{59} = 16.43 \text{ [kg/s]}$$

$$m_{61} = 16.43 \text{ [kg/s]}$$

$$m_{62} = 15.38 \text{ [kg/s]}$$

$$m_{71} = 138.5 \text{ [kg/s]}$$

$$m_{oil} = 91.28 \text{ [kg/s]}$$

$$NO = 3.74$$

$$Pinch_{HE04} = 15[C]$$

$$P_{01} = 101.3 \text{ [kPa]}$$

$$P_{04} = 1317 \text{ [kPa]}$$

$$P_{07} = 1500 \text{ [kPa]}$$

$$P_{09} = 389.8 \text{ [kPa]}$$

$$P_{11} = 101.3 \text{ [kPa]}$$

$$P_{13} = 175 \text{ [kPa]}$$

$$P_{17} = 1500 \text{ [kPa]}$$

$$P_{20} = 250 \text{ [kPa]}$$

$$P_{22} = 1000 \text{ [kPa]}$$

$$P_{50} = 101.3 \text{ [kPa]}$$

$$P_{53} = 389.8 \text{ [kPa]}$$

$$P_{55} = 1500 \text{ [kPa]}$$

$$P_{57} = 3557 \text{ [kPa]}$$

$$P_{59} = 8434 \text{ [kPa]}$$

$$P_{61} = 20000 \text{ [kPa]}$$

$$P_{62} = 20000 \text{ [kPa]}$$

$$P_{71} = 20000 \text{ [kPa]}$$

$$Qv_{11} = 9001 \text{ [m}^3\text{/day]}$$

$$Qv_{15} = 0.0846 \text{ [Mm}^3\text{/day]}$$

$$Qv_{19} = 3799 \text{ [m}^3\text{/day]}$$

$$Qv_{21} = 0.008261 \text{ [m}^3\text{/s]}$$

$$Qv_{51} = 0.05904 \text{ [m}^3\text{/s]}$$

$$Qv_{70} = 12000 \text{ [m}^3\text{/day]}$$

$$Q_{AC03A} = 168.2 \text{ [kJ/s]}$$

$$Q_{AC04A} = 3783 \text{ [kJ/s]}$$

$$Q_{AC04C} = 2722 \text{ [kJ/s]}$$

$$Q_{C03} = 436.1 \text{ [kJ/s]}$$

$$Q_{HE02} = 3.271 \text{ [MJ/s]}$$

$$Q_{HE04} = 3.271 \text{ [MJ/s]}$$

$$Q_{HE,Wat} = 1.32 \text{ [MJ/s]}$$

$$\rho_{oil} = 876.2 \text{ [kg/m}^3\text{]}$$

$$m_{54} = 0.9266 \text{ [kg/s]}$$

$$m_{56} = 0.9266 \text{ [kg/s]}$$

$$m_{58} = 16.43 \text{ [kg/s]}$$

$$m_{60} = 16.43 \text{ [kg/s]}$$

$$m_{61A} = 15.38 \text{ [kg/s]}$$

$$m_{70} = 138.5 \text{ [kg/s]}$$

$$m_{gas} = 16.43 \text{ [kg/s]}$$

$$m_{wat} = 43.93 \text{ [kg/s]}$$

$$Pinch_{HE03} = 10[C]$$

$$P_{00} = 101.3 \text{ [kPa]}$$

$$P_{02} = 1317 \text{ [kPa]}$$

$$P_{05} = 141.2 \text{ [kPa]}$$

$$P_{08} = 1500 \text{ [kPa]}$$

$$P_{10} = 389.8 \text{ [kPa]}$$

$$P_{12} = 175 \text{ [kPa]}$$

$$P_{14} = 1500 \text{ [kPa]}$$

$$P_{19} = 101.3 \text{ [kPa]}$$

$$P_{21} = 900 \text{ [kPa]}$$

$$P_{23} = 950 \text{ [kPa]}$$

$$P_{52} = 389.8 \text{ [kPa]}$$

$$P_{54} = 389.8 \text{ [kPa]}$$

$$P_{56} = 1500 \text{ [kPa]}$$

$$P_{58} = 3557 \text{ [kPa]}$$

$$P_{60} = 8434 \text{ [kPa]}$$

$$P_{61A} = 20000 \text{ [kPa]}$$

$$P_{70} = 100 \text{ [kPa]}$$

$$Qv_{07} = 12800 \text{ [m}^3\text{/day]}$$

$$Qv_{14} = 1.415 \text{ [Mm}^3\text{/day]}$$

$$Qv_{17} = 1.5 \text{ [Mm}^3\text{/day]}$$

$$Qv_{20} = 0.04397 \text{ [m}^3\text{/s]}$$

$$Qv_{50} = 0.02556 \text{ [m}^3\text{/s]}$$

$$Qv_{62,s} = 17.74 \text{ [m}^3\text{/s]}$$

$$Qv_{in} = 0.1481 \text{ [m}^3\text{/s]}$$

$$Q_{AC03B} = 268 \text{ [kJ/s]}$$

$$Q_{AC04B} = 2907 \text{ [kJ/s]}$$

$$Q_{Av,Ex} = 23.6 \text{ [MJ/s]}$$

$$Q_{C04} = 9412 \text{ [kJ/s]}$$

$$Q_{HE03} = 2.759 \text{ [MJ/s]}$$

$$Q_{HE,Oil} = 1.674 \text{ [MJ/s]}$$

$$Q_{Loss,Comb} = 1.465 \text{ [MJ/s]}$$

$$rP_{C03A} = 3.848$$

$rP_{C03B} = 3.848$   
 $rP_{C04B} = 2.371$   
 $r_{P,C01} = 13$   
 $T_{00} = 25$  [C]  
 $T_{02} = 371.8$  [C]  
 $T_{03A} = 361.3$  [C]  
 $T_{05} = 516.5$  [C]  
 $T_{07} = 55$  [C]  
 $T_{09} = 62.19$  [C]  
 $T_{11} = 81$  [C]  
 $T_{13} = 65$  [C]  
 $T_{15} = 81$  [C]  
 $T_{19} = 62.19$  [C]  
 $T_{21} = 96$  [C]  
 $T_{23} = 300$  [C]  
 $T_{51} = 81$  [C]  
 $T_{53} = 126$  [C]  
 $T_{55} = 172$  [C]  
 $T_{57} = 147.2$  [C]  
 $T_{59} = 124$  [C]  
 $T_{61} = 124$  [C]  
 $T_{62} = 40$  [C]  
 $T_{71} = 25$  [C]  
 $T_{min,Ex} = 150$  [C]  
 $T_{out,Gas} = 40$  [C]  
 $T_{out,Wat} = 55$  [C]  
 $WisOP02 = 7.678$  [kJ/s]  
 $WisOP04 = 2764$  [kJ/s]  
 $W_{C03} = 0.3588$  [MJ/s]  
 $W_{C03B} = 0.268$  [MJ/s]  
 $W_{C04A} = 3.093$  [MJ/s]  
 $W_{C04C} = 2.907$  [MJ/s]  
 $W_{P01} = 8.718$  [kJ/s]  
 $W_{P03} = 1.101$  [kJ/s]  
 $W_{T01} = 33.6656$  [MJ/s]  
 $x_{O07} = 0.1083$

$rP_{C04A} = 2.371$   
 $rP_{C04C} = 2.371$   
 $SG_{Oil} = 0.8762$   
 $T_{01} = 25$  [C]  
 $T_{03} = 124$  [C]  
 $T_{04} = 996.8$  [C]  
 $T_{06} = 467.5$  [C]  
 $T_{08} = 62.19$  [C]  
 $T_{10} = 81$  [C]  
 $T_{12} = 81$  [C]  
 $T_{14} = 62.15$  [C]  
 $T_{17} = 61$  [C]  
 $T_{20} = 62.19$  [C]  
 $T_{22} = 96$  [C]  
 $T_{50} = 81$  [C]  
 $T_{52} = 219.6$  [C]  
 $T_{54} = 40$  [C]  
 $T_{56} = 40$  [C]  
 $T_{58} = 40$  [C]  
 $T_{60} = 40$  [C]  
 $T_{61A} = 124$  [C]  
 $T_{70} = 25$  [C]  
 $T_{AD} = 1016.8$  [C]  
 $T_{out,AC} = 40$  [C]  
 $T_{out,Oil} = 55$  [C]  
 $WisOP01 = 6.538$  [kJ/s]  
 $WisOP03 = 0.8261$  [kJ/s]  
 $W_{C01} = 20.6956$  [MJ/s]  
 $W_{C03A} = 0.0908$  [MJ/s]  
 $W_{C04} = 8.908$  [MJ/s]  
 $W_{C04B} = 2.907$  [MJ/s]  
 $W_{Net} = 12.97$  [MJ/s]  
 $W_{P02} = 10.24$  [kJ/s]  
 $W_{P04} = 3.685$  [MJ/s]  
 $x_{g07} = 0.6019$   
 $x_{w07} = 0.2897$

### C.4.1 Mass and energy balances

Following tables summarize the mass and energy balances obtained from data calculated by the program. In addition, the calculated values were put together with those obtained from Hysys for results comparison.

Table 29 – Mass balances per system in EES model, kg/h.

| <b>System</b>      |               |               |                |               |
|--------------------|---------------|---------------|----------------|---------------|
|                    | <i>Inlets</i> |               | <i>Outlets</i> |               |
| Separation plant   | 07            | 545899        | Oil            | 328596        |
|                    | 05            | 211141        | 17             | 59145         |
|                    | 56            | 3336          | 50             | 1008          |
|                    |               |               | 51             | 2328          |
|                    |               |               | Wat            | 158157        |
|                    |               | 06            | 211141         |               |
| <i>Subtotals</i>   |               | <i>760375</i> |                | <i>760375</i> |
| Gas turbines       | 01            | 207360        | 05             | 211141        |
|                    | 03            | 3781          |                |               |
| <i>Subtotals</i>   |               | <i>211141</i> |                | <i>211141</i> |
| Gas boost          | 50            | 1008          | 56             | 3336          |
|                    | 51            | 2328          |                |               |
| <i>Subtotals</i>   |               | <i>3336</i>   |                | <i>3336</i>   |
| Gas injection      | 17            | 59145         | 62             | 55365         |
|                    |               |               | 03             | 3781          |
| <i>Subtotals</i>   |               | <i>59145</i>  |                | <i>59145</i>  |
| Seawater injection | 70            | 498600        | 71             | 498600        |
| <i>Subtotals</i>   |               | <i>498600</i> |                | <i>498600</i> |

Table 30 – Mass balances per system in Hysys model, kg/h.

| <b>System</b>      |               |               |                |               |
|--------------------|---------------|---------------|----------------|---------------|
|                    | <i>Inlets</i> |               | <i>Outlets</i> |               |
| Separation plant   | FLUID         | 540922        | OIL            | 324558        |
|                    | A07a          | 109816        | B11            | 54216         |
|                    | A07b          | 109816        | B13            | 2910          |
|                    | B18           | 4108          | B15            | 1625          |
|                    | B26           | 571           | B20a           | 2054          |
|                    | B27           | 696           | B20b           | 2054          |
|                    | B29           | 595           | A09            | 219633        |
|                    |               |               | WATER          | 159476        |
| <i>Subtotals</i>   |               | <i>766525</i> |                | <i>766526</i> |
| Gas turbines       | B20a          | 2054          | A07a           | 109816        |
|                    | B20b          | 2054          | A07b           | 109816        |
|                    | AIR           | 107773        |                |               |
|                    | AIRb          | 107773        |                |               |
| <i>Subtotals</i>   |               | <i>219654</i> |                | <i>219633</i> |
| Gas boost          | B11           | 54216         | B26            | 571           |
|                    | B12           | 2910          | B29            | 595           |
|                    | B14           | 1625          | B17            | 57585         |
| <i>Subtotals</i>   |               | <i>58751</i>  |                | <i>58751</i>  |
| Gas injection      | B17           | 57585         | GAS            | 52716         |
|                    |               |               | B18            | 4108          |
|                    |               |               | B27            | 696           |
|                    |               |               | G03            | 66            |
| <i>Subtotals</i>   |               | <i>57585</i>  |                | <i>57586</i>  |
| Seawater injection | H01           | 498993        | H02            | 498993        |
| <i>Subtotals</i>   |               | <i>498993</i> |                | <i>498993</i> |



Table 31 – Power demand distribution according to EES and Hysys models, kW.

| System             | Equipment       |                 | Value         |              |
|--------------------|-----------------|-----------------|---------------|--------------|
|                    | <i>Hysys</i>    | <i>EES</i>      | <i>Hysys</i>  | <i>EES</i>   |
| Separation plant   | P-B01           | P02             | 25.48         | 10.24        |
|                    | P-B02           | P01             | 0.32          | 8.72         |
|                    | P-E01           | P03             | 14.47         | 1.10         |
|                    | E-B05           | NI              | 111.38        | 0            |
|                    |                 | <i>Subtotal</i> | <i>151.65</i> | <i>20.06</i> |
| Gas boost system   | C-C01           | C03A            | 71            | 90.8         |
|                    | C-C02           | C03B            | 246           | 268          |
|                    |                 | <i>Subtotal</i> | <i>317</i>    | <i>359</i>   |
| Gas injection      | C-D01           | C04A            | 2685          | 3093         |
|                    | C-D02           | C04B            | 2509          | 2907         |
|                    | C-D03           | C04C            | 2324          | 2907         |
|                    | C-D04           | NI              | 2014          | 0            |
|                    | <i>Subtotal</i> | <i>9531</i>     | <i>8908</i>   |              |
| Seawater injection | P-H01           | P04             | 4569          | 3685         |
|                    |                 | <i>Subtotal</i> | <i>4569</i>   | <i>3685</i>  |
| <b>Total</b>       |                 |                 | <b>14569</b>  | <b>12972</b> |

*NI- Not included.*

Table 32 – Heat rejection distribution according to EES and Hysys models, kW.

| System        | Equipment       |            | Value        |              | T, °C |
|---------------|-----------------|------------|--------------|--------------|-------|
|               | <i>Hysys</i>    | <i>EES</i> | <i>Hysys</i> | <i>EES</i>   |       |
| Separation    | E-B03           | HE_Oil     | 1819         | 1674         | 65    |
|               | E-B04           | HE_Wat     | 1210         | 1320         | 61    |
|               | <i>Subtotal</i> |            | <i>3029</i>  | <i>2994</i>  |       |
| Gas turbines  | E-E01’*         | Exh. Gas   | 21570        | 23601        | 471   |
|               | R-A01           | Comb.      | 543          | 1465         | 1046  |
|               | R-A01b          | NI         | 543          | 0            | 1046  |
|               | <i>Subtotal</i> |            | <i>22656</i> | <i>25066</i> |       |
| Gas boosting  | E-C01           | AC03A      | 393          | 168          | 108   |
|               | E-C02           | AC03B      | 301          | 268          | 149   |
|               | <i>Subtotal</i> |            | <i>694</i>   | <i>436</i>   |       |
| Gas injection | F-D01           | AC04A      | 3983         | 3783         | 126   |
|               | F-D02           | AC04B      | 3116         | 2907         | 111   |
|               | F-D03           | AC04C      | 3426         | 2722         | 109   |
|               | F-D04           | NI         | 2882         | 0            | 105   |
|               | <i>Subtotal</i> |            | <i>13407</i> | <i>9412</i>  |       |
| <b>Total</b>  |                 |            | <b>39786</b> | <b>37909</b> |       |

\*Considering a min. allowed temp. of 150 °C for exhaust gases.

NI- Not included.

## APPENDIX D – Exergy balances per equipment



## D.1 EXERGY BALANCES

Table 33 presents the formulation of the exergy balances carried out for each equipment conforming the plant.

Table 33 – Exergy balances per equipment.

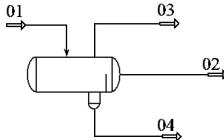

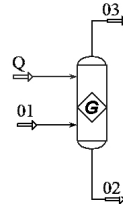
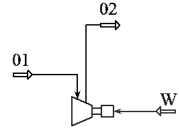
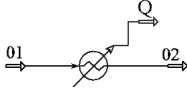
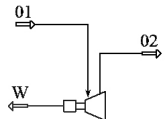
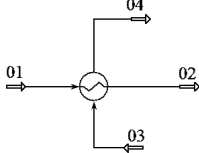
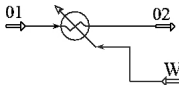
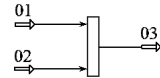
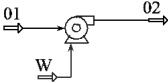
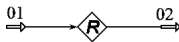
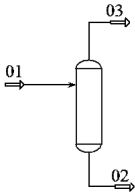
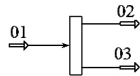

| Equipment             | Figure  | Formulation   |
|-----------------------|---|---|
| Three phase separator |    | $B_D = B_{01} - (B_{02} + B_{03} + B_{04})$                               |
| Air cooler            |    | $B_L = B_{01} - B_{02}$   |
| Combustor             |    | $B_L = (1 - \frac{T_0}{T}) Q$<br>$B_D = B_{01} - (B_{02} + B_{03} + B_L)$ |
| Compressor            |   | $B_D = B_{01} - B_{02} + W$   |
| Cooler                |  | $B_L = B_{01} - B_{02}$   |
| Expander              |  | $B_D = B_{01} - (B_{02} + W)$   |
| Heat exchanger        |  | $B_D = B_{01} - B_{02} + B_{03} - B_{04}$                                 |

Table 33 – Exergy balances per equipment (*cont.*).

| Equipment            | Figure  | Formulation                        |
|----------------------|---|------------------------------------|
| Heater<br>(electric) |  | $B_D = B_{01} + W - B_{02}$        |
| Mixer                |  | $B_D = B_{01} + B_{02} - B_{03}$   |
| Pump                 |  | $B_D = B_{01} + W - B_{02}$        |
| Recycle              |  | $B_D = 0$                          |
| Separator            |  | $B_D = B_{01} - (B_{02} + B_{03})$ |
| Tee                  |  | $B_D = B_{01} - (B_{02} + B_{03})$ |
| Valve                |  | $B_D = B_{01} - B_{02}$            |

## D.2 RESULTS

Tables 34 through 38 present the detailed exergy balances for both cases (Hysys and EES).

Table 34 – Exergy losses per system, kW.

| System           | Stream       |                 | Value        |              |
|------------------|--------------|-----------------|--------------|--------------|
|                  | <i>Hysys</i> | <i>EES</i>      | <i>Hysys</i> | <i>EES</i>   |
| Separation plant | HE-B03       | HE_Oil          | 197          | 176          |
|                  | HE-B04       | HE_Wat          | 124          | 133          |
|                  | A09          | 06              | 14152        | 17291        |
|                  | WATER        | Wat             | 2496         | 2462         |
|                  |              | <i>Subtotal</i> | <i>16968</i> | <i>20063</i> |
| Gas turbines     | A07a         | 05              | 8241         | 19287        |
|                  | A07b         | NI              | 8241         |              |
|                  | HR-A01a      | Comb.           | 379.1        | 1006         |
|                  | HR-a01b      | NI              | 379.1        |              |
|                  |              | <i>Subtotal</i> | <i>17240</i> | <i>20293</i> |
| Gas boost        | HE-C01       | AC03A           | 49           | 27           |
|                  | HE-C02       | AC03B           | 56           | 56           |
|                  | B26          | NI              | 2673         |              |
|                  |              | <i>Subtotal</i> | <i>2777</i>  | <i>83</i>    |
| Gas injection    | HF-D01       | AC04A           | 655          | 698          |
|                  | HF-D02       | AC04B           | 458          | 461          |
|                  | HF-D03       | AC04C           | 482          | 432          |
|                  | HF-D04       | NI              | 387          |              |
|                  | B27          | NI              | 268          |              |
|                  |              | <i>Subtotal</i> | <i>2249</i>  | <i>1590</i>  |
| Recirculations   | A07a         |                 | 8241         | 19287        |
|                  | A07b         |                 | 8241         |              |
|                  | B26          |                 | 2673         |              |
|                  | B27          |                 | 268          |              |
| <i>Total</i>     |              | <i>19812</i>    | <i>22743</i> |              |

*NI- Not included.*

Table 35 – Exergy destruction rate per equipment, kW.

| System/Equip.           |            | Type       | Value         |               | $T_0 S_{gen}$ |
|-------------------------|------------|------------|---------------|---------------|---------------|
| <i>Separation plant</i> |            |            |               |               |               |
| <i>Hysys</i>            | <i>EES</i> |            | <i>Hysys</i>  | <i>EES</i>    | <i>Hysys</i>  |
| M-B01A                  | NI         | Mixer      | 7.0           |               | 2.7           |
| M-B03                   | NI         | Mixer      | 0.0           |               | 0.0           |
| V-B01                   | V01        | 3 Ph. Sep. | 0.0           | 327.52        | 0.0           |
| V-B02                   | V02        | 3 Ph. Sep. | 12.1          | 75.91         | 11.2          |
| L-B01                   | NI         | Valve      | 166.5         |               | 166.5         |
| L-B02                   | NI         | Valve      | 32.8          |               | 32.8          |
| L-B03                   | NI         | Valve      | 0.2           |               | 0.2           |
| L-E01                   | NI         | Valve      | 0.0           |               | 0.0           |
| L-B04                   | NI         | Valve      | 57.2          |               | 57.2          |
| L-B00                   | NI         | Valve      | 1425.5        |               | 1425.5        |
| L-B05                   | NI         | Valve      | 34.7          |               | 34.7          |
| E-B01                   | HE03       | Heat Ex.   | 170.8         | 102.37        | 170.8         |
| E-E01                   | HE02       | Heat Ex.   | 545.8         | 797.84        | 545.8         |
| E-B02                   | HE04       | Heat Ex.   | 1301.8        | 756.61        | 1301.8        |
| P-B01                   | P02        | Pump       | 2.6           | 2.09          | 2.6           |
| P-E01                   | P03        | Pump       | 1.7           |               | 1.7           |
| P-B02                   | P01        | Pump       | 0.0           | 2.20          | 0.0           |
| V-B03                   | NI         | Separator  | 3.7           |               | 3.6           |
| R-E01                   | NI         | Recycle    | 0.0           |               | 0.0           |
| R-B01                   | NI         | Recycle    | -0.1          |               | 0.0           |
| R-B02                   | NI         | Recycle    | -0.6          |               | 0.0           |
| R-B03                   | NI         | Recycle    | 0.0           |               | 0.0           |
| R-B04                   | NI         | Recycle    | 0.0           |               | 0.1           |
| E-B05                   | NI         | Heater     | 118.3         |               | 118.3         |
| Y-B01                   | NI         | Tee        | 0.0           |               | 0.0           |
| <i>Subtotal</i>         |            |            | <i>3879.9</i> | <i>2064.5</i> |               |
| <i>Gas turbines</i>     |            |            |               |               |               |
| T-A02                   | T01        | Expander   | 162.0         | 1465.53       | 162.0         |
| T-A01                   | NI         | Expander   | 121.1         |               | 121.1         |
| T-A03                   | NI         | Expander   | 239.1         |               | 239.1         |
| C-A02                   | C01        | Comp.      | 478.8         | 982.68        | 478.8         |
| C-A01                   | NI         | Comp.      | 474.4         |               | 474.4         |
| R-A01                   | Comb.      | Gibbs R.   | 8003.4        | 14821.02      | 8383.6        |

*NI*–Not included.



Table 35 – Exergy destruction rate per equipment (*Cont.*), kW.

| System/Equip.               |            | Type      | Value          |                | $T_0 S_{gen}$ |
|-----------------------------|------------|-----------|----------------|----------------|---------------|
| <i>Hysys</i>                | <i>EES</i> |           | <i>Hysys</i>   | <i>EES</i>     | <i>Hysys</i>  |
| M-A01                       | 3A         | Mixer     | 400.4          | 76.33          | 400.4         |
| L-A01                       | NR         | Valve     | 18.6           |                | 18.6          |
| <i>Total per turbine</i>    |            |           | <i>9897.6</i>  | <i>17345.6</i> |               |
| <i>Subtotal</i>             |            |           | <i>19795.1</i> | <i>17345.6</i> |               |
| <hr/>                       |            |           |                |                |               |
| <i>Gas boost system</i>     |            |           |                |                |               |
| M-C02                       | 17         | Mixer     | 26.4           | 1.19           | 26.4          |
| M-C01                       | 53         | Mixer     | 6.2            | 7.76           | 6.2           |
| C-C01                       | C03A       | Comp.     | 17.8           | 20.17          | 17.8          |
| C-C02                       | C03B       | Comp.     | 63.3           | 66.05          | 63.3          |
| V-C01                       | NI         | Separator | 0.9            |                | 0.9           |
| V-C02                       | NI         | Separator | 0.0            |                | 0.0           |
| R-C01                       | NI         | Recycle   | 0.0            |                | 0.0           |
| L-C01                       | NI         | Valve     | 195.0          |                | 195.0         |
| Y-C01                       | NI         | Tee       | 0.0            |                | 0.0           |
| <i>Subtotal</i>             |            |           | <i>309.6</i>   | <i>95.2</i>    |               |
| <hr/>                       |            |           |                |                |               |
| <i>Gas injection system</i> |            |           |                |                |               |
| C-D01                       | C04A       | Comp.     | 721.2          | 795.41         | 721.2         |
| C-D02                       | C04B       | Comp.     | 700.4          | 792.36         | 700.4         |
| C-D03                       | C04C       | Comp.     | 648.8          | 792.36         | 648.8         |
| C-D04                       | NI         | Comp.     | 566.8          |                | 566.8         |
| V-D01                       | NI         | Separator | 0.1            |                | 0.1           |
| V-D02                       | NI         | Separator | 0.1            |                | 0.1           |
| V-D03                       | NI         | Separator | 0.0            |                | 0.0           |
| V-D04                       | NI         | Separator | 6.6            |                | 6.6           |
| R-D01                       | NI         | Recycle   | 0.0            |                | 0.0           |
| R-D02                       | NI         | Recycle   | -15.1          |                | 0.7           |
| R-D03                       | NI         | Recycle   | -0.1           |                | 0.0           |
| Y-D02                       | NI         | Tee       | 0.0            |                | 0.0           |
| Y-D01                       | 61A        | Tee       | 0.0            | 333.13         | 0.0           |
| L-D02                       | NI         | Valve     | 766.0          |                | 766.0         |
| L-D01                       | NI         | Valve     | 197.8          |                | 197.8         |
| <i>Subtotal</i>             |            |           | <i>3592.6</i>  | <i>2713.3</i>  |               |

*NI-Not included.*

Table 35 – Exergy destruction rate per equipment (*Cont.*), kW.

| <b>System/Equip.</b>             |            | <b>Type</b> | <b>Value</b>  |              | <b><math>T_0 S_{gen}</math></b> |
|----------------------------------|------------|-------------|---------------|--------------|---------------------------------|
| <i>Hysys</i>                     | <i>EES</i> |             | <i>Hysys</i>  | <i>EES</i>   | <i>Hysys</i>                    |
| <i>Seawater injection system</i> |            |             |               |              |                                 |
| P-H01                            | P04        | Pump        | 503.1         | 933.44       | 503.1                           |
| Y-H01                            | NI         | Tee         | 0.0           |              | 0.0                             |
| L-H01                            | NI         | Valve       | 799.4         |              | 799.4                           |
| M-H01                            | NI         | Mixer       | 11.4          |              | 11.4                            |
| R-H01                            | NI         | Recycle     | 0.0           |              | 0.0                             |
| <i>Subtotal</i>                  |            |             | <i>1313.8</i> | <i>933.4</i> |                                 |
| <b>Total</b>                     |            |             | <b>28891</b>  | <b>23152</b> |                                 |

*NI-Not included.*

Table 36 – Exergy balances per system in EES model, kW.

| <b>System</b>      | <b>Inlets</b>    |                | <b>Outlets</b> |                |
|--------------------|------------------|----------------|----------------|----------------|
| Separation plant   | 07               | 4618923.61     | Oil            | 3868517.64     |
|                    | 05               | 19286.91       | 17             | 747765.57      |
|                    | 56               | 42170.93       | 50             | 12657.48       |
|                    | Work             | 20.06          | 51             | 29332.04       |
|                    |                  |                | Losses         | 20062.8        |
|                    |                  |                | Destr.         | 2064.5         |
| <i>Subtotals</i>   |                  | <i>4680401</i> |                | <i>4680400</i> |
| Gas turbines       | 01               | 2800.14        | 05             | 19286.91       |
|                    | 03               | 47808.39       | Work           | 12970          |
|                    |                  |                | Losses         | 1006           |
|                    |                  |                | Destr.         | 17346          |
|                    | <i>Subtotals</i> |                | <i>50609</i>   | <i>50609</i>   |
| Gas boosting       | 50               | 12657.48       | 56             | 42170.93       |
|                    | 51               | 29332.04       | Losses         | 83             |
|                    | Work             | 359            | Dest.          | 95.2           |
|                    | <i>Subtotals</i> |                | <i>42348</i>   | <i>42349</i>   |
| Gas injection      | 17               | 747765.57      | 62             | 704561.58      |
|                    | Work             | 8908           | 03             | 47808.39       |
|                    |                  |                | Losses         | 1590           |
|                    |                  |                | Destr.         | 2713.3         |
|                    | <i>Subtotals</i> |                | <i>756674</i>  | <i>756674</i>  |
| Seawater injection | 70               | 6923.87        | 71             | 9675.62        |
|                    | Work             | 3685           | Dest.          | 933.4          |
|                    | <i>Subtotals</i> |                | <i>10609</i>   | <i>10609</i>   |

Table 37 – Exergy balances per system in Hysys model, kW.

| <b>System</b>             | <b>Inlets</b> |                | <b>Outlets</b> |                |
|---------------------------|---------------|----------------|----------------|----------------|
| Separation plant          | FLUID         | 4742058        | OIL            | 4023631        |
|                           | A07a          | 8241           | B11            | 673297         |
|                           | A07b          | 8241           | B13            | 31901          |
|                           | B18           | 51667          | B15            | 19258          |
|                           | B26           | 2673           | B20a           | 25830          |
|                           | B27           | 268            | B20b           | 25830          |
|                           | B29           | 7292           | Losses         | 16968          |
|                           | Work          | 152            | Destr.         | 3879.9         |
| <i>Subtotals</i>          |               | <u>4820591</u> |                | <u>4820595</u> |
| Gas turbines              | B20a          | 25830          | WT-A03         | 7285           |
|                           | B20b          | 25830          | WT-A03b        | 7285           |
|                           | AIR           | 108            | Losses         | 17240          |
|                           | AIRb          | 108            | Destr.         | 19795.1        |
| <i>Subtotals</i>          |               | <u>51875</u>   |                | <u>51604</u>   |
| Gas boost system          | B11           | 673297         | B16            | 714395         |
|                           | B13           | 31901          | B29            | 7292           |
|                           | B15           | 19258          | Losses         | 2777           |
|                           | Work          | 317            | Destr.         | 309.6          |
| <i>Subtotals</i>          |               | <u>724773</u>  |                | <u>724773</u>  |
| Gas injection system      | B17           | 714395         | GAS            | 666416         |
|                           | Work          | 9531           | B18            | 51667          |
|                           |               |                | Losses         | 2249           |
|                           |               |                | Destr.         | 3593           |
| <i>Subtotals</i>          |               | <u>723926</u>  |                | <u>723925</u>  |
| Seawater injection system | H01           | 6924           | H02            | 10179          |
|                           | Work          | 4569           | Destr.         | 1313.8         |
| <i>Subtotals</i>          |               | <u>11493</u>   |                | <u>11493</u>   |

Table 38 – General exergy balance, kW.

| <b>Streams</b> |              |                  |                |                |
|----------------|--------------|------------------|----------------|----------------|
| <i>Inlets</i>  | <i>Hysys</i> | <i>EES</i>       | <i>Hysys</i>   | <i>EES</i>     |
|                | FLUID        | 07               | 4742058        | 4618923.61     |
|                | AIR          | 01               | 108            | 2800           |
|                | AIRb         | NI               | 108            | 0.00           |
|                | H01          | 70               | 6924           | 6923.87        |
|                |              | <i>Subtotals</i> | <i>4749197</i> | <i>4628648</i> |
| <i>Outlets</i> | <i>Hysys</i> | <i>EES</i>       | <i>Hysys</i>   | <i>EES</i>     |
|                | OIL          | Oil              | 4023631        | 3868518        |
|                | GAS          | 62               | 666416         | 704562         |
|                | H02          | 71               | 10179          | 9675.62        |
|                | Losses       | Losses           | 19812          | 22743          |
|                | Destr.       | Destr.           | 28891.1        | 23152.0        |
|                |              | <i>Subtotals</i> | <i>4748930</i> | <i>4628650</i> |



## **APPENDIX E – Oil characterization results**





This appendix presents the results concerning the oil characterization using the procedure described in Sec. 3.1, which are included within the Hysys calculation subroutines. These results are obtained from a minimum set of standardized data commonly encountered in the industry. As mentioned in AspenTech (2011), the more information provided, the greater the accuracy of the characterization. However, the lack of information is common when modeling this type of process. Given that the properties and composition of crude change over time and from a reservoir to another, the characterization of the crude shown here corresponds to a typical fluid (as shown in Tab. 8) and does not pretend to model an actual fluid in detail. Moreover, the scope of present work is rather focused on the energy efficiency of the processes than on the crude characterization.

Figures 53 through 56 present the calculated properties for the pseudocomponents generated in order to model the crude, which corresponds to as a mixture of 34 pseudocomponents, 7 pure hydrocarbons, CO<sub>2</sub>, Nitrogen, Oxygen and water. In addition, Tab. 39 shows the composition of the oily phase of the crude, which reports an average molecular weight of 250.7 kg/kmol.

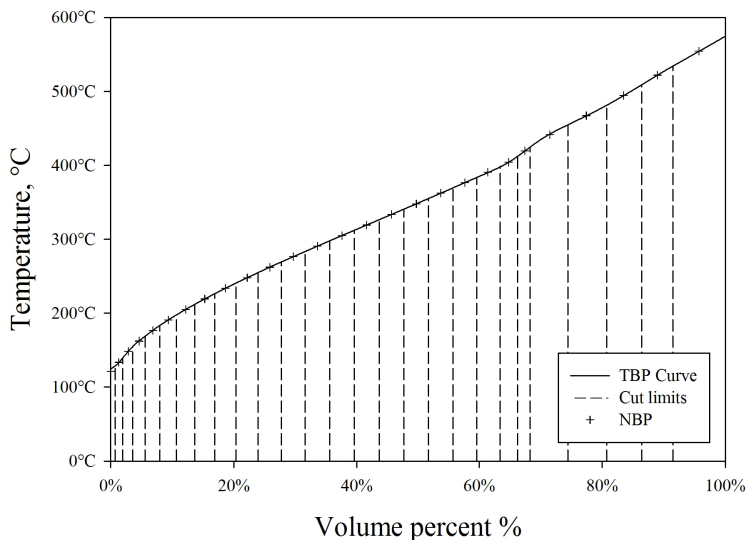
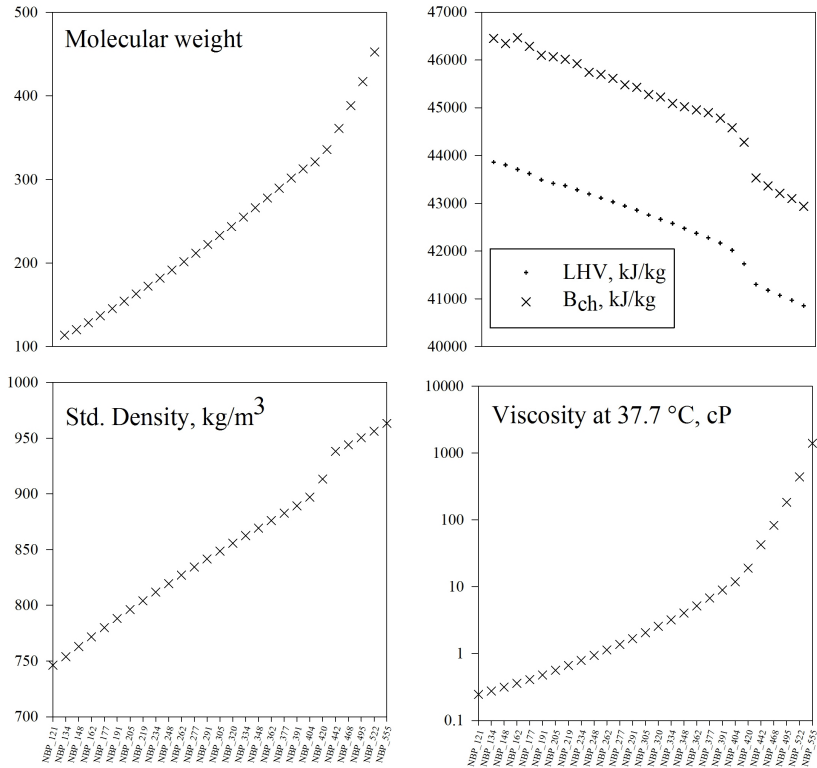


Figure 53 – TBP curve and normal boiling point (NBP) of each pseudocomponent.

Table 39 – Crude composition (oily phase).

| <b>Hypo name</b> | <b>mass frac.</b> |
|------------------|-------------------|
| NBP[0]121*       | 0.0061            |
| NBP[0]134*       | 0.0108            |
| NBP[0]148*       | 0.0139            |
| NBP[0]162*       | 0.0180            |
| NBP[0]177*       | 0.0213            |
| NBP[0]191*       | 0.0244            |
| NBP[0]205*       | 0.0272            |
| NBP[0]219*       | 0.0297            |
| NBP[0]234*       | 0.0320            |
| NBP[0]248*       | 0.0340            |
| NBP[0]262*       | 0.0357            |
| NBP[0]277*       | 0.0371            |
| NBP[0]291*       | 0.0382            |
| NBP[0]305*       | 0.0390            |
| NBP[0]320*       | 0.0396            |
| NBP[0]334*       | 0.0399            |
| NBP[0]348*       | 0.0399            |
| NBP[0]362*       | 0.0397            |
| NBP[0]377*       | 0.0393            |
| NBP[0]391*       | 0.0387            |
| NBP[0]404*       | 0.0293            |
| NBP[0]420*       | 0.0209            |
| NBP[0]442*       | 0.0659            |
| NBP[0]468*       | 0.0681            |
| NBP[0]495*       | 0.0620            |
| NBP[0]522*       | 0.0555            |
| NBP[0]555*       | 0.0940            |



### Pseudocomponents

Figure 54 – Some physical properties and lower heating value (LHV) of each pseudocomponent.

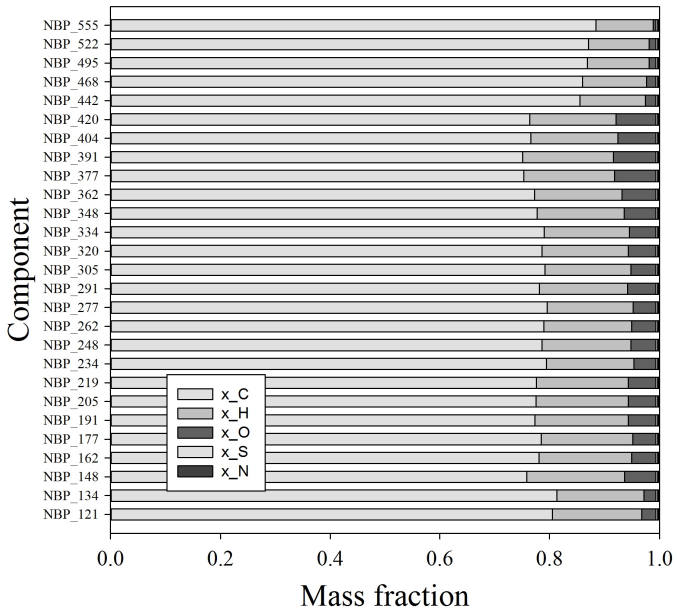


Figure 55 – Elemental composition of each pseudocomponent.

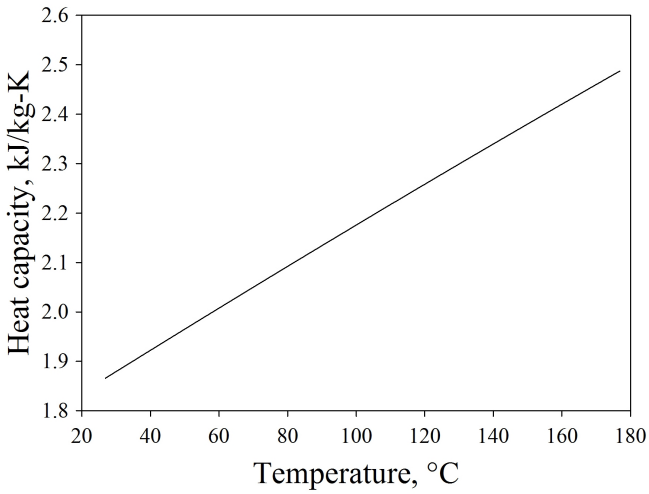


Figure 56 – Specific heat of crude (oily phase).